To the Graduate Council:

I am submitting herewith a dissertation written by Roger Charles Hart entitled "Coherent Cancellation Effects in the Multiphoton Ionization of Xenon." I have examined the final copy of this dissertation for form and content and recommend that it be accepted in partial fulfillment of the requirements for the degree of Doctor of Philosophy, with a major in Physics.

John O. Thomson, Major Professor

We have read this dissertation
and recommend its acceptance:

Accepted for the Council:

Associate Vice Chancellor
and Dean of the Graduate School

# Coherent Cancellation Effects in the Multiphoton Ionization of Xenon

A Dissertation

Presented for the

Doctor of Philosophy

Degree

The University of Tennessee, Knoxville

Roger Charles Hart

December 1991

# DEDICATION

This dissertation is dedicated to my parents

Charles Madison Hart

and

Alma Mavis Hart

whose faith, support, and guidance made it possible.

# ACKNOWLEDGMENTS

Many colleagues, collaborators, teachers, and friends have contributed in one way or another to the completion of the research described in this dissertation. Ray Garrett and Marvin Payne of the ORNL Photophysics group provided patient teaching and guidance. Steve Allman and Ron Phillips were always ready with technical support, good advice, and lots of laser lore. Ollie Thomson deserves special mention for giving an undergraduate physics student an early opportunity to do hands-on physics experiments (even if we didn't find any quarks).

This research was sponsored in part by the Office of Health and Environmental Research, U.S. Department of Energy under contract DE-AC05-840R21400 with Martin Marietta Energy Systems, Inc.

# ABSTRACT

Two experiments exploring various manifestations of the three-photon interference effect are described. In the first experiment, a transition in xenon allowed with both one and three photons is shown to exhibit a shift in the resonance wavelength which varies with the xenon density and the angle between the laser beams used for the three-photon excitation. The magnitude of the shift is shown to agree quite well with the predictions of a two-state model for the excitation which includes self-consistently the pumping rate due to the internally generated sum-frequency wave as well as that due to the laser fields. The second experiment demonstrates the suppression of the excitation of a two- and four-photon allowed transition by a three-photon interference effect occuring at an intermediate three- and one-photon allowed resonance. The degree of the suppression is measured by comparing the ionization with and without retroreflection of the near three-photon resonant laser beam. The observed suppression agrees well with the predictions of a three-state model in which the transition rate due to the internally generated third-harmonic light (plus an additional photon) is treated self-consistently. The diminution of the free third-harmonic wave which is necessary for the three-photon interference effect to occur is shown to be due mainly to a large phase mismatch between the free third harmonic and the laser field, rather than to absorption of the third harmonic. The suppression of wing absorption into the three-photon state by the three-photon interference effect is also demonstrated.

# TABLE OF CONTENTS

# LIST OF FIGURES

# CHAPTER I

## Introduction and Review of the Literature

The study of the interaction of electromagnetic radiation with atoms has long been one of the principle means of gaining information about atomic structure. Spectroscopic observation of the regularities in the spacing of the absorption and emission lines of hydrogen during the last decades of the nineteenth century provided, a few decades later, the principle impetus for the development of quantum mechanics; in the late 1940s the observation of the Lamb shift in hydrogen provided experimental confirmation for the developing theory of quantum electrodynamics. With the invention of the laser a new regime for experimentation became accessible. This bright, spectrally narrow, and (eventually) tunable light source could produce nonlinear effects that were both interesting in themselves and which further extended the spectroscopist's reach. But laser spectroscopy brought with it a fundamental change in emphasis: the old spectroscopy studied atoms, using light merely as a probe, while the new spectroscopy studies the combined light-atom system, often finding more of interest in the light than in the atom.

In both the experiments described in this dissertation the response of a medium to excitation with intense light is shown to be profoundly altered by interference between the applied light and light generated in the medium. In one experiment the apparent energy of an atomic transition is found to vary with the density of the medium and the angle between the laser beams which excite the transition; shifts as large as 200 Å are observed. Such shifts are *very* much larger than those due to the ac Stark effect or pressure-induced shifting. In the other experiment the excitation rate of a four-photon resonance is shown to decrease as the laser is tuned nearer an intermediate, enhancing

resonance; in the absence of any interference one would expect instead a significant increase.

The first section of this chapter gives a brief review of some of the physical concepts necessary to understand the theoretical and experimental work discussed here; a simple model of the three-photon interference effect is presented. In the second section the pertinent experimental and theoretical contributions in the literature are discussed and analyzed in terms of this simple model. Where appropriate, connection is made with the work presented in this dissertation.

## Introduction

The response of a medium to light can be described in terms of electric susceptibilities. If the light is not too intense, then

$$P = \chi^{(1)} E, \tag{1.1}$$

gives the electric polarization $P$ in terms of the linear susceptibility $\chi^{(1)}$ and the instantaneous electric field strength $E$. Here $E = E_0 \cos(kz - \omega t)$, with $E_0 = \sqrt{\frac{8\pi}{c} I}$ in cgs units for a light wave of intensity $I$. Then through $n = \sqrt{1 + 4\pi\chi}$, with n the index of refraction, all the familiar phenomena of linear optics (absorption and refraction, for example) can be described.

If the intensity is large, however, equation 1.1 is no longer an adequate description. If the induced dipole moment for an atom is calculated quantum mechanically including $E$ to higher orders, the polarization is found as an expansion in powers of $E$; the coefficients of that expansion are the nonlinear susceptibilities. Examples of such treatments may be found in chapter 2 of Ref. 1 and in chapter 2 of Ref. 2. Susceptibility treatments are not entirely adequate for all problems in nonlinear optics, being restricted mainly to the adiabatic-following limit, although most of the very wide range of known

nonlinear behavior is at least represented in such an expansion of $P$. The susceptibility approach is essentially an attempt to solve once and for all time the quantum mechanical side of the light-matter interaction problem; having the appropriate susceptibilities, one may treat the remainder of the problem purely in terms of electromagnetism. This is certainly convenient, but solutions found in that way can be no better than the analysis employed to find the susceptibilities in the first place.

Because of the all-inclusive nature of the susceptibility approach and the complexity it entails, any detailed discussion of the form or significance of the the various nonlinear terms in the susceptibility is outside the scope of this dissertation. The calculations of the atomic response under specific conditions of excitation carried out in later chapters are framed directly in terms of the atomic parameters, as this results in a description which is both more accurate and more easily understood. Nevertheless, a few introductory observations are best made in terms of the susceptibility formalism.

One of the simplest nonlinear effects is multiphoton absorption (MPA) or ionization (MPI), in which an atom initially in the ground state absorbs several photons and is left in an excited state; if the final state is a continuum state, the atom is ionized. For ionization the conservation of energy requires $n\hbar\omega > e(I.P.)$, where $n$ is the number of photons absorbed, $\omega$ is the frequency of the light in radians per second, $e$ is the electron charge, and $I.P.$ is the ionization potential of the atom (see Fig. 1.). As an example, the first $I.P.$ of xenon is at 97,798 $cm^{-1}$ ( corresponding to 12.1 eV ); one-photon ionization of xenon would thus require light with a wavelength shorter than 1022.5 Å, while ionization by five photons requires light shorter than 5113 Å in wavelength.

Absorption is proportional to $Im(\chi)$; the absorption of n photons (to either a bound or a continuum state) is proportional to $Im(\chi^{(2n-1)})$.[3] The m'th order susceptibility is

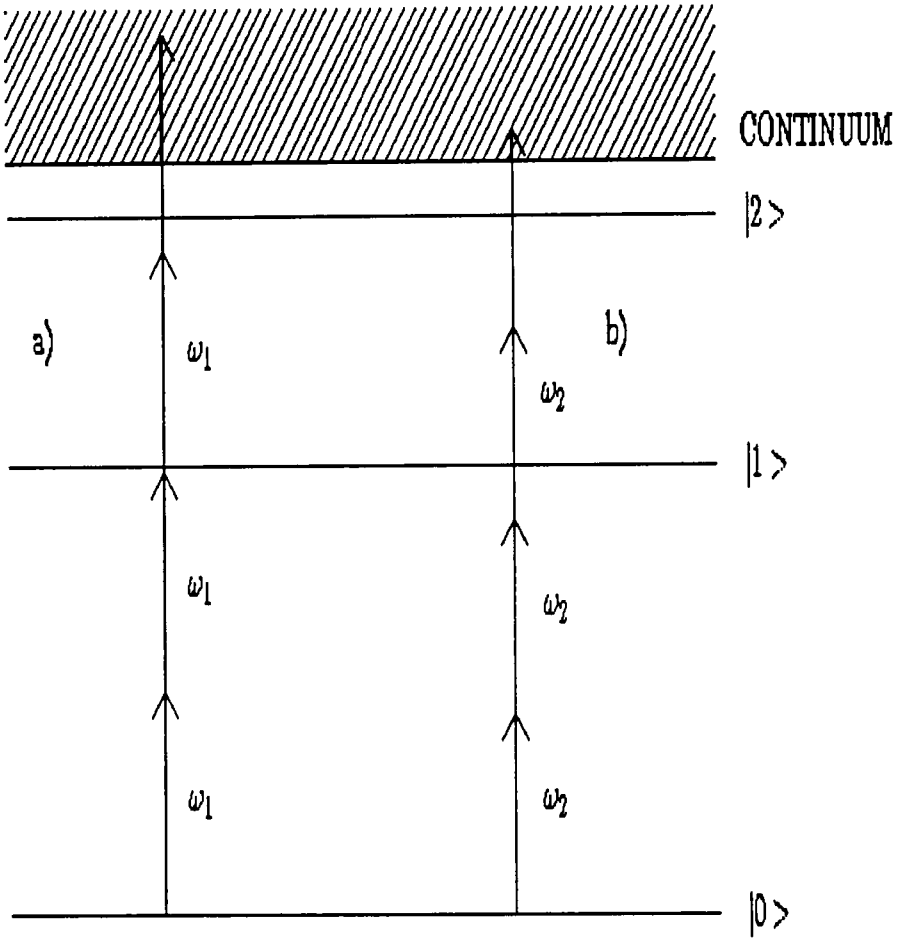


Figure 1. Ionization by MPI and REMPI

Multiphoton ionization by $n$ photons is due to the imaginary part of the $(2n-1)$'th order susceptibility. Resonant enhancement occurs when some number of laser photons is near-resonant with an allowed transition $|0> \rightarrow |1>$ as at a). Then the resonant denominator in one term of the susceptibility is small, resulting in a much larger transition rate.

of the form

$$\chi^{(m)}(-\omega_\sigma;\omega_1\cdots\omega_m) = K\widehat{P}_T$$
$$\times \sum_{gb_1\cdots b_m} \frac{\vec{\epsilon}_\sigma^{\,*}\cdot\vec{Q}_{gb_1}\,\vec{\epsilon}_1\cdot\vec{Q}_{b_1b_2}\cdots\vec{\epsilon}_m\cdot\vec{Q}_{b_mg}}{(\Omega_{b_1g}-\omega_1-\cdots-\omega_m)(\Omega_{b_2g}-\omega_2-\cdots-\omega_m)\ldots(\Omega_{b_mg}-\omega_m)}. \qquad (1.2)$$

(With the grouping of some constants and parameters into $K$ and some minor changes in notation, this is equation 2.15 in Ref. 3.) Here $\Omega_{ij} = (E_i - E_j)/\hbar \pm i\Gamma$, where $E_i$ the energy of stationary atomic state $|i>$ and $\Gamma$ is a phenomenologically introduced absorption or damping factor. $\vec{\epsilon}_m$ is the polarization vector of the light at angular frequency $\omega_m$, and $\omega_\sigma = \omega_1 + \cdots + \omega_m$. The dipole matrix element is given by $\vec{Q}_{ij} = <i|\vec{Q}|j>$, with $\vec{Q} = e\vec{r}$ being the electric dipole operator. The summation is taken over all states of the atom, and implies an integration over continuum states; here $g$ represents the ground state. $\widehat{P}_T$ is the overall permutation operator, which indicates the expression is to be summed over all permutations of $(\epsilon_i, \omega_i)$.[3]

Equation 1.2 is a complicated expression, not least because it is written for the general case of excitation by light of $m$ different colors (with frequencies $\omega_1$ through $\omega_m$), and also because it represents a portion of the response of a complicated system (an atom) to a complicated perturbation. Still, the important features of 1.2 are simply stated: the expression contains a product of dipole matrix elements in the numerator of each term, and a product of detunings in the denominator. The rightmost term in the denominator of 1.2 involves detunings between single frequencies $\omega_m$ and transitions $\Omega_{b_mg}$ between the ground state and levels $b_m$. The next term to the left (not written) involves similar detunings between sums of two frequencies and the various $\Omega$'s. If some exciting frequency $\omega$ or some sum of j exciting frequencies is nearly equal to some atomic transition frequency $\Omega$, then the denominator of that term will be small. If the transition is allowed by the electric dipole selection rules for that number of photons, then the numerator will not be zero, and the susceptibility will be large. This is resonant enhancement. If the resonance providing the enhancement is lower in energy than the

final state, it is referred to as an intermediate resonance. In ionization, of course, the final state is in the continuum, where, except for autoionizing resonances, there is a continuous distribution of states, and so no evident enhancement. But if the laser is tuned through resonance with an intermediate level, a peak in the ionization will be seen. This is resonantly enhanced multiphoton ionization (REMPI).

With the $\Omega_{ij}$'s real, a susceptibility of the form given in equation 1.2 becomes singular on resonance; phenomenological terms of the form $i\Gamma$ are often added to the detunings in the denominators to represent the effect of damping (by collisional dephasing, for example), and thus avoid singularities. In the absence of damping, higher-order terms of the susceptibility are needed to take proper account of the large changes produced in the atom by on-resonance excitation. (This discussion of singularities follows that given in Ref. 3 , section 2.5.)

REMPI is a useful probe of the atom. For example, determination of the energies of high-lying states in noble gases by observation of one-photon absorption requires a source of vacuum ultraviolet (VUV) light and an evacuated monochromator; observation of the enhancement of the ionization as a laser is tuned through multiphoton resonance with the state provides the same information, but requires only the generation of light at some subharmonic of the resonant wavelength, and a means to detect the ionization produced. For example, the xenon $4f$ levels require VUV light at about 1100 Å for one-photon excitation, while four-photon resonant excitation (with one additional photon ionizing) requires light at only 4400 Å, which is easily within the capabilities of modern lasers. Additionally, studies of the pressure-induced broadening and shifting of resonant transitions are difficult to perform by observing one-photon absorption, since substantial densities are necessary to produce the broadening and shifting, and the medium is then quite opaque to on-resonance light. Similar studies may be conducted using three-photon excitation of the resonant level (with ionization by additional photons), thus avoiding the absorption problem.[4]

The nonlinear terms in the susceptibility are also responsible for frequency-mixing processes.

$$P_{NL}^{(n)}(\omega_\sigma) = \chi^{(n)}(-\omega_\sigma; \omega_1 \cdots \omega_n) E_1(\omega_1) \cdots E_n(\omega_n)$$

represents a polarization of the medium at the frequency $\omega_\sigma = \omega_1 + \cdots + \omega_n$. Polarizations occur at all sums and differences of the frequency (or frequencies) of the incident light, provided the susceptibility for that particular mixture of frequencies is not zero due to symmetry considerations. These polarizations are source terms for the growth of electromagnetic fields, though in general these fields are quite weak. Resonant enhancement of the susceptibility will, of course, increase the magnitude of the polarization quite substantially, but the generation of significant amounts of light at a sum or difference frequency also requires the generated light be phase matched with the laser. Consider third-harmonic generation. Laser light at frequency $\omega$ propagates in the $+\hat{z}$ direction according to $E_0(e^{i(k_\omega z - \omega t)} + c.c)$, where $c.c$ indicates the complex conjugate and $k_\omega$, the magnitude of the propagation vector, is given by $k_\omega = \omega n(\omega)/c$, with $n(\omega)$ the index of refraction at frequency $\omega$. For the third-harmonic light the magnitude of the propagation vector is $k_{3\omega} = 3\omega n(3\omega)/c$. The phase matching condition simply requires that third-harmonic light generated at some point $z_1$ be in phase with third harmonic generated at some later point $z_2$. A substantial phase mismatch will result in destructive interference between components of the third-harmonic originating at various points in the medium and thus a reduction in the intensity of the generated light. The time for a point of constant phase of the laser field to traverse the distance $\Delta z = z_2 - z_1$ is

$$\Delta t = \frac{\Delta z}{v} = \frac{n(\omega)}{c} \Delta z.$$

The phase of the third harmonic generated at $z_1$ will advance in the time $\Delta t$ and the distance $\Delta z$ by

$$k_{3\omega} \Delta z - 3\omega \frac{n(\omega)}{c} \Delta z = (k_{3\omega} - 3k_\omega) \Delta z,$$

so phase matching requires $\Delta k = k_{3\omega} - 3k_\omega = 0$.

Frequency mixing processes have proved useful for the generation of tunable light at wavelengths outside the region accessible with dye lasers.[5,6] Of more fundamental physical significance, however, is the fact that sum-frequency generation can drastically alter the atomic response to excitation when the laser is tuned near a transition allowed in both one and a higher odd number of photons. There is no equivalent effect involving an even number of photons, since even-harmonic generation is not allowed in centrosymmetric media (such as atomic vapors or noble gases) by parity considerations.

Consider the excitation of an atomic state $|1>$ which is coupled to the ground state $|0>$ in both one and three photons as shown in Fig. 2. A laser of frequency $\omega_L$, with $\omega_L$ chosen so that $3\omega_L \simeq (E_1 - E_0)/\hbar$, couples together the amplitudes $a_0$ and $a_1$ of states $|0>$ and $|1>$. But the third-harmonic field at $3\omega_L$ also couples these states, so the evolution of the amplitude of state $|1>$ depends on the relative amplitudes and phases of the couplings due to the three-photon laser field and the third-harmonic field. This is referred to as the three-photon interference effect. Under rather general circumstances the amplitude and phase of the coupling due to the generated field is such as to cancel the coupling due to the laser field, and so no excitation of state $|1>$ takes place. This is the three-photon cancellation effect. There are analogous effects in any situation in which a resonance is coupled to the ground state in both one and some odd number of photons; the effect is referred to in general as the odd-photon interference effect or the (2n+1) photon interference effect.

The equation of motion of the amplitude $a_1$ of state $|1>$ is

$$\frac{\partial a_1}{\partial t} = -i\Omega_{01}^{*(eff)} e^{-i\delta t} a_0,$$

where several terms have been omitted for clarity. Here

$$\Omega_{01}^{eff} = e^{-i\Delta k_r z}\Omega_{01}^{(3)} + \Omega_{01}^{(1)}$$

is the effective Rabi frequency which describes the coupling of states $|0>$ and $|1>$ by both the laser field and the third-harmonic field. $\Omega_{01}^{(3)}$ is the three-photon Rabi frequency

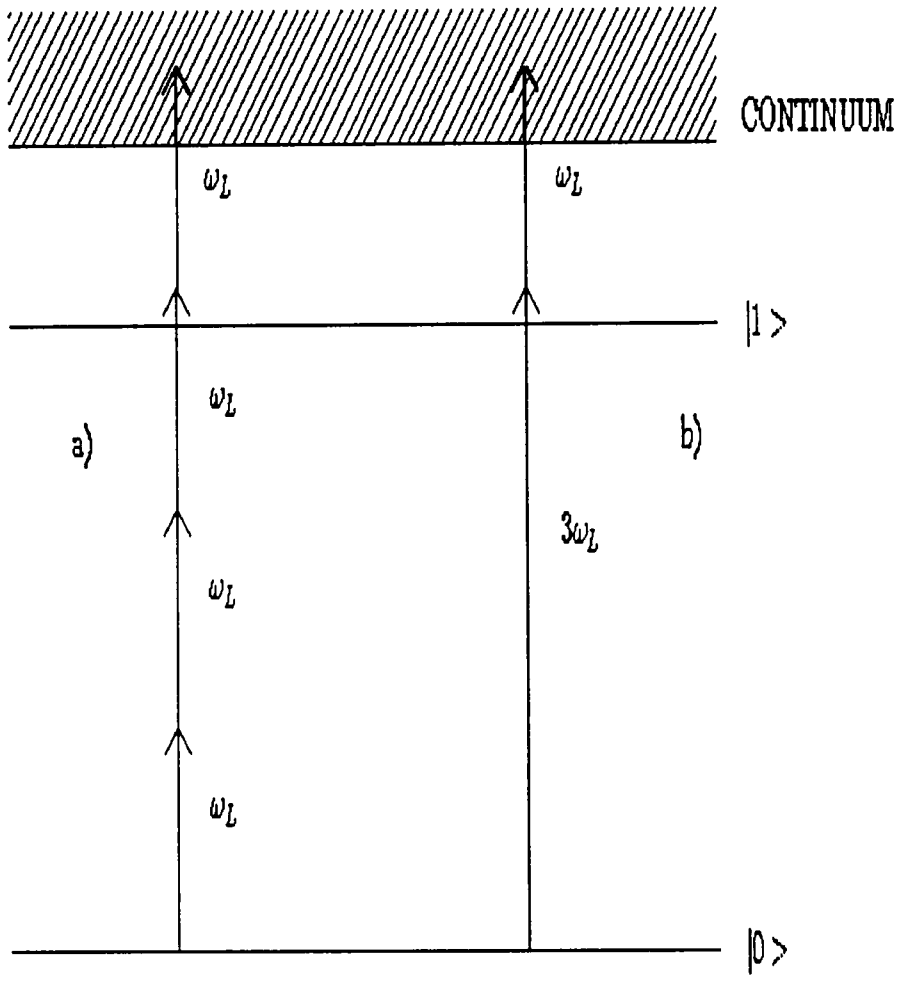


Figure 2. Simultaneous Coupling of States |0> and |1> by Two Fields

At a) the three-photon laser field couples |0> and |1>, and at b) the states are coupled by the third-harmonic field generated in the medium by the laser field. One additional photon ionizes from |1>. Under suitable conditions interference between the two pathways between |0> and |1> can result in the near-total cancellation of the excitation of |1>, and thus of the enhancement of the ionization due to |1>.

due to the laser, and $\Omega_{01}^{(1)}$ is the one-photon Rabi frequency due to the third-harmonic field. $\delta$ is the detuning from three-photon resonance, and $\Delta k_r$ is the phase mismatch between the laser field and the third-harmonic field. As is shown several places in the literature (Refs. 17 and 15, for example), and as will be shown in Chapters II and IV of this dissertation, the contribution from the third-harmonic field has two components: one is a local, adiabatic polarization term, while the other is due to propagating third-harmonic light generated at other (smaller z) locations. The adiabatic term will be found to have the same magnitude as the term due to the laser, but to be $\pi$ out of phase with it, so the adiabatic term cancels the laser. The magnitude of the nonlocal term of the polarization at the third-harmonic frequency will be shown to depend on the magnitude of the absorption at $3\omega_L$ and on the phase mismatch between the laser and the third harmonic. Thus questions concerning resonant enhancement at an odd-photon resonance or the cancellation of the enhancement are really questions about the propagation and absorption of the internally generated odd-harmonic light.

In the case discussed here (three-photon resonant enhancement by a one-photon allowed transition plus ionization by additional photons) there are at least five ways to create an ion: 1) MPI by laser photons enhanced by the intermediate three-photon resonance; 2) MPI by one third-harmonic photon plus additional laser photons; 3) direct MPI due to the non-resonant terms in the susceptibility; 4) wing absorption of a third-harmonic photon by the nearby resonance followed by ionization by laser photons; 5) dissociative absorption of a third-harmonic photon by dimers. Pathway 3) is in general extremely small, since it is unenhanced by any resonances. Dissociative absorption (item 5) is absorption by a dimer (in xenon a Van der Waals molecule) followed by dissociation of the dimer into one ground state atom and one atom in the nearby excited state, followed by ionization of the excited state atom. 1) is the pathway affected (and in fact eliminated) by the three-photon cancellation, while pathways 2), 4) and 5) all involve the absorption of a third-harmonic photon.

# Review of the Literature

The two experiments reported in this dissertation show in different ways the consequences of the complex interaction between applied and internally generated light. A semi-classical treatment of three-photon cancellation is given in Chapter II, where the cancellation effect is shown to form a fundamental part of the three-photon shift effect. Chapter III reports the experimental confirmation of the predictions made in Chapter II. Chapters IV and V deal with the effect of three-photon interference on the excitation of a four-photon resonance. In the remainder of this chapter the principle experimental observations concerning odd-photon cancellation and related effects are reviewed and explained qualitatively in terms of the model just described. Also, a brief overview of the relevant theoretical literature is given.

The first observation of three-photon cancellation came in 1977 when Aron and Johnson[7] reported the absence of a three-photon resonant enhancement peak at the $6s[\frac{3}{2}]_1^O$ level (referred to as the $6s$) in the MPI spectrum of xenon; their work was conducted with xenon pressures of 1 Torr and greater, corresponding to room temperature number densities of $3.2 \times 10^{16}$ cm$^{-3}$ or more, and with a focused, linearly polarized laser. Somewhat later, Compton *et al.*[8] examined the same transition with xenon at lower densities in an atomic beam and found the resonance easily observable. Miller *et al.*[9,10] reported that with a pressure of 0.05 Torr the $6s$ resonance was easily observed; as the pressure was raised the relative magnitude of the on-resonance ionization decreased, becoming undetectable for pressures greater than 0.3 Torr. Cancellation of the three-photon resonance requires the propagating, nonlocal component of the third-harmonic light be made small. For low enough number density the absorption is small; third-harmonic light can propagate over considerable distances and excitation can take place through the absorption of the third-harmonic light plus additional laser photons. At

larger densities, the absorption is strong enough to prevent the growth of much third-harmonic light, so no excitation can occur by that mechanism and the resonance appears canceled.

Glownia and Sander[11] found that excitation of the xenon $6s[\frac{3}{2}]_1^O$ with counterpropagated circularly polarized light showed resonant enhancement. Counterpropagated means that in addition to a laser beam traveling in the $+\hat{z}$ direction there is also a beam traveling in the $-\hat{z}$ direction; this may be accomplished by splitting the beam and directing it into both ends of the cell, or by simply retroreflecting the forward beam back through the cell. Now $\Delta M_J = \pm 1$ for a circularly polarized photon (with the sign depending on the sense of polarization), so three photons all traveling in the same direction require $\Delta M_J = \pm 3$. Thus the J=1 three-photon level cannot be coupled to the J=0 ground state by three photons traveling in one direction. There can be no enhancement by the three-photon level, and also no third-harmonic field. However, two photons from the $+\hat{z}$ direction plus one from the $-\hat{z}$ direction (for example) give $\Delta M_J = \pm 1$ for three photons, so excitation by this counterpropagated pathway can be enhanced by the three-photon level. Although not directly relevent to the demonstration of a method of 'overcoming' the three-photon interference effect (since that effect is absent due to $\Delta M_J$ selection rules), this clever experiment nevertheless shows that normal resonance enhancement can be seen if the three-photon state is coupled to the ground state only by the counterpropagated pathway.

Jackson *et al.*[12,13] found the absent resonant enhancement could also be restored by retroreflecting a linearly polarized laser beam back on itself. This experiment differs from that of Glownia and Sander in that the excitation pathway consisting of three photons all traveling in the same direction is permitted. However, as noted earlier, this copropagated pathway shows no resonant enhancement due to three-photon cancellation. The additional pathway produced by counterpropagating the laser beam has a phase

mismatch given by

$$\Delta k = k_{3\omega} - (2k_{\omega} - k_{\omega}) = k_{3\omega} - k_{\omega}.$$

The explanation accepted at the time (1983) (Ref. 12, but also Ref. 14) was that the phase mismatch for this component of the excitation was so large that very little third-harmonic field would be generated, and thus no cancellation of that excitation pathway could occur. Subsequent work,[4,15,16,17,18,19] some of which is described in Chapters II and III of this dissertation, has shown this explanation to be incorrect.

All the workers mentioned above used focused laser beams for excitation. Three-photon cancellation has also been observed with unfocused excitation,[20] and with other resonances in xenon and in other noble gases ( xenon $6s'[\frac{1}{2}]_1^o$, krypton $5s[\frac{3}{2}]_1^o$, argon $4s[\frac{3}{2}]_1^o$, all Ref. 10). Five-photon cancellation was reported at the xenon $5d[\frac{3}{2}]_1^o$ and argon $5s[\frac{3}{2}]_1^o$ levels in Ref. 21. In all these cases ionization at the wavelength of the resonance was either absent or much reduced from its expected value when unidirectional excitation was employed.

Also reported in Ref. 21 are observations of a five-photon resonant enhancement peak at the argon $3d[\frac{5}{2}]_3^o$ level, produced without counterpropagation of the laser; counterpropagated excitation produced little additional ionization. Since this state is not coupled to the ground state in one photon, there is no resonant enhancement at the frequency of the fifth harmonic. No significant fifth-harmonic field is generated and no interference or cancellation occurs.

So far only on-resonance excitation has been discussed. Discussion of the various off-resonance effects reported requires a more detailed model of phase matching. As noted above, the phase mismatch $\Delta k$ is given by

$$\Delta k = k_{3\omega_L} - 3k_{\omega_L} = \frac{3\omega_L}{c}(n(3\omega_L) - n(\omega_L)). \tag{1.3}$$

In xenon the lowest lying one-photon allowed state is the $6s[\frac{3}{2}]_1^o$ at an energy of 67,068.047 $cm^{-1}$ (corresponding to 8.3 eV). A laser tuned near three-photon resonance

with that state is clearly very far from one-photon resonance with any transition, and so $n(\omega_L)$ is very nearly unity. To calculate $n(3\omega_L)$ one could use equation 1.2 with m = 1 to find the linear susceptibility and thus the index of refraction; since the detuning from three-photon resonance $\delta = 3\omega_L - (E_1 - E_0)/\hbar$ is only a few hundred wavenumbers the summation over off-resonance states is unnecessary, and one merely has to use the Wigner-Eckart theorem to evaluate the matrix element in terms of a reduced matrix element, which itself can be evaluated in terms of an oscillator strength.

A more transparent approach is taken in Ref. 22, sections 2.6.1 and 2.6.2, in which the forced oscillation of a damped classical oscillator of resonant frequency $\omega_{01}$ is solved. The amplitude of the oscillation is then related to the induced dipole moment, from which an index of refraction $n$ may be found. For a detuning $\delta \ll 3\omega_L$ the real part of the index reduces to

$$n = 1 - \frac{\pi N e^2}{(3\omega_L)m} \frac{\delta}{\delta^2 + (\frac{\gamma}{2})^2}.$$

This is equation 2.56b of Ref. 22 written in cgs units and with $\delta = \omega_L - \omega_{01}$; $\gamma$ is the full width at half maximum (FWHM) of the absorption profile of the transition. Weighting the contribution by the resonance to the index of refraction with the absorption oscillator strength $F_{01}$ and assuming $|\delta| \gg |\frac{\gamma}{2}|$, one finds

$$n(3\omega_L) = 1 - \frac{c}{3\omega_L} \frac{\kappa_{01}}{\delta},$$

with

$$\begin{aligned} \kappa_{01} &= \frac{\pi N e^2 F_{01}}{mc} \\ &= \frac{2\pi(3\omega_L)N|D_{01}|^2}{\hbar c} \\ &= 0.0265 N F_{01}. \end{aligned} \tag{1.4}$$

Here $N$ is the number density in $\text{cm}^{-3}$, $D_{01}$ is the electric dipole matrix element between |0> and |1> in esu (so that $|D_{01}|^2$ has units of ergs-$\text{cm}^3$), $e$ is the electron charge, and $\delta$ is in units of radians per second. $\kappa_{01}$ has units of $\text{cm}^{-1}\ \text{s}^{-1}$.

Using equation 1.3 and recalling that $n(\omega_L) \simeq 1$, one finds

$$\Delta k_r \simeq \frac{3\omega_L}{c}(n(3\omega_L) - 1) \simeq -\frac{\kappa_{01}}{\delta}, \tag{1.5}$$

where $\Delta k_r$ indicates the real part of the phase mismatch. Equation 1.5 agrees with forms found in the literature (for example, Ref. 23, equation 20b).

Equation 1.5 shows that one cannot have substantial third-harmonic generation in a pure gas with an unfocused laser beam; $\Delta k$ is large for small detunings, and the resonant enhancement is small for large detunings. Suppose, however, that one were to add to the medium a buffer gas, chosen so that the phase mismatch per unit density due to the buffer gas $\Delta k_b'$ is positive for the frequencies employed. If neither $\omega_L$ nor $3\omega_L$ is too near a one-photon allowed transition in the buffer gas, then $\Delta k_b'$ will be essentially independent of $\delta$, but will depend on the number density $N_b$ of the buffer gas, and

$$\Delta k_r = -\frac{N_a}{\delta}\kappa_{01}' + N_b \Delta k'$$

will give the net phase mismatch. Here $\kappa_{01}' = \kappa_{01}/N_a$ with $N_a$ the number density of the near-resonant gas. By varying the ratio $N_a/N_b$ one can make $\Delta k_r = 0$ for any reasonable positive detuning. Phase matching on the negative detuning side of the resonance would require $\Delta k_b'$ negative; since negative (anomalous) dispersion is found only over a relatively small range of detunings on the high energy side of a resonance, this would require a coincidence nature has not seen fit to provide.

This phase matching mechanism was explored in the experiment reported in Ref. 20. This study was performed at the xenon $6s[\frac{3}{2}]_1^O$ three-photon resonance with an unfocused, linearly polarized laser beam. A variable amount of argon was added to the xenon as a positively dispersive buffer gas. A narrow peak in the ionization could be seen, blue-shifted with respect to the resonance, with the magnitude of the blue shift going as $\delta = CP_A/P_B$, with $P_a, P_b$ the partial pressures of xenon and argon, as predicted by the phase matching model for third-harmonic production described above. This blue-shifted peak is due to ionization by absorption of one third-harmonic photon

plus two additional laser photons; as discussed in Ref. 20, ionization by this pathway is far more likely than direct five-photon MPI. The peak is narrow because substantial amounts of third-harmonic light and thus ionization are produced only in a narrow range of detunings around the phase matching point; the width of the peak is found to vary inversely with the density of near-resonant gas $N_a$. Retroreflection of the laser of course produced an additional ionization peak at the three-photon resonance.

In the study of the xenon $6s[\frac{3}{2}]_1^O$ three-photon resonance reported in Refs. 9 and 10, in which the laser was focused and not retroreflected, a peak in the ionization was observed at a wavelength slightly to the blue of the resonance; the detuning of the blue-shifted peak from three-photon resonance and the width of the peak were both observed to increase with pressure. Also given are tuning profiles of the third-harmonic output which also show a blue shift with increasing pressure; the shift as well as the width of the third-harmonic profiles were found to be linear with pressure. Generally similar behavior was observed at the xenon $6s'[\frac{1}{2}]_1^O$, the krypton $5s[\frac{3}{2}]_1^O$ and the argon $4s[\frac{3}{2}]_1^O$. These results may also be understood in terms of the phase matching behavior of third-harmonic generation.

If a laser beam with diffraction limited divergence and a Gaussian radial intensity distribution is focused it is found[24,22] that the beam area varies as $(1 + (2z/b)^2)$, where z is along the direction of propagation with z = 0 at the position of the focal spot, and $b = kw_0^2 = 2\pi\lambda F^2/w_s^2$ is the confocal parameter in terms of the magnitude of the propagation vector $k$, the radius of the focal spot $w_0$, the wavelength $\lambda$, the focal length $F$, and the radius $w_s$ of the beam at the lens. $b$ is the distance between the points at which the on-axis amplitude has decreased to $1/\sqrt{2}$ of its value at the focal point. The phase of the wavefront has a variation in addition to $\exp(ikz)$ which is given by $\exp(-i\tan^{-1}(2z/b))$, so there is an additional phase shift of $\pi$ as z goes from $-\infty$ to $+\infty$. This position dependent phase shift due to focusing has a profound effect on the generation of third-harmonic light. In Ref. 24 the far-field (large z) intensity of the

third-harmonic light in the absence of absorption is found to be

$$\begin{aligned} I_{3\omega_L} &= -\pi \Delta k_r b \exp\left(\frac{\Delta k_r b}{2}\right) && \Delta k_r < 0 \\ &= 0 && \Delta k_r \geq 0. \end{aligned} \tag{1.6}$$

(This is equation III. 22 of Ref. 24, with some signs changed to agree with the definition of $\Delta k$ used here.) As in the unfocused case, no third-harmonic is generated on the red (positively dispersive) side of the resonance. On the blue side of the resonance the intensity of the third-harmonic depends on the value of $\Delta k_r b$, reaching a maximum at $\Delta k_r b = -4$. Using the previous definition of $\Delta k_r$ one finds

$$\delta_{Max} = N\frac{\kappa'_{01} b}{2}$$

for the relation between number density N and the detuning $\delta_{Max}$ of the peak of the third-harmonic profile; this is just the sort of behavior reported in Ref. 10.

As in the unfocused case discussed previously, ionization by absorption of one third-harmonic photon plus additional laser photons is much more likely than direct MPI by laser photons alone. The shape of the ionization profile as the laser is tuned across the resonance will not, of course, exactly match that of the third-harmonic generation profile, since the enhancement due to the nearby resonance in the rate of ionization by the third-harmonic will vary as $1/\delta^2$.

In the study of Ref. 4 the laser beam was unfocused and retroreflected. This study was conducted to study the broadening and shifting of a resonant transition due to the pressure of the resonant gas. As mentioned earlier, such studies are difficult to perform with one-photon absorption, since the medium becomes essentially opaque to resonant light at even modest pressures. An earlier study[25,26] by other workers employed the reflection method to overcome this difficulty, while in Ref. 4 three-photon resonantly enhanced MPI was employed. The resonance to be studied was three-photon resonant with the laser, with ionization occurring through the absorption of additional laser photons. The laser beam was retroreflected to overcome the three-photon cancellation.

Tuning the laser through three-photon resonance with the transition should produce a peak in the ionization; from the position (in frequency) and width of the ionization peak the pressure shift and broadening of the transition could be found. At four of the five three-photon resonances studied (xenon $6s[\frac{3}{2}]_1^O$, $6s'[\frac{1}{2}]_1^O$, $5d[\frac{3}{2}]_1^O$, and krypton $5s[\frac{1}{2}]_1^O$) a peak was seen, but only at a slightly blue-shifted position, the degree of the shift increasing linearly with pressure. No data on any possible shift was obtained for the remaining resonance (the xenon $7s[\frac{3}{2}]_1^O$) due both to weak signal levels and to an unfavorable combination of oscillator strength and resonance wavelength. Pressure-dependent shifts were, of course, expected, since the energy levels of the atoms are perturbed during collisions. The predicted shift, expressed as a fraction of the predicted pressure-broadened width, was in the range 0.05 to 0.25; the shift was expected to be to the red. In the study described in Refs. 25 and 26 in which one-photon excitation of the transition was employed, a red shift was in fact observed. The shift observed in Ref. 4, however, gave a value of shift to observed width of about 0.5, and was to the *blue*. Neither the magnitude nor the direction of the shift was understood at the time. More recent work[15,16,17,18,19], some of which is described in Chapters II and III of this dissertation, has provided an explanation for this shift in terms of the effect of the badly phase mismatched third-harmonic field produced by two photons from one propagation direction and one from the other direction. In every analysis of the problem previous to those presented in references 19 and 16 the effect of the third-harmonic field had been neglected on the grounds that, being very badly phase matched, it was of negligible intensity. This was, in retrospect, a serious oversight.

A substantial body of literature has been produced to explain these and related observations. Needless to say, all treatments agree in predicting the suppression of on-resonance enhancement for unidirectional excitation, that being the observed phenomena. However, the models employed vary widely in the sophistication and completeness with which the effects of pressure broadening and laser bandwidths and mode structure

are included. The earliest treatments are those due to Payne, Garrett, and Baker[27] (1980) and Payne and Garrett [28] (1982), in which the excitation of a two-level atom simultaneously pumped by a laser field and a self-consistently derived third-harmonic field is found. In Ref. 27 the effects due to focusing the laser are treated only approximately, the $\pi$ phase change being simply imposed on a cylindrical geometry. Ref. 28 treats the problem in an unfocused geometry in a more detailed way, dealing with both excitation by a transform-limited laser and excitation by broad bandwidth, multimode laser light. The pressure dependence of the onset of on-resonance cancellation is found, and found to agree with previously reported experiment, although the experiments were done with focused laser beams. Since the beam is unfocused, making the third harmonic badly phase mismatched for small detunings, little off-resonance excitation due to third-harmonic generation and absorption is predicted.

Jackson and Wynne[13] (1982) and Jackson, Wynne, and Kes[12] (1983) make the same simplifying assumption about the geometry, but do not treat the third-harmonic generation in a self-consistent way, instead simply introducing the perturbation theory result. In addition, they employ a slowly varying amplitude and phase approximation (SVAP) in their calculation of the amplitude of the third-harmonic field which is valid on-resonance only if the pressure-broadened width of the transition is much larger than the laser bandwidth. Thus their model cannot establish the pressure threshold for the onset of the effect. Also, laser bandwidth effects are not considered.

Poirier[29] (1983) gives a treatment of pressure-induced third-harmonic generation in which the laser field is treated classically, while the third-harmonic field is treated quantum mechanically. No account is taken of propagation or other collective effects, and furthermore, it is assumed the system is always phase matched, even at zero detuning. For low densities, Rabi flopping between the ground and excited states is predicted, leading to considerable ionization, since it is only while the population is in the excited state that ionization can occur. At higher densities, the Rabi flopping is suppressed

during the early part of the pulse by 'radiation damping' due to the third-harmonic field, and most of the population remains in the ground state; after some time, the Rabi flopping returns. If the length of the laser pulse is short enough, there is not enough time for the Rabi flopping to begin, resulting in a reduction of ionization for increased density. Thus this model does predict a suppression of the ionization with increased pressure. However, Poirier's model predicts a laser intensity dependence of the onset of cancellation which is not observed. Much more serious, however, is the fact that the experiments described above, in which cancellation is easily observable, employed laser intensities generally thought inadequate to drive Rabi flopping.

Payne and Garrett [14] (1983) give a treatment of the three-photon interference effect for the case of a diffraction-limited, focused Gaussian beam from a broadband, multimode laser. As in their earlier work [27,28], the third-harmonic field is treated self-consistently. They find the third-harmonic field to be the same as it would be in the absence of the interference effect; note that this is a result of their calculations, rather than an assumption as in Refs. 13, 12, and 30.

Wynne [30] (1984), seeking to explain the cancellation effect in terms of more general principles, discusses the problem in terms of a 'renormalization' of the nonlinear polarization. By this he means, evidently, that the adiabatic part of the third-harmonic field (the driven wave, in his terminology) alters the value of the nonlinear polarization in such a way that, in the limit where the dielectric constant (and thus the index of refraction) at the frequency of the third-harmonic is very large compared to the dielectric constant at the laser frequency, the net nonlinear polarization goes to zero. In other words, if there is enough absorption to damp the propagating part of the third-harmonic polarization, and if $n^2(\omega_L) - n^2(3\omega_L)$ is large, then cancellation occurs. In a later work,[31] Wynne attempts to generalize the notion farther, discussing both two-photon cancellation and odd-photon cancellation as examples of 'nonlinear optical balance'. Dissipation in a system of coupled waves in a lossy nonlinear medium is found to provide a mech-

anism for minimizing the net excitation of the medium; the minimization is described as 'robust' since the effect of the dissipation is to return the system to the minimum excitation condition even if the applied excitation is altered.

Agarwal and Tewari[32] (1984) give a fully quantum mechanical treatment for the simultaneous excitation of a two-level atom by both a near three-photon resonant laser and the third-harmonic field, although only in a plane wave approximation, and without including laser bandwidth effects in detail. The treatment is, in general, similar to that of Payne and Garrett[28] (1982). In a later work Tewari[33] (1988) investigates the density dependence of the onset of a collective atomic response. At sufficiently low pressures the atoms interact with the laser and third-harmonic fields independently, while at higher pressures the atoms interact through the third-harmonic field. He finds the transition from one regime to the other to occur when the linear density reaches 250 atoms per wavelength of the fundamental. Finally, Payne *et al.*[23] (1986) give a detailed description for the unfocused geometry which includes effects due to foreign gases, collisions, and dimer absorption.

A fascinating experimental demonstration of the three-photon interference effect is reported by Chen, Yin, and Elliot[34] (1990). Third-harmonic light is generated in Hg vapor using the $6s\,^1S_0 \rightarrow 6p\,^1P_0$ three-photon transition using a focused laser beam at a wavelength of about 554 nm. Both the fundamental and the third harmonic are passed through a cell containing a variable density of Ar and then refocused into a second cell containing Hg vapor at a much lower density than in the first. No significant generation of third-harmonic light is considered to occur in the second cell due to the low Hg density. Ionization is observed in the second cell due to both the three-photon resonant laser field and the one-photon resonant third-harmonic field, plus in each case two additional laser photons. The Ar in the cell between the first and second Hg cells serves as a phase shifter due to the difference in the index of refraction of Ar at the fundamental and third-harmonic frequencies. Variation of the Ar density produces a sinusoidal variation

in the ionization in the second cell which is in excellent agreement with prediction.

This concludes the review of literature pertaining specifically to the three-photon cancellation effect. In summary, with unfocused laser beams no resonant enhancement in the MPI spectrum is observed at a three- and one-photon allowed transition provided the density of the medium is sufficiently high. Counterpropagation of the laser beam is observed to bring back the missing enhancement peak, but careful observation reveals a pressure-dependent blue shift in the position of the resonance line. If the laser is focused, a blue-shifted peak in the ionization spectrum is seen even with unidirectional excitation; as with the unfocused case, the magnitude of the shift increases with increasing number density.

The absence of the resonant enhancement with an unfocused laser is explained by considering the simultaneous coupling of the ground state to the three-photon resonant state by both the internally generated third-harmonic field and by the laser field. If the density of the medium is large enough, then the propagating, non-local part of the third-harmonic field is strongly absorbed, and the remaining, local portion of the polarization at the third-harmonic frequency is found to exactly cancel the excitation of the three-photon state by the laser field. If the laser is focused, phase matching can occur at a blue-side detuning determined by the oscillator strength of the transition, the number density of the medium, and the confocal parameter of the focused beam. Near the phase matched detuning, the propagating third-harmonic light can become intense enough to produce substantial ionization, and thus a peak in the MPI spectrum is seen.

As will be shown in Chapters IV and V of this dissertation, if the three-photon resonant laser is focused a three-photon interference effect can be induced at a detuning closer to resonance than the phase matching point by either absorption of the third harmonic or by a sufficiently large phase mismatch. In Chapter IV a brief review of work relevant to the influence of interference at an intermediate three-photon resonance on the excitation of a four-photon resonance will be given.

# CHAPTER II

## Theory of the Three-photon Shift

In this chapter a semiclassical model for the three-photon excitation of a three- and one-photon allowed transition $|0> \rightarrow |1>$ is developed. As is discussed in Chapter I, under such conditions of excitation a polarization at the sum of the exciting frequencies occurs in the medium; the interaction of the generated and applied fields can cause substantial changes in the atomic response. In the treatment given here ( which follows closely that given in Ref. 16 ) the three-photon excitation is by two unfocused laser beams of different wavelengths. The frequencies $\omega_1$ and $\omega_2$ are chosen so that two photons of frequency $\omega_1$ from one beam plus one photon of frequency $\omega_2$ from the other beam are nearly resonant with the $|0> \rightarrow |1>$ transition, while neither $\omega_1$ nor $\omega_2$ is near three-photon resonance with the $|0> \rightarrow |1>$ transition; it is assumed that neither $\omega_1$ nor $\omega_2$ nor any combination of $\omega_1$ and $\omega_2$ (aside from $2\omega_1 + \omega_2$) is near resonance with any allowed transition. With such a combination of wavelengths excitation will occur only in the region where the beams intersect; it is then possible to introduce an angle $\theta$ between the beams and study only the ionization resulting from excitation at the angle $\theta$. This generalizes the situation discussed in Chapter I, in which parallel and anti-parallel (unidirectional and counterpropagated) excitation was found to produce radically different atomic responses (in the parallel case no on-resonance excitation; in the anti-parallel case excitation, but with a shift).

In Refs. 18 and 19 Friedberg, Hartmann, and Manassah present a derivation of the principle results given here by using a susceptibility based treatment. Ref. 19 is restricted to the collinear ($\theta = \pi$) case, while Ref. 18 treats the more general case of

non-collinear excitation. Though more complex, the treatment presented in Refs. 16, 15, and here provides a better insight into the interaction of the laser fields and the internally generated field which is responsible for the angle- and pressure-dependent three-photon shift.

## Description of the Model

The model developed here will use a two-state basis (illustrated in Fig. 3) consisting of the ground state $|0>$ and the excited state $|1>$; dipole transitions between $|0>$ and $|1>$ are assumed to be allowed with both one and three photons. Transitions from $|1>$ to the continuum will be represented by an ionization rate $\Gamma_I$. The effect of all the other states in the atom on the three-photon excitation of $|1>$ will be represented in terms of a reduced three-photon Rabi frequency $\Omega_{01}^{(3)}$; a reduced Rabi frequency, as defined here, is simply half the Rabi frequency as normally defined. ac Stark shifts will be neglected. In Fig. 3 $\delta_1 = 2\omega_1 + \omega_2 - (E_1 - E_0)/\hbar$ is the detuning from three-photon resonance; here $E_1$ is the energy of state $|1>$ and $E_0$ that of state $|0>$. Both lasers are assumed to be linearly polarized with the directions of polarization parallel. In Fig. 4 the geometry of the pumping scheme is illustrated; $\theta$ is the angle between the two laser beams. For convenience the $+\hat{z}$ direction is taken along $\vec{k}_M = 2\vec{k}_1 + \vec{k}_2$, where $\vec{k}_1$ and $\vec{k}_2$ are the propagation vectors for light at frequencies $\omega_1$ and $\omega_2$. In general the subscript $M$ (as in $\omega_M$, $\lambda_M$, $k_M$, *etc.* ) will indicate the quantity has to do with the mixing frequency, wavelength, propagation vector, and so forth. Now $k(\omega) = \omega n(\omega)/c$, but for the situation under consideration, with $\omega_1$ and $\omega_2$ far off resonance with any one-photon allowed transition, $n(\omega) = 1$ to good accuracy, so $k_i = \omega_i/c$ with $i = 1, 2$. Note that $k = 2\pi/\lambda$, where $\lambda$ is the wavelength. The number density $N$ of the nonlinear medium is assumed large enough to permit making an adiabatic-following approximation in the calculation of the atomic response, and to provide rapid enough off-diagonal relaxation to

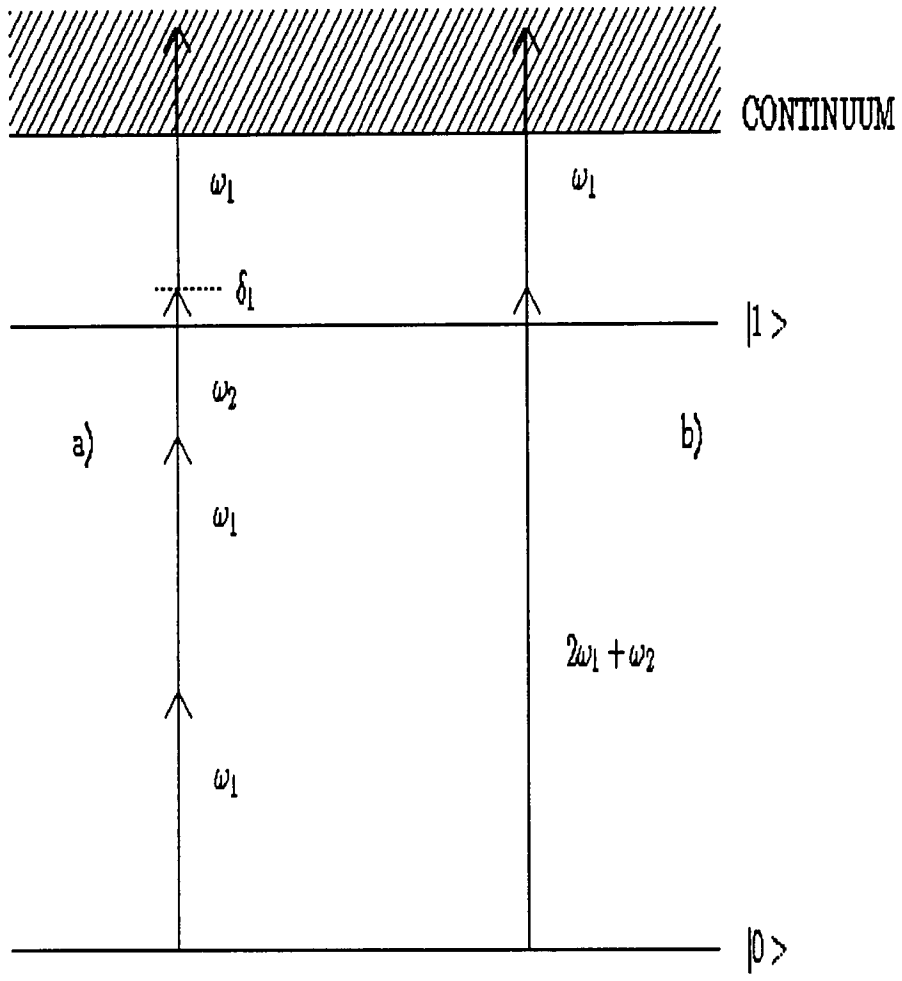


Figure 3. Three-photon Excitation and Sum-frequency Generation

State |1> (the xenon $5d[\frac{3}{2}]_1^O$) is coupled to the ground state |0> by a) two photons of frequency $\omega_1$ (corresponding to $\lambda_1 \simeq 2920$ Å) plus one of frequency $\omega_2$ ($\simeq 6500$ Å), and b) the sum frequency $\omega_M = 2\omega_1 + \omega_2$. The detuning from three-photon is resonance is $\delta_1 = 2\omega_1 + \omega_2 - (E_1 - E_0)/\hbar$.

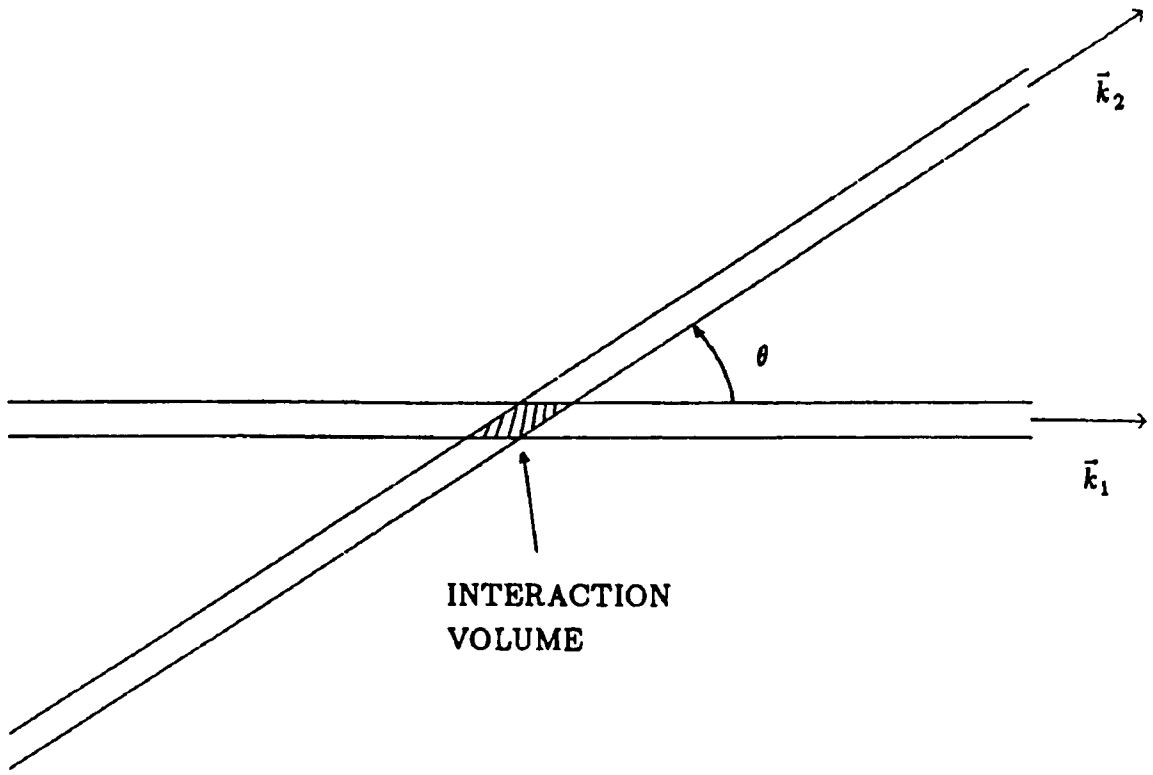


Figure 4. Geometry of the Pumping Scheme

The interaction region is the intersection of beam 1 of frequency $\omega_1$ and propagation vector $k_1 = \omega_1 n(\omega_1)/c$ and beam 2 of frequency $\omega_2$ and propagation vector $k_2 = \omega_2 n(\omega_2)/c$. $\theta$ is the angle between the beams, and $\vec{k}_M = 2\vec{k}_1 + \vec{k}_2$ is the resultant propagation vector.

make valid what is essentially a rate equation treatment. Furthermore, it is assumed that very little population is transferred from the ground state. With the number densities ($N \geq 1.6 \times 10^{18}$ cm$^{-3}$) and laser intensities ($I_{Laser} \approx 10^8$ Watts/cm$^2$ or less) employed in the experiment described in Chapter III these assumptions and approximations are perfectly valid.

A density matrix treatment will be employed. The density matrix operator is given by $\rho = \ll \Psi\Psi^{\dagger} \gg$, where $\Psi$ is the state vector, the superscript $^{\dagger}$ indicates the Hermitian adjoint, and $\ll \gg$ indicates an ensemble average. The expectation value of an operator $Q$ will then be found to be $\ll Q \gg = Tr(\rho Q)$, where $Tr$ indicates the trace. The equation of motion for the density matrix is given by

$$i\hbar \frac{\partial \rho}{\partial t} = [\mathcal{H}, \rho] - i\hbar \left( \frac{\partial \rho}{\partial t} \right)_{Relax}, \tag{2.1}$$

where $\mathcal{H}$ is the Hamiltonian and $[A, B] = AB - BA$ is the commutator of the operators $A$ and $B$. The term $\left(\frac{\partial \rho}{\partial t}\right)_{Relax}$ on the right hand side of equation 2.1 allows the inclusion of non-energy conserving relaxation mechanisms such as ionization. Such processes correspond to a non-Hermitian part of the Hamiltonian which may be evaluated using $\mathcal{H}\rho - \rho\mathcal{H}^{\dagger}$ instead of the commutator. A density matrix formulation is most useful in nonlinear optics for treating problems where either laser bandwidth effects or the effects of collisional perturbations must be taken into account. To deal with the effect of a broadband, multimode laser the ensemble average would be taken over the time history of the laser pulse (expressed in terms of the autocorrelation function describing the laser statistics). Collisional effects may be included by taking the ensemble average over interatomic distances and including in $\mathcal{H}$ an interatomic potential term. In the problem at hand, in which the pressure-broadened width of the $|0> \rightarrow |1>$ transition is assumed larger than the laser bandwidth, the lasers may be assumed to have transform limited bandwidths without loss of generality, and bandwidth effects can be ignored. Collision effects, however, cannot be eliminated from the model, since they contribute both a shift in the energy of the transition and a pressure-broadened width. Nevertheless, explicit

calculations of these quantities will not be given here, as they are unrelated to the topic under discussion, and somewhat complicated; the collisional shift and width will merely be introduced phenomenologically where appropriate. Another reason for using a density matrix approach (the principal reason here) is that it makes calculation of the polarization somewhat more straightforward than the alternative approach of applying Schrödinger's equation to the state vector directly.

## Solution for the Excitation

The wavefunction $\Psi$ for the two-state model is written in the Schrödinger representation as

$$\Psi(z,t) = a_0(z,t)e^{-i\omega_0 t}|0> + a_1(z,t)e^{-i\omega_1 t}|1>, \tag{2.2}$$

where $a_0$ and $a_1$ are the amplitudes of $|0>$ and $|1>$, and the rapid part of the time dependence has been written explicitly. $|0>$ and $|1>$ are eigenstates of the Hamiltonian $\mathcal{H}_0$ of the unperturbed atom, so that

$$\mathcal{H}_0|i> = \hbar\omega_i|i>, \qquad i = 0, 1. \tag{2.3}$$

Treating the combined effect of the lasers and the sum-frequency field as a time-dependent perturbation $V = -\hat{\mathcal{D}} \cdot \vec{E}$, where $\hat{\mathcal{D}}$ is the electric dipole operator and $\vec{E}$ is the electric field, and defining $\mathcal{H}^{(eff)} = \mathcal{H}_0 + V$, one finds

$$\begin{aligned}\mathcal{H}^{(eff)} =& \hbar\omega_0|0><0| + \hbar\omega_1|1><1| + \\ & V_{01}|0><1| + V_{10}|1><0| - i\hbar\frac{\Gamma_I}{2}|1><1|,\end{aligned} \tag{2.4}$$

where the non-Hermitian term allows for ionization from state $|1>$, and $V_{ij} = <i|V|j>$. Here $\Gamma_I = \sigma_I(\omega_1)F_1 + \sigma_I(\omega_2)F_2$ is the ionization rate from state $|1>$ in terms of the

photoionization cross-sections $\sigma_I(\omega)$ and photon fluxes $F_1$ and $F_2$ at frequencies $\omega_1$ and $\omega_2$. In the experiment to be described the excited state $|1>$ can be ionized by one photon of either color, but $E_1 + \hbar\omega_2$ is just slightly above the first I.P. for xenon, while the corresponding quantity involving $\omega_1$ is far above threshold; as a result, the photoionization cross-section $\sigma_I(\omega_2)$ is much larger than $\sigma_I(\omega_1)$.

The components of $\rho$ are

$$\rho(z,t) = \begin{pmatrix} a_0 a_0^* & a_0 a_1^* e^{i\omega_{10}t} \\ a_1 a_0^* e^{-i\omega_{10}t} & a_1 a_1^* \end{pmatrix}, \tag{2.5}$$

where $a_0^*$ indicates the complex conjugate of $a_0$, and $\omega_{10} = (E_1 - E_0)/\hbar$. Then the equations of motion for the components of the density matrix are

$$\begin{aligned} \frac{\partial \rho_{00}}{\partial t} &= -2\, Im(V_{10}\rho_{01}/\hbar), \\ \frac{\partial \rho_{01}}{\partial t} &= -i\frac{V_{01}}{\hbar}(\rho_{11} - \rho_{00}) \\ &\quad + i[\omega_{10} + \Delta_{bl} + i(\Gamma_P + \Gamma_i/2)]\rho_{01}, \\ \frac{\partial \rho_{11}}{\partial t} &= 2\, Im(V_{10}\rho_{01}/\hbar) - \Gamma_I \rho_{11}. \end{aligned} \tag{2.6}$$

$Im$ indicates the imaginary part. Since $\rho_{10} = \rho_{01}^*$ there is no need to consider the equation for $\rho_{10}$. Here $\Gamma_P$ is the half-width at half maximum of the pressure broadened line, and $\Delta_{bl}$ is a small pressure-dependent blue shift in the resonant frequency due to the transfer of coherence in collisions between excited and ground-state atoms. $\Gamma_P$ and $\Delta_{bl}$ have been introduced phenomenologically. Defining $\kappa_{01}$ as before to be

$$\kappa_{01} = \frac{2\pi\omega_M N |D_{01}|^2}{\hbar c}, \tag{2.7}$$

where $\omega_M = 2\omega_1 + \omega_2$, $N$ is the number density of the medium, and $D_{01}$ is the dipole matrix element between $|0>$ and $|1>$, one has

$$\begin{aligned} \Delta_0 &= \frac{\kappa_{01}\lambda_M}{4\pi} \\ \Gamma_P &= 2.33\Delta_0, \\ \Delta_{bl} &= 0.22\Delta_0. \end{aligned} \tag{2.8}$$

Here $\lambda_M = 2\pi c/\omega_M$ is the vacuum wavelength of the sum-frequency light. The value given for $\Gamma_P$ is found in the impact theory limit for the self-broadening of a resonance transition. The impact theory of pressure broadening is discussed briefly later in this chapter; for a more extensive, yet elementary discussion see chapter 10 of Ref. 35. Values similar to that used for $\Delta_{bl}$ have been found by several workers[36,37,38]. The physical origin of this shift is the transfer of coherence in collisions between an excited state atom and a ground state atom in which the excitation is transferred. Due to the coherence between the atomic wavefunctions the dipole-dipole potential between the atoms is repulsive, and so leads to a blue shift in the energy of the transition. In the experiment to be described in Chapter III the transition of interest is the xenon $5p^6 \rightarrow 5d[\frac{3}{2}]_1^O$ with an energy $\hbar\omega_{10}$ of 83890.47 $cm^{-1}$, so $\lambda_M \approx 1192$ Å. Using $\kappa_{01} = 0.0265 N F_{01}$ with $F_{01} \approx 0.35$ and $N = 3.23 \times 10^{16}$ $cm^{-3}$ per Torr at 300 K, one finds $\kappa_{01} = 3 \times 10^{14}$ $Torr^{-1}$ $cm^{-1}$ $s^{-1}$. So for a pressure of 100 Torr, $\Delta_0 = 2.85 \times 10^{10}$ radians per second, $\Gamma_P = 6.65 \times 10^{10}$ radians per second, corresponding to a FWHM of 0.7 $cm^{-1}$, and $\Delta_{bl}$ is only 0.03 $cm^{-1}$.

Evaluating $V_{01}$ using techniques described in chapters 4 and 9 of Ref. 39 one finds

$$\begin{aligned} \frac{V_{01}}{\hbar} &= -\Omega_{01}^{(3)} e^{i\omega_M t} e^{-ik_M z} - \frac{D_{01} E_0^L}{2\hbar} e^{i\omega_M t}, \\ &= -( \Omega_{01}^{(3)} + \Omega_{01}^{(1)} e^{-i\Delta k_r z} ) e^{-ik_M z} e^{i\omega_M t}, \end{aligned} \tag{2.9}$$

where $E_0^L$ is the amplitude of the local sum-frequency mixing field described by

$$\begin{aligned} E_M^L &= \frac{1}{2} [\, E_0^L e^{i\omega_M t} + \ c.c. \,], \\ &= \quad E_M^{L+} + E_M^{L-}, \end{aligned} \tag{2.10}$$

$\Omega_{01}^{(3)}$ is the reduced three-photon Rabi frequency due to the laser fields, and

$$\Omega_{01}^{(1)} = \frac{D_{01} E_0^L}{2\hbar} e^{i(k_M + \Delta k_r)z} \tag{2.11}$$

is the reduced one-photon Rabi frequency due to the sum-frequency field. In equation 2.11 $\Delta k_r$ is the real part of the phase mismatch.

To evaluate the magnitude of $k_M$ one merely applies the cosine formula $k_M^2 = (2k_1)^2 + k_2^2 - 2(2k_1)k_2\cos(\phi)$ to the triangle formed by $2k_1$, $k_2$ and $k_M$, where $\phi$ is the interior angle between the vectors $2k_1$ and $k_2$. Then using $(2k_1 + k_2)^2 = 4k_1^2 + k_2^2 + 4k_1k_2$ and $\cos(\theta) = 1 - 2\sin^2\left(\frac{\theta}{2}\right)$, with $\theta = \pi - \phi$ being the angle between the propagation directions of the beams, one finds

$$k_M^2 = (2k_1 + k_2)^2\left[1 - \frac{8k_1k_2}{(2k_1 + k_2)^2}\sin^2\left(\frac{\theta}{2}\right)\right]. \tag{2.12}$$

What is desired in this analysis is the ionization rate as a function of the detuning from three-photon resonance, the angle between the laser beams, and the other parameters in the problem. The ionization rate from state $|1>$ is simply proportional to the population of $|1>$, which is given by $\rho_{11} = a_1a_1^*$. The third of equations 2.6 shows that the driving term for $\rho_{11}$ is the imaginary part of $V_{10}\rho_{01}$. Equation 2.9 shows $V_{01}$ to depend upon the three-photon Rabi frequency due to the lasers, which is treated as known, and upon the one-photon Rabi frequency due to the sum-frequency field, which is to be determined. As will be shown, the intensity of the sum-frequency field depends on the induced nonlinear polarization, which depends on $\rho_{01}$. But the second of equations 2.6 shows $\rho_{01}$ to depend on $V_{01}$. Clearly, a self-consistent solution of the problem requires solving simultaneously for $\rho_{01}$ and $V_{01}$.

The solution will proceed as follows. The strength of the sum-frequency field will be found in terms of $\rho_{01}$, taking into account propagation effects and the phase mismatch. The expression so derived will be used to eliminate the sum-frequency field from the expression for $\frac{\partial\rho_{01}}{\partial t}$, yielding an integro-differential equation which will be solved in the adiabatic limit for $\rho_{01}$. An expression for the excitation will then follow almost directly.

An atom at position $z_1$ will interact with two optical-frequency fields: that due to the lasers, and that due to the sum-frequency generation occurring not only at $z_1$ but at all other values of $z$ in the interaction region. The propagation of the sum-frequency light is described by a wave equation derived from Maxwell's equations with the polarization as a source term. Maxwell's equations describe the behavior of macroscopic (space

averaged) fields, while the fields which appear in equations 2.9 and 2.10 are microscopic (local) fields. For the laser fields at frequencies $\omega_1$ and $\omega_2$ this distinction is irrelevant: $\omega_1$ and $\omega_2$ are by assumption far off-resonance with any atomic transition, and so the polarization occurring at frequencies $\omega_1$ and $\omega_2$ is negligibly small. The polarization induced at $\omega_M = 2\omega_1 + \omega_2$ is not negligibly small, however, since $\omega_M \simeq \omega_{10}$, and the local and space-averaged fields are not the same. To relate the two one uses the Lorenz-Lorentz approximation in the form

$$E_M^{L+} = E_M^+ + \frac{4\pi}{3}\mathcal{P}_M^+. \tag{2.13}$$

Here $E_M^{L+}$ is the positive-frequency part of the local sum-frequency field, $E_M^+$ is the positive-frequency part of the space-averaged sum-frequency field described by

$$\begin{aligned} E_M &= \frac{1}{2}\left[E_0 e^{i\omega_M t} + c.c\right], \\ &= E_M^+ + E_M^-, \end{aligned} \tag{2.14}$$

and $\mathcal{P}_M^+$ is the positive frequency part of the polarization at $\omega_M$. Since $\omega_{10} \approx \omega_M$, the polarization is dominated by the contribution of the nearby $|0> \rightarrow |1>$ transition. In order to treat this resonant contribution in the proper degree of detail, the polarization is divided into a resonant and a nonresonant part, so $\mathcal{P}_M = \mathcal{P}_M^{RES} + \mathcal{P}_M^{NR}$, where $\mathcal{P}_M^{NR}$ is the nonresonant contribution due to all the far off-resonance transitions from the ground state. Since polarization is the total induced dipole moment per unit volume, the resonant contribution to the polarization $\mathcal{P}_M^{RES}$ due to the amplitude of state $|1>$ will be given by

$$\mathcal{P}_M^{RES} = N\,Tr(\hat{\rho}\hat{D}), \tag{2.15}$$

with $\hat{D}$ the electric dipole operator and $N$ the number density of the nonlinear medium. Equation 2.15 may be evaluated using equation 2.5 and $\hat{D}_{ij} =< i|D|j >$ to find

$$\mathcal{P}_M^{RES\,+} = N\rho_{01}D_{10}. \tag{2.16}$$

Then

$$\mathcal{P}_M^+ = \chi_0 E_M^{L+} + N\rho_{01}D_{10}, \tag{2.17}$$

where $\chi_0$ is the linear susceptibility at frequency $\omega_M$ due to all the resonance transitions in the atom *except* $|0> \rightarrow |1>$; this is added as a correction to account for the effect on the index of refraction of all the resonance transitions which are not included in the truncated two-state basis employed. Since $\omega_M$ is far off-resonance for these transitions, $\chi_0$ will be very small.

Substituting equation 2.17 in equation 2.13 and neglecting $\frac{4\pi}{3}\chi_0$ with respect to 1 gives

$$E_M^{L+} = E_M^+ + \frac{4\pi}{3}N\rho_{01}D_{10}, \tag{2.18}$$

which, when substituted in 2.9, and using $D_{01}D_{10} = |D_{01}|^2$, produces

$$\frac{V_{01}}{\hbar} = -\frac{D_{01}E_M^+}{\hbar} - \frac{4\pi}{3\hbar}N|D_{01}|^2\rho_{01} - \Omega_{01}^{(3)}e^{i\omega_M t}e^{-ik_M z}. \tag{2.19}$$

It remains to solve for $E_M^+$ in terms of the off-diagonal element of the density matrix; that is, the field at the sum frequency $\omega_M$ at a position $z$ must be determined from Maxwell's equations and the polarization at $\omega_M$. Maxwell's equations [2] are

$$\begin{aligned}
\nabla \cdot \vec{E} &= 4\pi\rho_{CHARGE} \\
\nabla \cdot \vec{B} &= 0 \\
\nabla \times \vec{E} &= -\frac{1}{c}\frac{\partial \vec{B}}{\partial t} \\
\nabla \times \vec{B} &= \frac{1}{c}\frac{\partial \vec{E}}{\partial t} + \frac{4\pi}{c}\vec{J}
\end{aligned} \tag{2.20}$$

where $\rho_{CHARGE}$ is the charge density and $\vec{J} = \vec{J}_{DC} + \dot{\vec{\mathcal{P}}}$ is the current density expressed in terms of a DC current (which is 0 here) and a displacement current due to the time variation of the polarization.[2] Taking the partial with respect to time of the last of equations 2.20 and using the third of equations 2.20 and the definition of $J$ gives

$$\nabla \times \nabla \times \vec{E} + \frac{1}{c^2}\frac{\partial^2 \vec{E}}{\partial t^2} = -\frac{4\pi}{c^2}\frac{\partial^2 \vec{\mathcal{P}}}{\partial t^2}. \tag{2.21}$$

Using the identity $\nabla \times \nabla \times \vec{E} = \nabla(\nabla \cdot \vec{E}) - \nabla^2 \vec{E}$ and the first of equations 2.20 with $\rho_{CHARGE} = 0$, one finds

$$\nabla^2 \vec{E} - \frac{1}{c^2}\frac{\partial^2 \vec{E}}{\partial t^2} = \frac{4\pi}{c^2}\frac{\partial^2 \vec{\mathcal{P}}}{\partial t^2}. \tag{2.22}$$

Now $\vec{E}_M$ will have a rapid spatial dependence given by $e^{-ik_M z}$ in the $\hat{z}$ direction, while the variation in the transverse directions will be much slower, occurring on a length scale determined largely by the diameters of the laser beams, and so the transverse components of $\nabla^2 \vec{E}_M$ may be neglected to give

$$\frac{\partial^2 E_M^+}{\partial z^2} - \frac{1}{c^2}\frac{\partial^2 E_M^+}{\partial t^2} = \frac{4\pi}{c^2}\frac{\partial^2 \mathcal{P}_M^+}{\partial t^2}. \tag{2.23}$$

To find $\mathcal{P}_M^+$ in terms of $E_M^+$ one uses equation 2.17, substituting the value of $E_M^{L+}$ from equation 2.13, and again using $1 \simeq 1 - \frac{4\pi}{3}\chi_0$. One finds

$$\mathcal{P}_M^+ = \chi_0 E_M^+ + N\rho_{01} D_{10}. \tag{2.24}$$

Substituting this equation into 2.23, collecting terms in $\frac{\partial^2 E_M^+}{\partial t^2}$ on the left hand side, and defining $v_1^2 = c^2/(1 + 4\pi\chi_0)$ gives

$$\frac{\partial^2 E_M^+}{\partial z^2} - \frac{1}{v_1^2}\frac{\partial^2 E_M^+}{\partial t^2} = \frac{4\pi}{c^2} N D_{01}\frac{\partial^2 \rho_{01}}{\partial t^2}. \tag{2.25}$$

Note that $v_1$ is not the phase velocity $v(\omega_M) = c/n(\omega_M)$ of freely propagating light at $\omega_M$. Near a one-photon resonance $n$ differs substantially from one, and $v_{PHASE} \neq c$; rather, $v_1 \simeq c$.

As is noted in Ref. 23, a wave equation of the form

$$\frac{\partial^2 Y(z,t)}{\partial z^2} - \frac{1}{v^2}\frac{\partial^2 Y(z,t)}{\partial t^2} = \frac{\partial g(z,t)}{\partial t} \tag{2.26}$$

is solved for the interval $0 \leq z \leq L$ and the boundary condition $Y(0,t) = 0$ by

$$Y(z,t) = -\frac{v}{2}\int_0^L g(z', t - \frac{|z - z'|}{v})\, dz'. \tag{2.27}$$

Thus equation 2.25 has the solution

$$E_M^+ = -\frac{v_1}{2}\frac{4\pi}{c^2}ND_{10}\int_0^L dz'\frac{\partial\rho_{01}}{\partial t}\left(z', t - \frac{|z-z'|}{v_1}\right). \tag{2.28}$$

Using the second of equations 2.6, and recognizing that by far the largest time dependence is that involving $\omega_{10}$, one finds $\frac{\partial\rho_{01}}{\partial t} \simeq i\omega_M\rho_{01}$, where the further approximation $\omega_M \simeq \omega_{10}$ has been made. Using this to substitute for the partial of $\rho_{01}$ with respect to $t$ in equation 2.28, and recalling that $v_1 \simeq c$, equation 2.19 becomes

$$\frac{V_{01}}{\hbar} = i\kappa_{01}\int_0^L \rho_{01}\left(z', t - \frac{|z-z'|}{v_1}\right)dz' - \Omega_{01}^{(3)}e^{i\omega_M t}e^{-ik_M z} - \frac{4}{3}\Delta_0\rho_{01}, \tag{2.29}$$

where various parameters have been grouped into $\kappa_{01}$ and $\Delta_0$, which are defined in equations 2.7 and 2.8.

With the assumption that very little population is transferred either to state $|1>$ or to the continuum, $\rho_{00} \simeq 1$ and $\rho_{11} \simeq 0$, and the substitution of 2.29 into the second of equations 2.6 gives

$$\begin{aligned}\frac{\partial\rho_{01}}{\partial t} &= \frac{iV_{01}}{\hbar} + i\left[\omega_{10} + \Delta_{bl} + i(\Gamma_P + \frac{\Gamma_I}{2})\right]\rho_{01} \\ &= -\kappa_{01}\int_0^L \rho_{01}\left(z', t - \frac{|z-z'|}{v_1}\right)dz' - i\Omega_{01}^{(3)}e^{i\omega_M t}e^{-ik_M z} \\ &\quad + i\left[\omega_{10} + \Delta_{bl} + i(\Gamma_P + \frac{\Gamma_I}{2}) - \frac{4}{3}\Delta_0\right]\rho_{01}.\end{aligned} \tag{2.30}$$

The real terms inside the bracket multiplying $\rho_{01}$ in the last line in equation 2.30 give the frequency of the coupling, while the imaginary terms give the width, so one may define

$$\begin{aligned}\Delta_P &= \Delta_{bl} - \frac{4}{3}\Delta_0 \\ &= \Delta_0\left(a - \frac{4}{3}\right) \qquad \text{with } a = 0.22, \\ \Delta_T &= \Delta_P + i\Gamma_P.\end{aligned} \tag{2.31}$$

Here $\Delta_P$ is the sum of the shift due to collisional transfer of coherence and the Lorenz-Lorentz shift. In the last line of equation 2.31 $\Gamma_I$ has been neglected, since the width due

to pressure broadening is much larger than the power broadening due to the transition $|1> \rightarrow |Continuum>$.

Now define a new variable $S$ which retains only the slowly varying temporal and spatial dependencies in $\rho_{01}$:

$$S(z,t) = e^{-i\omega_M t} e^{ik_M z} \rho_{01}(z,t) \tag{2.32}$$

Taking $\frac{\partial S}{\partial t}$ and using the definition of $\Delta_T$ from equation 2.31 gives for equation 2.30

$$\begin{aligned}
&\left(\frac{\partial S(z,t)}{\partial t} + i\omega_M S(z,t)\right) e^{i\omega_M t} e^{-ik_M z} = \\
&- \kappa_{01} \int_0^L S\left(z', t - \frac{|z-z'|}{v_1}\right) \exp(-ik_M z) \exp(i\omega_M (t - \frac{|z-z'|}{v_1})) dz' \\
&- i\Omega_{01}^{(3)} e^{i\omega_M t} e^{-ik_M z} \\
&+ i[\omega_{10} + \Delta_T] e^{i\omega_M t} e^{-ik_M z} S(z,t).
\end{aligned} \tag{2.33}$$

Collecting terms in $S$, using $\delta_1 = \omega_M - \omega_{10}$, and dividing through by $e^{i\omega_M t} e^{-ik_M z}$ one finds

$$\begin{aligned}
\frac{\partial S(z,t)}{\partial t} = &-i[\delta_1 - \Delta_T] S(z,t) - i\Omega_{01}^{(3)} \\
&- \kappa_{01} \int_0^L S\left(z', t - \frac{|z-z'|}{v_1}\right) \exp\left(ik_M (z-z')\right) \exp\left(-i\omega_M \frac{|z-z'|}{v_1}\right) dz'
\end{aligned} \tag{2.34}$$

The change of variables from $\rho_{01}$ to $S$ has indeed produced an expression for $S$ which contains no rapid time dependence. Note that since $\mathcal{P}_M^{RES+} = N\rho_{01} D_{10}$ (equation 2.16), equation 2.34 is essentially an equation for the polarization of the medium.

If the lasers are tuned so that $|\delta_1 - \Delta_T| \gg \Gamma_L$, where $\Gamma_L$ is the effective three-photon laser bandwidth, then no real population can be created in state $|1>$, and the polarization (which is $\propto a_0 a_1^*$) will simply follow the temporal variation in the amplitude of the laser field; $\frac{\partial S}{\partial t}$ will then be very small. Setting $\frac{\partial S}{\partial t} \equiv 0$ is an adiabatic approximation. Note that the minimum value of $|\delta_1 - \Delta_T|$ is $\Gamma_P$, corresponding to $\delta_1 = \Delta_P$. The pressure-broadened line width $\Gamma_P$ corresponds to a loss of phase memory in the coherence between

states $|0>$ and $|1>$ in a time $\tau_C \approx 1/\Gamma_P$. If $\tau_C \ll \tau_L$, where $\tau_L$ is the duration of the laser pulse, then the polarization at a particular time in the laser pulse will depend mainly on the laser amplitude at that particular time, and very little on its value earlier in the pulse, so again the polarization will have just the time dependence of the laser. Thus if $\Gamma_P \gg \Gamma_L$ the adiabatic approximation is valid even for on-resonance excitation. A discussion of the adiabatic approximation is found in Ref. 3, section 2.6.1. (An interesting application of the three-photon interference effect to the direct measurement of collisional dephasing rates (albeit in the $5p^6 \rightarrow 6s$ and $5p^6 \rightarrow 6s'$ transitions in xenon) is described in Ref. 51.) With $\frac{\partial S}{\partial t} \equiv 0$, equation 2.34 becomes

$$S(z,t) = -\frac{\Omega_{01}^{(3)}}{(\delta_1 - \Delta_T)} + \frac{i\kappa_{01}}{(\delta_1 - \Delta_T)} \int_0^L S\left(z', t - \frac{|z-z'|}{v_1}\right) \exp(ik_M(z-z')) \exp\left(-i\omega_M \frac{|z-z'|}{v_1}\right) dz'. \tag{2.35}$$

Solution of equation 2.35 proceeds by assuming a trial solution of the form

$$S = S_0 + S_1 e^{p_1 z} + S_2 e^{p_2 z} \tag{2.36}$$

with $S_0$, $S_1$, $S_2$, $p_1$, and $p_2$ constant, substituting it into 2.35, and then finding the conditions (if any) under which the trial solution is correct. The form of the trial solution is suggested by the observation that, since $\omega_M \approx \omega_{10}$ and the oscillator strength $F_{01}$ is assumed not to be too small, the absorption length for the sum-frequency light should be much less than the length of the interaction region $L$, and so the polarization (and thus $S$) should be independent of $z$. The exponential terms allow for effects within a few absorption lengths of the ends of the interaction region. The apparent time independence of 2.36 is due to the adiabatic approximation, which assumes all the time dependence in $S$ is due to $\Omega_{01}^{(3)}(t)$. The details of solving equation 2.35 by this method will not be presented here; the process is lengthy, quite tedious, and, with the exception of revealing the conditions under which a solution of the form of equation 2.36 is valid, provides no insight whatsoever into the physics.

Substituting equation 2.36 into 2.35 and equating the $z$ independent terms gives, after some manipulation,

$$S_0 = \frac{-\Omega_{01}^{(3)}}{[\delta_1 - \Delta_T] + \kappa_{01}\frac{2\omega_M/v_1}{k_M^2-(\omega_M/v_1)^2}}, \tag{2.37}$$

which, with the use of equation 2.12 and the approximation $v_1 \approx c$, yields

$$S_0 = \frac{-\Omega_{01}^{(3)}}{[\delta_1 - \Delta_T] - \frac{\kappa_{01}}{4\pi}\frac{2\lambda_2+\lambda_1}{1-\cos(\theta)}}. \tag{2.38}$$

Here $\lambda_1$ and $\lambda_2$ are the laser wavelengths and $\theta$ is the angle between the laser beams.

To evaluate $p_1$ and $p_2$, equate the coefficients of $\exp(p_1 z)$ (or $\exp(p_2 z)$) to find an expression quadratic in $p_1$ or $p_2$; one solution is $p_1$ and the other is $p_2$. Defining for later convenience $p_\pm = im_\pm$, one finds

$$m_\pm = k_M \pm \frac{\omega_M}{v_1}\left(1 - \frac{2\kappa_{01}v_1}{(\delta_1 - \Delta_T)\omega_M}\right)^{\frac{1}{2}} \tag{2.39}$$

The proper identification of $m_+$ and $m_-$ with $p_1$ and $p_2$ will become clear a bit later.

$S_1$ and $S_2$ are determined using the remaining terms in the expression resulting from substituting equation 2.36 into equation 2.35. If $Re(p_1 L) \ll 0$

$$S_2 = S_0\left(\frac{p_2}{i(k_M + \omega_M/v_1)} - 1\right)e^{-p_2 L}, \tag{2.40}$$

and, if $Re(p_2 L) \gg 0$

$$S_1 = S_0\left(\frac{p_1}{i(k_M - \omega_M/v_1)} - 1\right). \tag{2.41}$$

Now $Re(pL) \ll 0$ implies $Im(mL) \gg 0$; as will be shown later, this implies $p_1 = im_-$. This slightly inobvious result is due to the $i\Gamma_P$ term concealed in $\Delta_T$ in equation 2.39. Similarly $p_2 = im_+$, so with $m_1 = m_-$ and $m_2 = m_+$ one finds from equations 2.36, 2.40, and 2.41

$$S(z,t) =$$
$$S_0\left[1-\left(1-\frac{m_1}{k_M-\omega_M/v_1}\right)e^{im_1 z}-\left(1-\frac{m_2}{k_M+\omega_M/v_1}\right)e^{-im_2(L-z)}\right]. \quad (2.42)$$

It is now necessary to investigate the values of $m_1$ and $m_2$. The maximum value of the second term under the radical in equation 2.39 occurs when $\delta_1 = \Delta_P$; then

$$m_2^{RES} = k_M + \frac{2\pi}{\lambda_M}\left(1 - i\frac{\kappa_{01}\lambda_M}{\pi\Gamma_P}\right)^{\frac{1}{2}}, \quad (2.43)$$

but, using the definitions of $k_{01}$ and $\Gamma_P$ (equations 2.7 and 2.8, respectively), one finds $\kappa_{01}\lambda_M/\pi\Gamma_P = 1.7$ for the xenon $5d[\frac{3}{2}]_1^O$, so

$$m_2^{RES} = k_M + \frac{2\pi}{\lambda_M}(1-1.7i)^{\frac{1}{2}}. \quad (2.44)$$

When evaluated with $\lambda_M = 1192$ Å this yields

$$Im(m_2^{RES}) \simeq -5\times 10^5 \mathrm{cm}^{-1}$$

so $Im(m_1)$ and $Im(m_2)$ are of the correct signs and, if $L$ is even a few millimeters, the correct magnitudes to satisfy the requirements for a solution of the form of equation 2.36.

A related question concerns how large $\delta_1$ can be for this form of the solution to remain valid. If $\delta_1 \gg \Gamma_P$, the radical in equation 2.39 can be expressed in the form

$$\frac{2\pi}{\lambda_M}\left(1-1.7i\frac{\Gamma_P^2}{\Delta^2}\right)^{\frac{1}{2}},$$

where $\Delta = \delta_1 - \Delta_P$. After a few more approximations one finds

$$Im(m_\pm) \simeq \mp\frac{2\pi}{\lambda_M}\frac{\Gamma_P^2}{\Delta^2} \quad (2.45)$$

so $|Im(m)| \gg 1$ yields $\Delta \ll 700\Gamma_P$, which means the solution should be valid for detunings of several hundred wavenumbers.

Since $m_1$ and $m_2$ are so large, the terms in 2.42 containing exponentials are vanishingly small except for regions of length $\approx 1/m$ near the end of the interaction region, and to good accuracy $S(z,t) = S_0$ for almost all $z$ in the overlap volume.

It remains only to find $\rho_{11}$. Using the definition of $S$ (equation 2.32) and the second of equations 2.6, one finds, after making the approximations $\rho_{00} \approx 1$ and $\rho_{11} \approx 0$, and neglecting $\Gamma_I$ and $\frac{\partial S}{\partial t}$,

$$\frac{V_{01}}{\hbar} = [\delta_1 - \Delta_{bl} - i\Gamma_P]\rho_{01}. \tag{2.46}$$

Substituting the complex conjugate of this equation into the third of equations 2.6 and using $|\rho_{01}|^2 = |S|^2$ one finds

$$\frac{\partial \rho_{11}}{\partial t} = 2\Gamma_P |S|^2 - \Gamma_I \rho_{11}, \tag{2.47}$$

so the excitation rate $R$ of $\rho_{11}$ is given by $2\Gamma_P|S|^2$, or

$$R = 2\Gamma_P \frac{|\Omega_{01}^{(3)}|^2}{\left[\delta_1 - \Delta_0\left(a - \frac{4}{3} + \left(\frac{2\lambda_2+\lambda_1}{(1-\cos(\theta))\lambda_M}\right)\right)\right]^2 + \Gamma_P^2}. \tag{2.48}$$

This expression shows a Lorentzian line shape for the excitation profile with a half-width at half maximum of $\Gamma_P$ and a line center at

$$\begin{aligned} \bar{\Delta}_P &= \Delta_0\left(a - \frac{4}{3} + \left(\frac{2\lambda_2 + \lambda_1}{(1-\cos(\theta))\lambda_M}\right)\right) \\ &= \Delta_P + \Delta_\theta \end{aligned} \tag{2.49}$$

Here $\Delta_0 a$ is the blue shift due to coherence transfer, $\frac{4}{3}\Delta_0$ is the Lorenz-Lorentz shift, which is to the red, and the last term is the pressure- and angle-dependent blue shift $\Delta_\theta$. Equation 2.48 describes the line shape expected of the atomic transition, with the added (and unusual) feature of the shift $\Delta_\theta$. Naïvely one would think of the energy of an atomic transition as being determined by the internal structure of the atom, and independent of all else; this is, of course, not true, since the energy levels of the atom can be perturbed in various ways by the atom's environment. ac Stark shifts and pressure

shifts are familiar examples of such perturbations. The shift discussed here is very unusual in that it depends on the wavelength combination used for the excitation and the angle between the laser beams as well as the number density of the medium and the oscillator strength of the transition.

For clarity and future convenience, equations 2.38 and 2.48 will be rewritten in terms of $\bar{\Delta}_P$:

$$S = -\frac{\Omega_{01}^{(3)}}{\delta_1 - \bar{\Delta}_P - i\Gamma_P} \tag{2.50}$$

$$R = 2\Gamma_P \frac{|\Omega_{01}^{(3)}|^2}{[\delta_1 - \bar{\Delta}_P]^2 + \Gamma_P^2}. \tag{2.51}$$

Also, several equivalent forms for $\Delta_\theta$ are presented:

$$\begin{aligned} \Delta_\theta &= -\kappa_{01} \frac{2\frac{\omega_M}{v_1}}{k_M^2 - \left(\frac{\omega_M}{v_1}\right)^2} \\ &= \frac{\kappa_{01}}{4\pi} \frac{2\lambda_2 + \lambda_1}{1 - \cos(\theta)} \\ &= \Delta_0 \frac{2\lambda_2 + \lambda_1}{(1 - \cos(\theta))\,\lambda_M} \end{aligned} \tag{2.52}$$

$\Delta_\theta$ is proportional to the product of number density $N$ and oscillator strength $F_{01}$ through the coefficient $\kappa_{01} \simeq 0.0265 N F_{01}$, so as the density of the medium is increased $\Delta_\theta$ will increase. $\Delta_\theta$ is inversely proportional to $1 - \cos(\theta)$, so for $\theta \approx 0$, corresponding to both laser beams traveling in nearly the same direction, $\Delta_\theta$ will be large, while for $\theta = \pi$, $\Delta_\theta$ will take on its smallest value. The dependence of $\Delta_\theta$ on the wavelengths $\lambda_1$ and $\lambda_2$ is not quite so obvious. To good accuracy

$$\frac{2}{\lambda_1} + \frac{1}{\lambda_2} = \frac{1}{\lambda_M} \approx \frac{2\pi c}{\omega_{10}},$$

where $\omega_{10}$ is the frequency of the $|0> \rightarrow |1>$ transition. Evaluating $\frac{\partial \Delta_\theta}{\partial \lambda_i} = 0$ (with $i = 1, 2$) with this constraint, one finds that $\Delta_\theta$ is maximized as $\lambda_1$ or $\lambda_2$ goes to zero, so use of wavelengths such that $\lambda_2 \ll \lambda_1$ (or $\lambda_1 \ll \lambda_2$) will produce larger shifts than the case $\lambda_1 = \lambda_2$.

## Three-photon Cancellation

The absence of resonant enhancement at a three- and one-photon allowed resonance when pumping with unidirectional light was discussed in Chapter I. Two special cases of the general model developed in the previous section are examined here: 1) excitation with $\theta = 0$, corresponding to unidirectional light, and 2) excitation with $\theta = \pi$, which is related to the case of excitation with retroreflected light discussed in Chapter I.

By comparison of equations 2.9 and 2.29, and using the definition of $S$ in equation 2.32, one may write

$$\Omega_{01}^{(1)} e^{-i\Delta k_r z} = \frac{4}{3}\Delta_0 S - i\kappa_{01} S e^{ik_M z} \int_0^L \exp(-ik_m z') \exp(-i\omega_M \frac{|z-z'|}{v_1}) dz'. \quad (2.53)$$

Although $S$ has the time dependence of $\Omega_{01}^{(3)}$, it can be moved out of the integral without loss of accuracy because of the assumption of transform limited lasers. The temporal envelope of such lasers varies only on the time scale of the pulse length, which is much larger than the retardation of the time over the dimensions of the interaction region; thus $\Omega_{01}^{(3)}(t^{RETARDED}) \approx \Omega_{01}^{(3)}(t)$.

Evaluation of the integral in 2.53 is straightforward, and yields

$$\Omega_{01}^{(1)} e^{-i\Delta k_r z} = \frac{4}{3}\Delta_0 S + \kappa_{01} S \left[ \frac{\exp\left(i(k_M - \frac{\omega_M}{v_1})z\right) - 1}{k_M - \frac{\omega_M}{v_1}} + \frac{1 - \exp\left(-i(k_M + \frac{\omega_M}{v_1})(L-z)\right)}{k_M + \frac{\omega_M}{v_1}} \right]. \quad (2.54)$$

The exponential terms inside the braces in equation 2.54 represent sum-frequency light propagating to point $z$ from the remainder of the interaction region; if the density is high and the detuning is not too large, this light will be strongly absorbed. If these terms are neglected, equation 2.54 becomes

$$\Omega_{01}^{(1)} e^{-i\Delta k_r z} = \frac{4}{3}\Delta_0 S + \kappa_{01} \frac{2\frac{\omega_M}{v_1}}{k_M^2 - \left(\frac{\omega_M}{v_1}\right)^2} S, \quad (2.55)$$

but with the use of equation 2.52 this is just

$$\Omega_{01}^{(1)} e^{-i\Delta k_r z} = \frac{4}{3}\Delta_0 S - \Delta_0 \frac{2\lambda_2 + \lambda_1}{(1 - cos(\theta))\,\lambda_M} S$$
$$= \frac{4}{3}\Delta_0 S - \Delta_\theta S \tag{2.56}$$

Clearly, if $\theta$ is small, the second term will be much larger than the first, so

$$\Omega_{01}^{(1)} e^{-i\Delta k_r z} = \frac{\Delta_\theta \Omega_{01}^{(3)}}{\delta_1 - \Delta_\theta - i\Gamma_P}, \tag{2.57}$$

where $\Delta_P = -1.11\Delta_0$ has been neglected in comparison with $\Delta_\theta$. From equation 2.9 one can define an effective Rabi frequency for the coupling between states |0> and |1> by

$$\Omega_{01}^{(eff)} = \Omega_{01}^{(3)} + \Omega_{01}^{(1)} e^{-i\Delta k_r z}, \tag{2.58}$$

where the first term is the three-photon Rabi frequency due to the laser field and the second is the one-photon Rabi frequency due to the sum-frequency field. In the limit as $\theta$ approaches 0 and $\Delta_\theta$ becomes very large, equation 2.57 becomes

$$\Omega_{01}^{(1)} e^{-i\Delta k_r z} = \frac{\Delta_\theta}{-\Delta_\theta} \Omega_{01}^{(3)} = -\Omega_{01}^{(3)}, \tag{2.59}$$

so $\Omega_{01}^{(eff)}$ goes to zero. What is seen here is the cancellation of excitation due to the laser by an equal and opposite excitation due to the local, adiabatic part of the nonlinear response of the medium. This is the three-photon cancellation effect. To reveal the effect the number density of the medium must be high enough to absorb the propagating, non-local part of the sum-frequency excitation.

Now suppose $\theta = \pi$. Then if $\lambda_1 = \lambda_2$, as in the study of Ref. 4, $\Delta_\theta = \frac{9}{2}\Delta_0$, and one finds for $\Omega_{01}^{(1)}$

$$\Omega_{01}^{(1)} e^{-i\Delta k_r z} = \frac{5.8\Delta_0 \Omega_{01}^{(3)}}{\delta_1 + 1.11\Delta_0 - 4.5\Delta_0 - i\Gamma_P}, \tag{2.60}$$

where the 5.8 in the numerator results from retaining the Lorenz term, and $\Delta_P$ has been evaluated in terms of $\Delta_0$. Here a small blue shift is seen due to the combination of the

$\Delta_\theta$ term and the smaller $\Delta_P$ term, which by itself produces a red shift; the net shift, amounting to $3.4\Delta_0$, is about 0.5 cm$^{-1}$ at 100 Torr for excitation of the xenon $5d[3/2]_1^o$ state. At the peak of the shifted line, with $\delta_1 = (-1.11 + 4.5)\Delta_0$,

$$\Omega_{01}^{(1)} e^{-i\Delta k_r z} = -\frac{5.8\Delta_0 \Omega_{01}^{(3)}}{i2.33\Delta_0},$$

where $\Gamma_P$ has been evaluated in terms of $\Delta_0$. The transition rate between states $|0>$ and $|1>$ is proportional to $|\Omega|^2$, so the rate due to the sum-frequency field is about $(5.8/2.33)^2 = 6.2$ times as large as the rate due to the laser alone. Then for $\theta = \pi$ one finds $\Omega_{01}^{(eff)} \simeq (1 - 2.5i)\Omega_{01}^{(3)}$ instead of $\Omega_{01}^{(eff)} = 0$ as for the $\theta = 0$ case. As noted in Chapter I, it was observed early on that the absent three-photon resonance could be made to reappear by retroreflecting the laser beam;[13] excitation by three photons from either the forward or reflected beam corresponds to the case $\theta = 0$, which produces no ionization due to the cancellation. Excitation by two photons from one direction plus one from the other corresponds to the $\theta = \pi$ case discussed here; as was observed in Ref. 4, ionization is then found, but at a slightly shifted wavelength. In the next section it is shown that this behavior can be understood in terms of the phase mismatch between the laser field and the sum-frequency light.

## The Three-photon Shift

As discussed in the previous section, if the angle between the laser beams of frequencies $\omega_1$ and $\omega_2$ is $\pi$, a small, pressure-dependent blue shift is observed in the position of the ionization peak, with the magnitude of the shift increasing with the density. If the angle between the beams is decreased from $\pi$, the shift will increase, becoming quite large for $\theta$ small. Two regimes of the shift $\Delta_\theta$ must be distinguished. In the large shift regime, where large means $\Delta_\theta \gg \Gamma_P$, the shifting mechanism may be understood solely in terms of phase matching between the laser field and the sum-frequency field. In the

small shift regime (that is, $\Delta_\theta \simeq \Gamma_P$) the angle-dependent shift $\Delta_\theta$ becomes comparable in magnitude with the other resonant shifts and no easy explanation in terms of a single, simple mechanism can be given. In this section and the following one the large shift regime will be explored in detail; nothing further will be said of the small shift regime until Chapter III, where it will be shown that the model given here agrees quite well with experiment even for the case where $\theta = \pi$.

From the first form of equation 2.52 one has $\Delta_\theta \propto (k_m^2 - (\omega_M/v_1)^2)^{-1}$. For $\theta = \pi$, $\vec{k}_M = 2\vec{k}_1 - \vec{k}_2$, while $\omega_M/v_1 \approx 2k_1 + k_2$, so $\Delta_\theta$ is small. As $\theta$ is decreased, the magnitude of $k_M$ increases as shown in equation 2.12, reaching a value, for $\theta = 0$, of $\vec{k}_M = 2\vec{k}_1 + \vec{k}_2 \approx \omega_M/v_1$, so $\Delta_\theta$ becomes very large. For $\theta$ fixed, $\Delta_\theta$ will vary proportionally with the number density, since the quantity $\kappa_{01} \propto N$.

If $\Delta_\theta$ is large compared with $\Delta_P$ (and thus $\Delta_0$), and the three-photon detuning $\delta_1$ is equal to $\Delta_\theta$, then from equation 2.57

$$\Omega_{01}^{(1)} e^{-i\Delta k_r z} = i\frac{\Delta_\theta}{\Gamma_P}\Omega_{01}^{(3)}. \tag{2.61}$$

$\Delta_\theta \gg \Delta_P$ implies $\Delta_\theta \gg \Gamma_P$, so the ratio of transition rates due the sum-frequency field and the laser field, given by

$$\left|\frac{\Omega_{01}^{(1)}}{\Omega_{01}^{(3)}}\right|^2 = \left|\frac{\Delta_\theta}{\Gamma_P}\right|^2, \tag{2.62}$$

will be very large. Thus, in the case where the shift $\Delta_\theta$ is large compared to the pressure-broadened line width, virtually all of the ionization will be due to the absorption of sum-frequency light. Recall from the previous section that even when $\theta = \pi$ and $\Delta_\theta$ is not large the transition rate due to the sum-frequency field was about six times as large as that due to the lasers. Note that since both $\Gamma_P$ and $\Delta_\theta$ are proportional to $\Delta_0$, the ratio in equation 2.62 is independent of the density.

The detuning of the ionization peak, provided $\Delta_\theta \gg \Gamma_P$, will be given by

$$\begin{aligned}\delta_1 &= \Delta_\theta \\ &= -\frac{2\kappa_{01}\omega_M/v_1}{k_M^2 - \left(\frac{\omega_M}{v_1}\right)^2} \\ &= -\frac{2\kappa_{01}}{\left(k_m - \frac{\omega_M}{v_1}\right)\left(k_m\frac{v_1}{\omega_M} + 1\right)}.\end{aligned} \tag{2.63}$$

But $k_m = \omega_M/c \approx \omega_M/v_1$, so equation 2.63 reduces to

$$k_M - \frac{\omega_M}{v_1} + \frac{\kappa_{01}}{\delta_1} = 0. \tag{2.64}$$

As is shown in Chapter I, the real part of the phase mismatch between the laser excitation and the sum-frequency light is given by

$$\begin{aligned}-\Delta k_r &= k_M - \frac{\omega_M n(\omega_M)}{c} \\ &\approx k_M - \frac{\omega_M}{c}\left(1 - \frac{c}{\omega_M}\frac{\kappa_{01}}{\delta_1}\right) \\ &\approx k_M - \frac{\omega_M}{c} + \frac{\kappa_{01}}{\delta_1},\end{aligned} \tag{2.65}$$

so by comparison of equations 2.64and 2.65the detuning of the peak is found to be such that $\Delta k_r = 0$; that is, in the case where the shift is large the maximum excitation occurs at the detuning where the sum-frequency light is phase matched to the laser.

In Chapter I the experiment of Ref. 4 (Ferrell *et al.*, 1987) was discussed, in which a peak due to the absorption of third-harmonic light was produced on the blue side of a three- and one-photon allowed resonance by phase matching the third harmonic to the unfocused laser with a positively dispersive buffer gas. As noted before, phase matching with unfocused, collinear laser beams is not possible without a buffer gas. If a positively dispersive buffer gas is added to the resonant gas, then at a detuning from three-photon resonance determined by the ratio of the densities of the resonant and buffer gases $\Delta k_r$ is zero; at this detuning there is no destructive interference among components of sum-frequency light generated at different values of $z$ and the sum-frequency intensity and the ionization are thus larger.

In the current experiment phase matching is accomplished with unfocused beams by using an angle between the beams, rather than a buffer gas. For $\theta = 0$, the situation is just as in the experiment of Ferrell *et al.* with no buffer gas: phase matching is impossible. As $\theta$ is increased, the length of the resultant vector $k_M$ decreases; phase matching with this shortened propagation vector requires a negative dispersion (an index of refraction less than one), which corresponds to a detuning on the blue side of the three-photon resonance. As $\theta$ approaches $\pi$, phase matching with the much shortened laser propagation vector requires an index of refraction much less than one; this is found for a blue-side detuning still closer to the resonance.

The dependence of $\Delta_\theta$ on the number density in the large shift regime can also be understood in terms of phase matching. The index of refraction at the laser frequencies $\omega_1$ and $\omega_2$ is very nearly unity, while the index of refraction at a small detuning from the one-photon resonant transition is large. Both vary proportionally with the density. Since the phase mismatch depends on the difference between $n(\omega_M)$ and $n(\omega_{LASER})$, $\Delta k_r$ is proportional to the number density $N$. That is, $\Delta k_r \propto N(n(\omega_M) - n(\omega_{LASER}))$, where here $n(\omega)$ is the index of refraction per atom, and the lasers are assumed to be of the same color.

## The Large Shift Regime

The expression for the excitation rate $R$ (equation 2.51) predicts a Lorentzian line shape for the ionization profile with an amplitude and width independent of the shift, so as $\theta$ is decreased from $\pi$ one would expect to see what looks like an atomic line shifted from its $\theta = \pi$ position by an increasing amount. If the number density $N$ is increased for fixed $\theta$, a shift proportional to $N$ will also occur; the variation of the amplitude of the ionization signal with increasing density is somewhat complicated and will be discussed briefly in Chapter III. If $\theta \ll \pi$, so that $\Delta_\theta \gg \Gamma_P$, and the shifting process is

well described by the phase matching model described above, the amplitude and width of the line will not behave as predicted by equation 2.51 with $\Gamma_P = 2.33\Delta_0$. This is because absorption on the far wing of the resonant line is not accurately described by the same width parameter $\Gamma_P$ that is appropriate at small detunings from three-photon resonance. In the following a model for the shifting mechanism in the large shift regime is presented to make clear the relation between the observed line width and amplitude and the absorption coefficient on the far wing of the resonance. The development follows closely that given in Ref. 15, and to some degree that given in Ref. 23.

Since the detuning $\delta_1$ from three-photon resonance is assumed large compared to any width (*e.g.* laser bandwidth, pressure-broadened line width) or shift in the problem, one may employ a simple perturbation treatment to find the nonlinear polarization directly in terms of the applied laser field, and then apply Maxwell's equations with a slowly varying amplitude and phase (SVAP) approximation to find the flux of sum-frequency photons as a function of detuning, number density, and phase mismatch parameter. Since the ionization in this regime is due almost entirely to absorption of the sum-frequency light, this gives the line shape.

The positive-frequency part of the polarization at the sum frequency $\omega_M$ can be written as

$$P_M^+ = \chi^{(1)} E_M^+ + N\rho_{01} D_{10}, \tag{2.66}$$

where $\chi^{(1)}$ is the linear susceptibility at $\omega_M$, and $E_M^+$ is the positive-frequency part of the space-averaged electric field at frequency $\omega_M$ given by

$$\begin{aligned} E_M &= E_M^+ + E_M^- \\ &= \frac{1}{2}\left[E_M(z,t)e^{i\omega_M t}e^{-ik_r z} + c.c.\right]. \end{aligned} \tag{2.67}$$

Here $E_M(z,t)$ contains only the slowly varying parts of the temporal and spatial dependencies, and $k_r$ is the real part of the propagation vector for light at $\omega_M$, so

$$k_r = Re\left[\frac{\omega_M n(\omega_M)}{c}\right], \tag{2.68}$$

where $Re$ indicates the real part.

From the second of equations 2.6, assuming $\rho_{00} \approx 1$ and $\rho_{11} \approx 0$ and neglecting $\Delta_{bl}$, $\Gamma_P$ and $\Gamma_I$ with respect to $\omega_{10}$, one finds

$$\frac{\partial \rho_{01}}{\partial t} = i\frac{V_{01}}{\hbar} + i\omega_{10}\rho_{01}. \tag{2.69}$$

Assuming $\rho_{01} \approx \exp(i\omega_M t)\,\rho'_{01}$, where $\rho'_{01}$ varies slowly with respect to time, and writing $V_{01}/\hbar = -\Omega_{01}^{(3)} \exp(i\omega_M t)\exp(-ik_M z)$, one finds

$$\rho_{01} = -\frac{\Omega_{01}^{(3)}}{\delta_1} e^{i\omega_M t} e^{-ik_M z}. \tag{2.70}$$

Inserting 2.66 with 2.70 into the wave equation 2.22 yields

$$\nabla^2 E_M^+ - \frac{1}{c^2}\frac{\partial^2 E_M^+}{\partial t^2} = \frac{4\pi}{c^2}\chi^{(1)}\frac{\partial^2 E_M^+}{\partial t^2} + \frac{4\pi}{c^2} N D_{01} \frac{\partial^2 \rho_{01}}{\partial t^2}. \tag{2.71}$$

Evaluating the time derivatives, neglecting the time dependence of $E_M(z,t)$ and $\Omega_{01}^{(3)}$, and using $n^2(\omega_M) = 1 + 4\pi\chi^{(1)}$, one finds

$$\nabla^2 \left(E_M(z) e^{i\omega_M t} e^{-ik_r z}\right) + \frac{\omega_M^2 n^2(\omega_M)}{c^2} E_M(z) e^{i\omega_M t} e^{-ik_r z} = - \frac{8\pi}{c^2}\omega_M^2 N D_{01} \frac{\Omega_{01}^{(3)}}{\delta_1} e^{i\omega_M t} e^{-ik_M z}, \tag{2.72}$$

where the extra factor of 2 on the right hand side comes from the $\frac{1}{2}$ in equation 2.67.

If the spatial dependence of $E_M$ is as described by equation 2.67, that is, the dependence can be factored into a product of two terms each with a different characteristic length for the variation, then

$$\left|\frac{\partial^2 E_M(z)}{\partial z^2}\right| \ll \left|k_M \frac{\partial E_M(z)}{\partial z}\right|, \tag{2.73}$$

will hold, and the second partial of $E_M$ with respect to time may be neglected: this is the slowly varying amplitude and phase (SVAP) approximation.[2] As is pointed out in Ref. 2, making the SVAP amounts to neglecting the wave radiated in the backward $(-\hat{z})$ direction; this wave is very badly phase mismatched under the conditions assumed here

($\theta$ small), so its intensity may be neglected. With the assumption that the transverse variation in $E_M$ is slow compared to $k_r$, and making the SVAP approximation, one finds for $\nabla^2 E_M^+$

$$\frac{\partial^2}{\partial z^2}\left(E_M(z)e^{-ik_r z}e^{i\omega_M t}\right) = -2ik_r\frac{\partial E_M(z)}{\partial z}e^{-ik_r z}e^{i\omega_M t} - k_r^2 E_M(z)e^{-ik_r z}e^{i\omega_M t}, \quad (2.74)$$

so equation 2.72 becomes

$$\frac{\partial E_M(z)}{\partial z} - \frac{1}{2ik_r}\left(\frac{\omega_M^2 n^2(\omega_M)}{c^2} - k_r^2\right)E_M(z) = i\frac{4\pi}{c}\frac{ND_{01}\omega_M}{n(\omega_M)}\frac{\Omega_{01}^{(3)}}{\delta_1}e^{i\Delta k_r z}, \quad (2.75)$$

where $\Delta k_r = k_r - k_M$.

A useful simplification can be made to the left hand side of 2.75.

$$\begin{aligned}\frac{1}{2ik_r}\left(\frac{\omega_M^2 n^2(\omega_M)}{c^2} - k_r^2\right) &= \frac{1}{2ik_r}\left(\frac{\omega_M n(\omega_M)}{c} - k_r\right)\left(\frac{\omega_M n(\omega_M)}{c} + k_r\right)\\ &\simeq -i\left(\frac{\omega_M n(\omega_M)}{c} - k_r\right),\end{aligned}$$

since from equation 2.68 the last parenthesis on the right hand side in the first line is $k + k_r = 2k_r + ik_i$, and $k_i \ll k_r$. Here $k_r$ and $k_i$ are the real and imaginary parts of $k$. $n(\omega_M) = n_r(\omega_M) + in_i(\omega_M)$, so the quantity in the parenthesis in the second line is $i\omega_M n_i(\omega_M)/c$, and

$$\frac{1}{2ik_r}\left(\frac{\omega_M^2 n^2(\omega_M)}{c^2} - k_r^2\right) = \frac{\omega_M n_i(\omega_M)}{c} = \frac{\beta}{2},$$

where $\beta$ is the absorption coefficient. Thus equation 2.75 sets the spatial rate of change of $E_M(z)$ equal to the difference between a driving term proportional to the laser field and an absorption term.

An equation of the form

$$\frac{dE(z)}{dt} = A(z) - \alpha E(z)$$

with $E(0) = 0$ has the obvious solution

$$E(z) = e^{-\alpha z}\int_0^z A(z')e^{\alpha z'}dz',$$

so $E_M(z)$ is given by

$$E_M(z) = e^{-\beta z/2}\frac{4\pi}{c}\frac{ND_{01}\omega_M}{n(\omega_M)}\frac{\Omega_{01}^{(3)}}{\delta_1}\frac{\exp\left(i(\Delta k_r - i\frac{\beta}{2})z\right) - 1}{\Delta k_r - i\frac{\beta}{2}}. \tag{2.76}$$

The flux $F_M$ of photons at $\omega_M$ is then

$$\begin{aligned} F_M &= \frac{c|E_M(z)|^2}{8\pi\hbar\omega_M} \\ &= \kappa_{01}N\frac{|\Omega_{01}^{(3)}|^2}{\delta_1^2}\frac{\left[1 + e^{-\beta z} - 2e^{-\beta z/2}\cos(\Delta k_r z)\right]}{(\Delta k_r)^2 + \beta^2/4}. \end{aligned} \tag{2.77}$$

If $\beta L/2 \gg 1$, then the last two terms in 2.77 will be vanishingly small over most of the interaction region, and

$$\begin{aligned} F_M(\Delta k_r, \beta) &= \frac{c|E_M(z)|^2}{8\pi\hbar\omega_M} \\ &= \kappa_{01}N\frac{|\Omega_{01}^{(3)}|^2}{\delta_1^2}\frac{1}{(\Delta k_r)^2 + \left(\frac{\beta}{2}\right)^2}. \end{aligned} \tag{2.78}$$

Note that in the opposite limiting case of $\beta = 0$, equation 2.77 can be put into the form of $\mathrm{sinc}^2(\Delta k_r z)$, where $\mathrm{sinc}(x) = \sin(x)/x$; this is the phase matching profile expected for an unfocused geometry.

From equation 2.65 one finds the detuning $\delta_0$ for $\Delta k_r = 0$ to be $\delta_0 = \kappa_{01}/(\omega_M/c - k_M)$. Expanding 2.65 in a Taylor series about $\delta_0$ gives to first order

$$\Delta k_r \simeq \frac{\kappa_{01}}{\delta_0^2}(\delta_0 - \delta_1), \tag{2.79}$$

but as shown earlier $\Delta_\theta = \delta_0$, and with the use of 2.79 in equation 2.78 one finds after some manipulation and the approximation $\delta_1 \approx \Delta_\theta$

$$F_M = \frac{N\Delta_\theta^2}{\kappa_{01}}\frac{|\Omega_{01}^{(3)}|^2}{(\delta_1 - \Delta_\theta)^2 + \left(\frac{\beta\Delta_\theta^2}{2\kappa_{01}}\right)^2}. \tag{2.80}$$

If $R$ is the excitation rate per atom and $N$ is the number density, then $NR$ should be the number of excited atoms produced per second per cm$^3$. Similarly, if $F_M$ is the

number of photons per second per cm$^2$, and $\beta$ is the fractional absorption per cm, then $\beta F_M$ should be the number of excited atoms produced per second per cm$^3$, so

$$\begin{aligned} R &= \frac{\beta F_M}{N} \\ &= 2\frac{\beta\Delta_\theta^2}{2\kappa_{01}} \frac{|\Omega_{01}^{(3)}|^2}{(\delta_1 - \Delta_\theta)^2 + \left(\frac{\beta\Delta_\theta^2}{2\kappa_{01}}\right)^2}. \end{aligned} \tag{2.81}$$

With the definition of

$$\Gamma_{EFF} = \frac{\beta\Delta_\theta^2}{2\kappa_{01}} \tag{2.82}$$

equation 2.81 becomes

$$R = 2\Gamma_{EFF} \frac{|\Omega_{01}^{(3)}|^2}{(\delta_1 - \Delta_\theta)^2 + \Gamma_{EFF}^2}, \tag{2.83}$$

so $R$ is described by a Lorentzian of half-width at half maximum $\Gamma_{EFF}$.

Recall that $\beta L/2 \gg 1$ was necessary to reduce 2.77 to the form of 2.83. If the number density $N$ is increased with $\theta$ fixed, $\Delta_\theta$ will increase, but $\beta$ at the detuning $\delta = \Delta_\theta$ will remain fixed, since $\beta \propto N^2/\delta^2$ and $\Delta_\theta \propto N$. However, if the number density is held constant and $\theta$ is decreased, $\Delta_\theta$ will increase, $\beta$ will decrease, and at some minimum angle $\theta_{MIN}$ the condition on $\beta L$ will no longer be met. $\theta_{MIN}$ is defined by

$$\frac{\kappa_{01}\Gamma_P \mathrm{L}}{\Delta_\theta(\theta_{MIN})} \simeq 1.$$

If $\theta < \theta_{MIN}$ the excitation profile will begin to resemble the phase matching profile for sum-frequency generation; the Lorentzian form is found only when the absorption is strong enough to make $F_M$ independent of $z$ over most of the interaction region.

If the absorption is given by

$$\beta = \frac{2\kappa_{01}\Gamma_P}{\delta_1^2}, \tag{2.84}$$

that is, if $\Gamma_{EFF} = \Gamma_P$, then equation 2.81 is the same as equation 2.51 in the limit $\Delta_\theta \gg \Delta_P$, and the excitation profile of the shifted line would have the same width and

amplitude as if it were unshifted. However, equation 2.84 is not an accurate estimate of $\beta$ for $\delta_1$ large.

A transition in an isolated atom has, of course, a spectral width $\Gamma_0$ related to the lifetime of the excited state against spontaneous decay $\tau$ by $\Gamma_0 = \tau^{-1}$. Alternatively, this may be regarded as the power broadening of the transition by emission stimulated by the vacuum field (Ref. 3, p. 26). If the number density is substantial, then atom-atom interactions (*e.g.* collisions) will perturb the atoms and increase the width of the transition. The interaction between atoms may be described by an atom-atom potential which will depend on the distance between the atoms, among other things. The distance between the interacting atoms can be described by the impact parameter $b$. Since one would expect $V_{ab} \propto r^{-n}$, where $V_{ab}$ is the interatomic potential, large impact parameters will be associated with small shifts in the energy levels of the atoms, which will correspond to absorption at small detunings from resonance.

More specifically, the broadening of a resonance line at detunings small compared to the inverse collision time may be accurately described by the impact theory of resonance broadening; this should apply with fair accuracy for detuning of 1 $cm^{-1}$ or less. Here the collision time $\tau_c \propto b/v$, where $v$ is the relative velocity of the atoms. The atom-atom potential is modeled by a dipole-dipole interaction leading to an $r^{-3}$ dependence of $V_{ab}$. The dipole-dipole potential has no non-zero diagonal elements and cannot lead directly to a substantial broadening of the transition for large values of $b$. However, in collisions between atoms of the same element, one of which is in the excited state, there is a high probability of an exchange of excitation between the atoms, and with it the possibility of a change in $M_J$. This disturbance of the state vector results in a broadening of the line. Quantitative analyses based on these ideas lead to results for $\Gamma_P$ similar to the value used here. Reasonable agreement with experiment has been found for the core of the line even at densities where the assumptions of the theory are no longer entirely valid.[4]

However, impact theory cannot accurately model the far wings of the line shape. The far wings (that is, $\delta_1 \gg \Gamma$, where $\Gamma$ is the half-width at half maximum) correspond to large energy shifts and small impact parameters. One approach to dealing with this regime is the quasi-static theory of line broadening, where absorption occurs when the atom-atom interaction shifts the atomic energy levels into resonance; the interacting pair of atoms may be thought of as an unbound molecule. When a dipole-dipole interaction potential is employed, the line shape is Lorentzian, as in the impact theory, but a different value of the line width is found. To accurately model very far wing absorption at detunings of 20 $cm^{-1}$ or more would require including higher-order multipoles. In chapter III shifts of as much as 600 $cm^{-1}$ are reported; as expected, the widths are not those predicted by the impact theory.

Since in general $\Gamma_{EFF} \neq \Gamma_P$ for $\delta_1 \gg \Gamma_P$, the amplitude and width of the shifted peak described by equation 2.81 will not be the same for small and large values of the shift. For small shifts the shifted peak should look very much like an atomic line. For shifts $\gg \Gamma_P$ but with $\theta > \theta_{MIN}$ the peak is Lorentzian but with a different amplitude and width than in the small shift regime. For very large shifts such that $\theta \leq \theta_{MIN}$ the lineshape goes over to a $sinc^2$ phase matching profile, and, due to the small absorption coefficient, the ionization becomes small.

Observation of $\Delta_\theta$ versus $N$ or $\theta$ in the regime where $\Delta_\theta \gg \Gamma_P$ provides a method for the measurement of the oscillator strength $F_{01}$ of the $|0> \rightarrow |1>$ transition with extreme accuracy. Using two-color excitation with an angle between the beams allows one to make the shift many times the pressure-broadened width of the line or the laser bandwidths, so the shift can be determined with very high accuracy. An example of this will be given in Chapter III. Note also that fitting equation 2.81 to the observed excitation profile would provide an excellent way to measure the effective value of $\beta$ at large detunings from the three-photon resonance and so study the line broadening due to atom-atom interactions at very small impact parameters.

# CHAPTER III

## The Three-photon Shift Experiment

In this chapter experimental observations are presented of the resonant enhancement of ionization in xenon by three- and one-photon allowed states using two-color excitation with an angle between the laser beams. In the first section the experimental apparatus, conditions, and procedures are described. Three sets of observations are reported in the second section. A three-photon transition between the $5p^6$ ground state of xenon and the $5d[\frac{3}{2}]_1^O$ state (referred to as the $5d$) is pumped with two laser beams of different colors with an angle $\theta$ of 180° between them. The variation of the width and blue shift of the transition with pressure is reported and compared with prediction; comparison is also made with the similar observations of Ferrell.[4] Excellent agreement with the theory described in Chapter II and Refs. 16 and 18 is found. The lack of a shift in the xenon $5d[\frac{5}{2}]_3^O$ state is described; this is in accord with prediction, since this $J = 3$ state is not coupled to the ground state by a one-photon transition. The angle- and pressure-dependent shift of the $5p^6 \rightarrow 5d[\frac{3}{2}]_1^O$ transition when $\theta$ is in the range of 10° to 28° is reported for xenon pressures of 50 to 800 Torr. The predicted linear dependence of shift on pressure is found for shifts of less than 250 $cm^{-1}$; the shift data in this region is used to determine a new value for the oscillator strength of 0.346. A sublinear dependence of shift on pressure for shifts greater than 250 $cm^{-1}$ is shown to be explainable in terms of a more detailed model for phase matching which includes the contribution to the index of refraction due to all the resonant transitions in the xenon atom rather than just the near-resonant $5p^6 \rightarrow 5d$. Excellent agreement is found between experimental values for

the shift and the predictions of the detailed model. The variation of the width of the shifted peak with the shift is discussed in terms the absorption coefficient.

## Experimental Apparatus and Procedures

Laser beams of two different frequencies $\omega_1$ and $\omega_2$ were crossed at an angle $\theta$ in a cell containing a known pressure $P_{Xe}$ of pure xenon gas; both beams were linearly polarized with the directions of polarization parallel. Ionization was measured using a wire-type proportional counter in the cell. The ionization signal was recorded as the frequency sum $2\omega_1 + \omega_2$ of the laser beams was scanned across the position of the resonant enhancement. Comparison of the frequency of the resonant enhancement at high and low xenon pressures and with various angles between the laser beams allows the determination of the value of the pressure- and angle-dependent shift.

Frequency-doubled light at 532 nm from a Quanta-Ray DCR-10 Nd:YAG flash-lamp pumped laser was used to pump two dye lasers simultaneously. The DCR-10 gave about 350 mJ of green (532 nm) light in a beam with an annular transverse intensity distribution; this beam was split into two equal intensity beams and directed into the dye lasers, both of which were Quanta-Ray PDL-1's. The PDL-1 consists of a Hänsch-type oscillator pumped with about 4% of the pump energy, an optional preamplifier stage, and an amplifier stage. The oscillator stage consists of a 4% reflective output coupler, a side-pumped dye cell into which the pump beam is focused with a cylindrical lens, a prism beam expander, and a diffraction grating which forms the rear reflector of the cavity. The prism beam expander enlarges the laser beam in the vertical direction to make it cover the grating surface. Frequency selection is achieved by adjusting the angle of the grating with a sine-bar drive. An air-spaced etalon can be introduced into the laser cavity to reduce the laser bandwidth. With the etalon in place, tuning must be done by changing the gas density in the cavity, thus changing the index of refraction

and the optical path length between the etalon surfaces. The tuning range is restricted to only a few Å if this method is employed. In the present experiment the amplifier cell was illuminated longitudinally with the pump beam, giving an output beam with an annular transverse intensity distribution like that of the pump beam. The pulse length (FWHM) was approximately 7 ns with a repetition rate of 10 Hz.

In the experiment to which most of this chapter is devoted one laser (Laser 1) was operated with Kiton Red 620 dye at a wavelength of about 5840 Å. This light was doubled in frequency using a KDP (potassium dihydrogen phosphate) doubling crystal to give a wavelength of 2920 Å. The total energy output at 5840 Å was 5 to 10 mJ per pulse; the doubling efficiency was poor (due to the lack of a suitable KDP crystal), so the energy per pulse in the UV was on the order of hundreds of $\mu$J. The angle between the incident laser beam and the optical axis of the non-centrosymmetric doubling crystal must be adjusted to phase match the frequency-doubled light to the laser light; since the phase matching angle depends on the wavelength, the UV light could not be scanned in wavelength with a simple, fixed-angle doubler of the type available. As this laser operated at a fixed frequency, the intracavity etalon could be employed to reduce the bandwidth to about 0.05 Å, which corresponds to about 0.15 $cm^{-1}$ at 5840 Å. This estimate for the bandwidth is based on observations with a viewing etalon.

The other laser (Laser 2) was operated with DCM dye in the wavelength region between 6100 Å and 6500 Å, providing about 10 mJ per pulse over most of that region. Since this laser had to be scanned over a wide wavelength range, the intracavity etalon could not be used. The laser bandwidth with the diffraction grating operated in fifth order was about 0.3 Å, corresponding to about 0.7 $cm^{-1}$ at 6500 Å. The dye concentrations used in both lasers were those recommended by the laser manufacturer.

With the lasers operating as described the effective three-photon bandwidth $\Gamma_L$ is approximately $\sqrt{4(0.15\ cm^{-1})^2 + (0.7\ cm^{-1})^2} \approx 0.75\ cm^{-1}$. The four under the radical is due to the frequency doubling of the light from Laser 1 to produce photons at frequency

$\omega_1$; as a result, the bandwidth of Laser 1 enters four times into the expression for the bandwidth. If Laser 1 had been operated without the intracavity etalon, the three-photon bandwidth would have been approximately $\sqrt{5}(0.7\ \text{cm}^{-1}) \approx 1.5\ \text{cm}^{-1}$, so the bandwidth would have been doubled.

Both laser beams were passed through 3:1 beam-reducing telescopes prior to entering the xenon cell. This was done primarily to increase the light intensity and thus the signal level. With unfocused, untelescoped beams the ionization signal was too small and noisy to allow the collection of reliable data. Focusing the beams increased the signal strength to an adequate level, but introduced an additional width into the resonance peak. This was thought to be due to the angle dependence of the position of the enhancement peak: the focused beams produced excitation with a range of intersection angles, resulting in a range of shifts which appeared as a broadening of the peak. Telescoping the beams proved to be a workable compromise. It was found the telescoped beams had a more or less Gaussian transverse profile instead of the annular profile of the untelescoped beams. The dimensions of the telescoped beams were measured using a one-dimensional CCD photodiode array. The UV beam was found to be 0.031 cm by 0.11 cm (FWHM), and the red ($\approx$ 6500 Å) beam was 0.088 cm by 0.038 cm. Assuming all the energy to be concentrated within the measured widths (which modestly overestimates the intensity) these areas lead to typical intensities of about $10^8$ watts/cm$^2$ for the red beam and $10^7$ watts/cm$^2$ for the UV.

Temporal overlap of the beams at the crossing region was ensured by carefully equalizing the path lengths. Since this can be done to within a few centimeters, and since the length of the light pulse is approximately seven feet (the speed of light having the convenient value of 1 foot per nanosecond), excellent overlap could be achieved.

The xenon cell was a stainless steel cube 11 cm on a side. Large (3" diameter) windows were mounted on the front and back sides of the cell to allow the passage of the crossed laser beams. One window was of quartz to transmit the UV light without

significant attenuation. Inside the cell was a wire-type proportional counter, consisting of a thin, smooth wire strung tautly between insulating supports. The wire was connected to the input of a charge-sensitive preamplifier. A positive voltage of a few hundred to a few thousand volts with respect to the body of the cell was placed on the wire through a large ($\approx$ 100 M$\Omega$) dropping resistor contained in the preamplifier. Electrons liberated by the ionization of xenon atoms during a laser pulse drift to the wire under the influence of the applied electric field. In the region very near the wire, where the field is quite large, avalanche multiplication occurs; the charge is then collected by the wire and passes through the dropping resistor. The FET input stage of the preamplifier is coupled to the charge-collection wire side of the dropping resistor through a capacitor. The charge-sensitive preamp generates an output pulse with a height proportional to the integral of the input voltage pulse. Additional amplification was provided by a pulse-shaping amplifier. A timing signal from the YAG pump laser, time delayed with a gate-and-delay generator, was used to trigger a sample-and-hold circuit at the peak of the voltage pulse from the amplifier. The output from the sample-and-hold circuit was digitized by an analog to digital converter (ADC) installed in an LSI-11 minicomputer.

A major difficulty to be overcome in this experiment was a very large amount of background ionization produced whenever the UV light was passed through the cell (note that the UV passed in one window and out the other). No similar ionization was produced by the red laser alone. This background was thought to be due to the amplification of photoelectrons ejected from the walls of the xenon cell by scattered UV light. The signal due to this ionization was large enough to completely obscure any resonantly enhanced MPI signal from the xenon. Plating the interior surfaces of the cell with a high work function metal such as gold would probably have eliminated this problem. Instead, a cylindrical, wire-mesh electrode was placed in the cell surrounding the charge-collection wire, the diameter of the electrode being large enough to place the mesh near the inner surface of the cell. The ends of the cylinder were also covered with

wire mesh, with the laser beams passing in and out of the space enclosed by the electrode through rectangular slots in each end. The electrode was supported on insulated feed-throughs which connected it to a high-voltage power supply; thus its potential with respect to the cell could be varied independently of the voltage on the charge-collection wire. It was initially thought that operation with a negative voltage with respect to the cell would cause the electrode to repel any photoelectrons ejected from the walls of the cell and prevent their reaching the wire. This did not work. Adequate suppression of the background could be had, however, by placing a positive voltage equal to ten or twenty percent of the wire voltage on the electrode.

The xenon pressure $P_{Xe}$ was measured with an MKS Barotron capacitive manometer with a range of 0 to 1000 Torr. The manometer was checked at $\approx 0$ Torr by comparison with a Hastings thermocouple-type pressure gauge, and at atmospheric pressure by comparison with a mercury column manometer. No significant error was observed. The Barotron gauge is claimed by its manufacturer to be accurate to within 0.5% over its range; due to a lack of suitable manometers for comparison, this claim could not be verified. On the basis of previous experience with the Barotron in question, an accuracy of a few percent seems reasonable, however.

The angle between the laser beams was found by measuring the distance between the beams at two locations a known distance apart; since the angles employed ranged from 10° to 28°, determination of $\theta$ to a few percent was possible. The principle limitation to the accuracy of the measurement was the diameter of the laser beams.

A typical data-taking run began with the setting of the angle $\theta$. The pulsed output signal representing the ionization was displayed on an oscilloscope, and the tunable laser scanned by hand to find three-photon resonance. The laser beams were then adjusted in the vertical and horizontal planes to maximize the MPI signal and thus the spatial overlap between the beams. A careful measurement of $\theta$ was made after this adjustment.

Data logging was done with the LSI-11 minicomputer. A computer-controlled step-

ping motor drive was connected to the tunable dye laser. A data acquisition program stepped the wavelength in increments across the desired wavelength region. The ionization signal strength from a specified number of laser pulses was averaged at each wavelength and recorded, along with the laser wavelength, in a computer file; the laser was then driven to the next wavelength and the process repeated. The recorded excitation profile thus consisted of a file of wavelengths and ionization levels. Determination of the centroid wavelengths and widths of the resonances was done by hand from plots of this data.

## Experimental Results and Comparison with Theory

As discussed earlier, Ferrell *et al.* report in Ref. 4 on a pressure-dependent blue shift in the peak of the excitation profile when a counterpropagated laser beam is tuned near several three- and one-photon allowed resonances in xenon. With one-color laser excitation ($\lambda \approx 3576$ Å), the shift observed for the $5d[\frac{3}{2}]_1^O$ was $\approx 5.6 \times 10^{-3}$ Torr$^{-1}$cm$^{-1}$ (as measured from Fig. 10 in Ref. 4). This situation corresponds to that studied in Chapter II with $\lambda_1 = \lambda_2$ and $\theta = 180°$; evaluation of the formulas for $\bar{\Delta}_P = \Delta_P + \Delta_\theta$ (equations 2.31 and 2.52) using $F_{01} = 0.346$ for the absorption oscillator strength gives $\bar{\Delta}_P = 5.1 \times 10^{-3}$ cm$^{-1}$ Torr$^{-1}$, which is in good agreement with Ferrell's result.

As explained in the previous chapter, one color excitation gives the smallest shift; making the ratio $\lambda_2/\lambda_1$ larger should give a larger shift. Furthermore, it was predicted that the amplitude and width of the shifted line should be the same as the atomic (unshifted) line; that is, the width of the peak should increase with pressure according to $\Gamma_P = 2.33\Delta_0$.

To test these predictions, two-color, three-photon resonant excitation of the xenon $5d[\frac{3}{2}]_1^O$ state with $\lambda_1 \approx 2820$ Å and $\lambda_2 \approx 7760$ Å was employed. The UV (2820 Å) and IR (7760 Å) beams were counterpropagated, so $\theta = 180°$. Later in this sec-

tion a value of 0.346 for the oscillator strength $F_{01}$ for this transition is found by analysis of the shift *vs.* pressure data for small values of $\theta$. Evaluating $\bar{\Delta}_P = \Delta_P + \Delta_\theta$ with this oscillator strength and the values of $\lambda_1$ and $\lambda_2$ given above, one finds $\Delta_P = -1.65 \times 10^{-3}\text{cm}^{-1}$ Torr$^{-1}$ and $\Delta_\theta = 1.15 \times 10^{-2}\text{cm}^{-1}$ Torr$^{-1}$, where the shift is given in wavenumbers (cm$^{-1}$) per Torr of Xenon. Then the total shift is $\bar{\Delta}_P = 9.85 \times 10^{-3}\text{cm}^{-1}$ Torr$^{-1}$, which is about 1.9 times as large as in Ferrell's experiment. The pressure-broadened half-width is $\Gamma_P = 3.48 \times 10^{-3}\text{cm}^{-1}$ Torr$^{-1}$. If only $\lambda_2$ is scanned, these values give a total shift at 7760 Å of 0.00593 Å per Torr and a half-width of 0.00209 Å per Torr.

In Fig. 5 the wavelength of the centroid of the excitation profile is plotted *vs.* the xenon pressure for six values of $P_{Xe}$. The shift is quite linear in pressure up to 800 Torr. The straight line has the slope for $\bar{\Delta}_P$ found above. The $P_{Xe} = 0$ intercept for the line was chosen by calculating the shift expected for $P_{Xe} = 50$ Torr (the lowest pressure data point) and adding that shift to the wavelength of the $P_{Xe} = 50$ Torr data point. Excellent agreement is found between the predicted and observed shifts for $P_{Xe} \leq 800$ Torr.

The lineshapes predicted in the previous chapter were Lorentzian, while those observed here were somewhat asymmetrical even at 50 Torr. For $P_{Xe} < 400$ Torr, the excitation profile was skewed modestly to the blue (shorter wavelength) side. At 400 Torr the profile was almost symmetrical, while for $P_{Xe} > 400$ Torr, the line was skewed substantially to the red side. Asymmetrical profiles are, of course, expected in the quasi-static pressure-broadening regime, which may account for the asymmetry observed at the higher pressures here. The asymmetry, in turn, may partly account for the lack of agreement between the expected and observed shifts at 1000 Torr. It is not obvious that the centroid is actually the best measure of the position of the line center when the profile is broad and asymmetrical, though the quality of the fit obtained for lower pressures, both with the data shown in Fig. 5 and with the other data sets to be presented later,

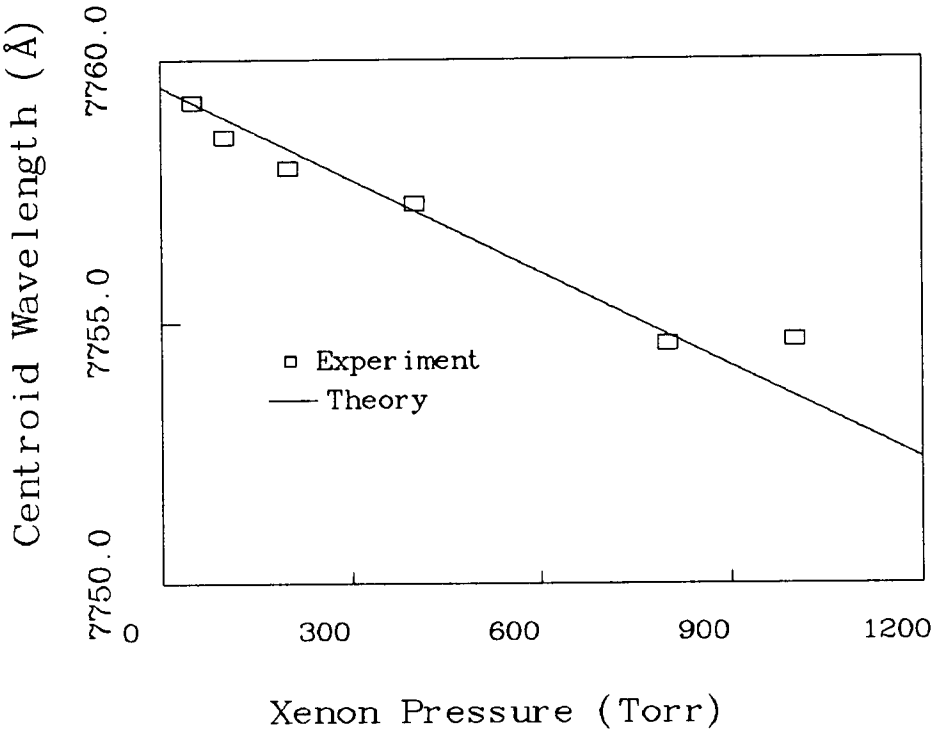


Figure 5. Centroid Position *vs.* Xenon Pressure for $\theta = 180°$

The wavelength of the centroid of the excitation profile of the xenon $5d[\frac{3}{2}]_1^O$ is plotted against the xenon pressure for $P_{Xe}$ ranging from 50 Torr to 1000 Torr. $\lambda_1 \approx 2820$ Å and $\lambda_2 \approx 7760$ Å, so the shift at a given pressure is larger than in the comparable study in Ref. 4. The straight line is the shift predicted in Refs. 16 and 19 and discussed in Chapter II of this work.

indicates it is in general a satisfactory measure.

In Fig. 6 the observed full width at half maximum (FWHM) of the excitation profiles is plotted *vs.* the xenon pressure. Comparison of the predicted and observed values requires consideration of the laser bandwidth. The observed FWHM of the 50 Torr profile is 1.8 Å, corresponding to 3 $cm^{-1}$, while the predicted FWHM from pressure broadening at that pressure is about 0.35 $cm^{-1}$, so the observed width should be due largely to the bandwidth of the laser excitation. Earlier in this chapter the effective three-photon bandwidth was estimated to be about 0.75 cm−1 for the case with $\lambda_2$ of about 6500 Å. For the observations discussed here, however, the frequency selection grating in the laser producing light at wavelength $\lambda_2$ had to be operated in third order instead of in fifth order. This results in a loss of spectral resolution by the grating and an increase in the bandwidth of the laser, which may account for the increase in the apparent bandwidth. No independent measurement of the bandwidth of the IR laser was made.

The straight line in Fig. 6 has the slope predicted for $2\Gamma_P$. The fit shown was achieved by adding 1.5 Å to the predicted widths. As is well known, the convolution of two Gaussian profiles is a Gaussian profile, with the widths adding in quadrature, while the convolution of two Lorentzian profiles is a Lorentzian with a width given by the sum of the widths of the component profiles. The expected lineshape here is Lorentzian, while the spectral profile of the lasers is thought to be approximately Gaussian; the convolution of the two gives a Voight profile. In Ref. 4 predicted pressure-broadened line widths are fitted fairly well to the observed excitation profile widths by treating both laser and line profiles as Gaussian. However, the laser bandwidth employed there was considerably smaller than here, which reduces its effect. It is not clear that there is a simple way to deal with including the effect of broad-bandwidth multi-mode laser excitation in the resonant pressure broadening problem. It is clear, however, that treating both the laser and the atomic line as Lorentzians gives an excellent fit to the data here for xenon

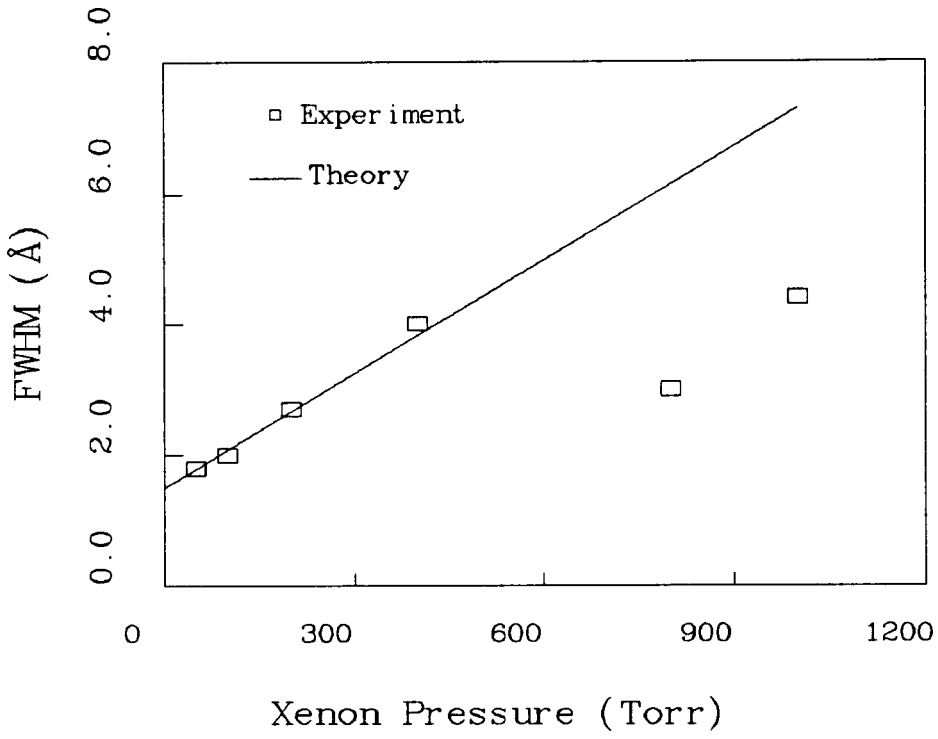


Figure 6. Width of the Excitation Profile *vs.* Xenon Pressure for $\theta = 180°$

The excitation conditions are the same as in Figure 6. The straight line has slope $2\Gamma_P$, where $\Gamma_P$ is the half-width at half-maximum of the transition found from the impact theory of pressure broadening as discussed in Chapter II.

pressures up to 400 Torr; in Ferrell's work the observed widths become larger than the predicted widths at only 200 to 250 Torr. In the data shown in Fig. 6, as in Ref. 4, the width decreases above a pressure of a few hundred Torr. It has been suggested (R. N. Compton, private communication) that the pressure range in which this decrease is observed may correspond to the pressure at which the rate of $M_J$ changing collisions between excited state atoms and ground state atoms becomes comparable to the laser pulse duration (see Ref. 51).

The prediction about the height of the shifted peak could not be tested with the apparatus employed. The shifts were produced here by varying the xenon pressure, but the gain of the proportional counter used to detect the ionization also changes with gas density, so the amplitudes of the ionization signals for different values of $P_{Xe}$ cannot be compared. In Ref. 4 absolute measurements of the ionization yield from the xenon $5d[\frac{3}{2}]_1^O$ were performed using the method described in Ref. 20, where an electron-emitting radioactive source ($^{55}$Fe) was placed in the cell. Knowing the W value for the mean energy of the emitted electrons, one can predict the number of electron-ion pairs produced per decay. Observation of the average height of the ionization pulse produced per decay then calibrates the sensitivity of the proportional counter at a given gas pressure. In Fig. 9 of Ref. 4 the absolute ionization signal at the center of the excitation profile from the xenon $5d[\frac{3}{2}]_1^O$ is shown to be linear in xenon pressure up to about 250 Torr; above this pressure the output levels off and becomes independent of pressure. This result does not contradict the predictions made here, however, since the study of reference 4 was made with a relatively broad bandwidth laser. For pressures less than 250 Torr the pressure-broadened width of the line is less than the three-photon laser bandwidth, so the output increases linearly with pressure. The independence of the signal with respect to pressure at high pressures may be understood by realizing that $R$ in equation 2.51 is the excitation rate per atom, so the total number of ions produced will go as $NR$, but at the peak of the excitation profile $NR = 2N|\Omega_{01}^{(3)}|^2/\Gamma_P$,

and since $\Gamma_P \propto N$, the pressure independence follows. This behavior is seen only if the pressure is high enough to make the assumption that the laser bandwidth $\Gamma_L$ is much less than $\Gamma_P$ valid. In the experiment reported on here, the laser bandwidths were even larger than those employed by Ferrell, so even with a calibrated ionization detector no useful information regarding ion yields could have been obtained.

The model presented in Chapter II predicts, for the case where the shift is not too large, a blue shift in the position of an otherwise unaltered atomic line. The data presented in Figs. 5 and 6 is in excellent quantitative agreement with that prediction. In combination with the observations by Ferrell *et al.*, these results completely confirm the model.

As discussed in Chapters I and II, three-photon interference in general, and the angle- and pressure-dependent shift described in Chapter II in particular, arise due to the generation in the nonlinear medium of a polarization at the sum frequency $\omega_M$. If, however, the three-photon excitation is tuned near a transition which is not dipole-allowed in one photon no significant polarization at $\omega_M$ will occur. In this case the cancellation and shifting effects discussed here should be absent.

To test this prediction, the $5p^6 \rightarrow 5d[\frac{5}{2}]_3^O$ transition was studied. In Fig. 7 are shown two excitation profiles for this transition. Here $\lambda_1 \approx 2972$ Å, $\lambda_2$ is about 6614 Å, and $\theta$ is 14.4°. The upper profile is at a xenon pressure of 100 Torr, while for the lower $P_{Xe} = 400$ Torr. If the transition were allowed in one photon, there would be essentially complete cancellation of on-resonance excitation, while a peak due to absorption of sum-frequency light would be found with a large (and pressure-dependent) shift. Here, with $\Delta J = 3$, the transition is not allowed with one photon. No cancellation and no shift are observed, thus demonstrating the importance of the sum-frequency field to cancellation and to the shifting process. The scans in Fig. 7 were taken with the intracavity etalons in place in both lasers to reduce the laser bandwidths and make any shift that took place more easily discernible. The FWHM of the narrower of the excitation profiles in

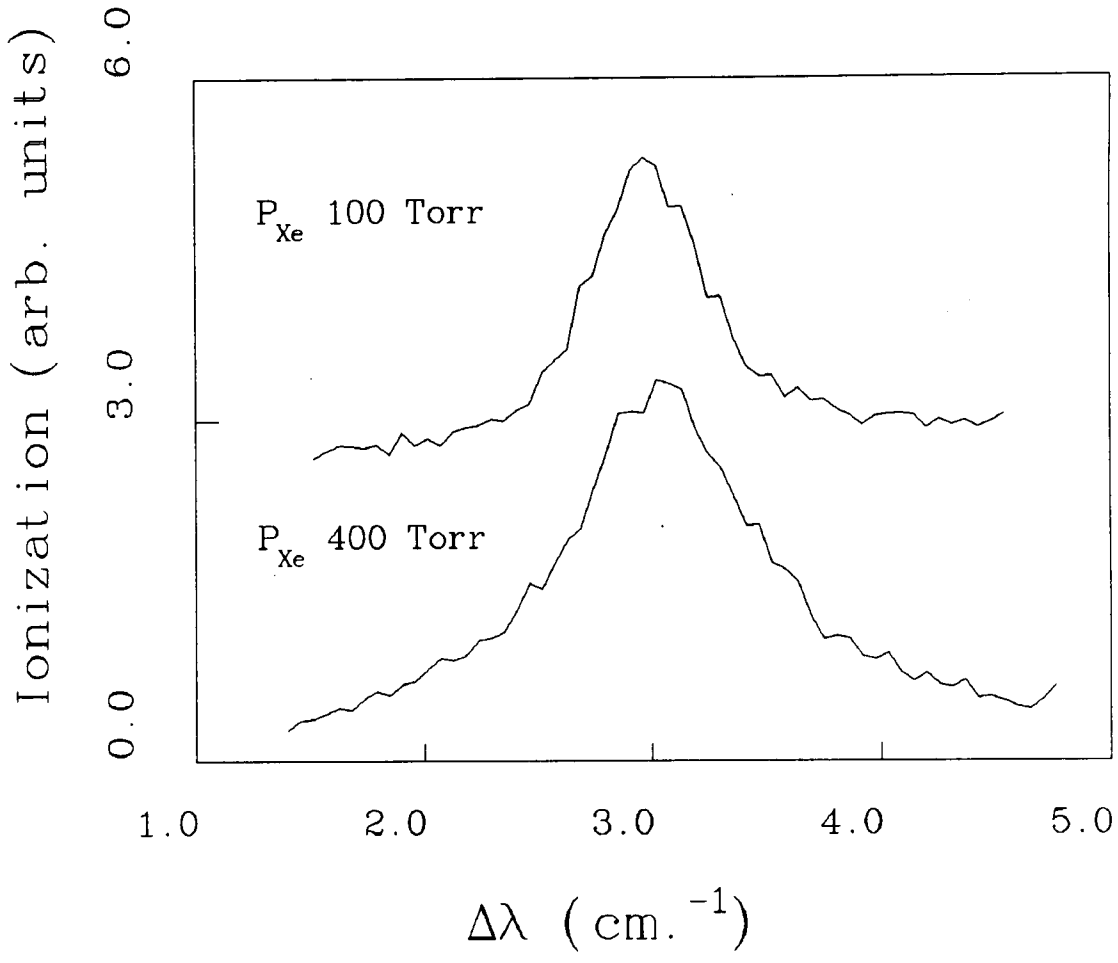


Figure 7. Excitation Profiles of the Xenon $5d[\frac{5}{2}]_3^o$

$\theta$ is 14.4°. No shift occurs because one-photon electric dipole transitions between the J=3 upper state and the J=0 ground state are not allowed. These scans were performed by pressure tuning one of the dye lasers; the horizontal axis is the shift from the zero cavity-pressure wavelength.

Fig. 7 is about 0.5 $cm^{-1}$, while the laser bandwidths with both etalons in place are expected to give a FWHM of about 0.33 $cm^{-1}$; the difference, as well as the increase in width between the 100 and 400 Torr profiles (from 0.5 $cm^{-1}$ to 0.85 $cm^{-1}$), is due to pressure-broadening mediated by multipole interaction terms of higher order than the dipole-dipole. The dipole-dipole broadening term is, of course, zero for a transition not allowed with one photon.

The remainder of this chapter is devoted to a study of the three-photon shift occurring at the xenon $5d[\frac{3}{2}]_1^O$ level when two-color laser excitation is employed with $\theta \ll \pi$. In Fig. 8 the angle between the beams is 22.8°. At a) the xenon pressure is 100 Torr; one peak is seen at about 649.1 nm; the unshifted (low pressure) position of the three-photon resonance is at about 650.185 nm (marked by the vertical line), so a shift of more than 10 Å has occurred. At b), a mirror was placed in the red (6500 Å) beam and adjusted to retroreflect the light; now excitation of the form $2\omega_1 + \omega_2$ can take place either by the absorption of two photons from the UV beam and one from the forward direction of the red beam, giving $\theta = 22.8°$ as before, or by the absorption of two photons from the UV beam and one from the retroreflected red beam, making $\theta = 157.2°$. The result is two values of $\Delta_\theta$ and two peaks. Since $\Delta_\theta \propto (1 + \cos\theta)^{-1}$, the shift for 157.2° is quite small, and the peak is nearly at the unshifted position of the resonance. In c), the xenon pressure is increased to 200 Torr; both peaks shift farther to the blue, with the shift being proportional to the density as predicted. The position of the unshifted resonance in Fig. 8 was determined by adding the calculated shift to the observed centroid position for each of the peaks and taking the average.

Note that the peaks corresponding to 22.8° are considerably narrower and taller than those showing only a small shift. As discussed in Chapter II, the shifted peak will have the amplitude and width of the atomic line only if $\Gamma_{EFF} = \Gamma_P$; this is not expected to be the case for detunings (shifts) of more than 20 $cm^{-1}$ or so. The $\theta = 22.8°$ shift shown in Fig. 8 for 100 Torr is about 26 $cm^{-1}$, so the difference in widths is not

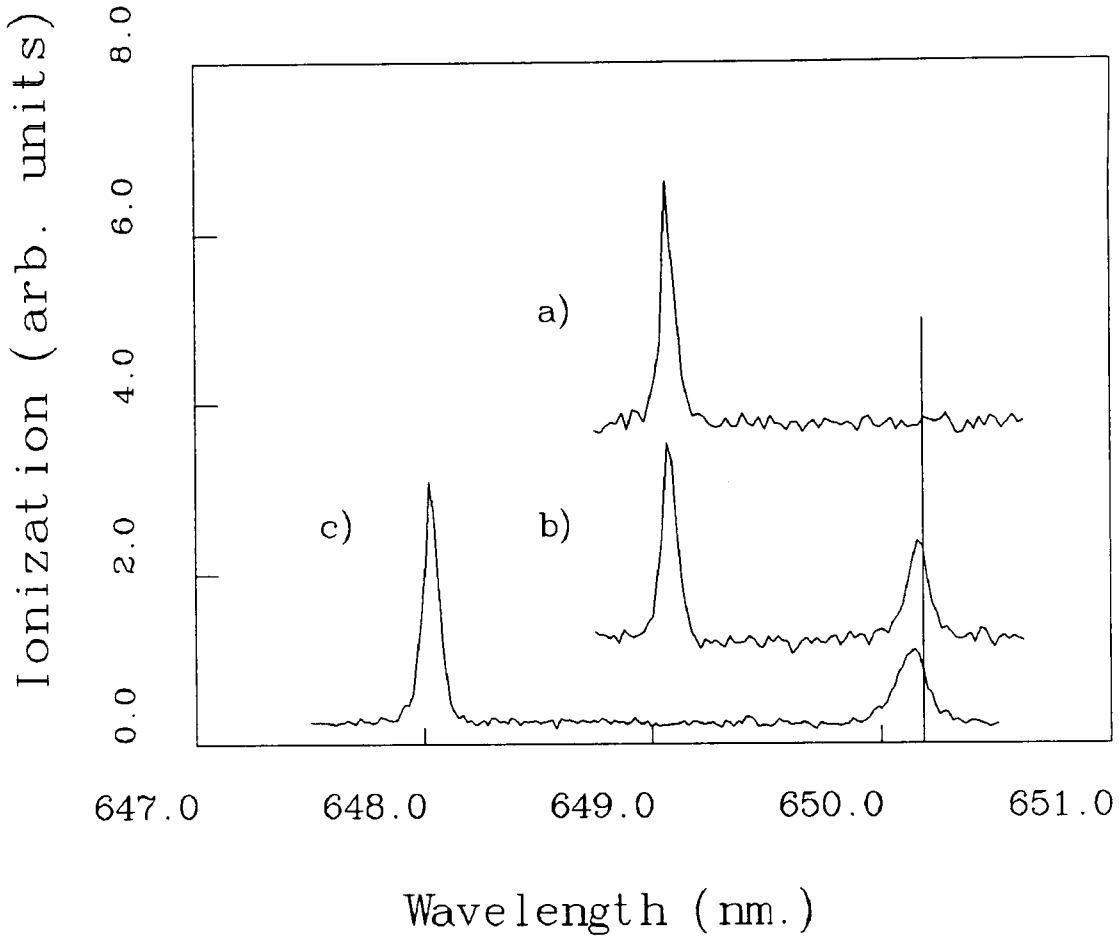


Figure 8. Pressure Shift of the Xenon $5d[\frac{3}{2}]_1^o$.

$P_{Xe}$ = 100 and 200 Torr with $\theta = 22.8°$. The position of the unshifted resonance is given by the vertical line at 650.185 nm. At a), $P_{Xe}$ = 100 Torr, and a shift of more than 1 nm. is seen. At b), one laser beam is retroreflected, giving an additional excitation pathway with $\theta = 157.2°$ and an additional peak. At c), $P_{Xe}$ = 200 Torr, and both peaks shift farther to the blue.

unexpected. Also, the peaks at the large shift are taller than those at the small shift; since the height of the peak of the excitation profile in the large shift regime should be proportional to $\Gamma_{EFF}^{-1}$, and since $\Gamma_{EFF} < \Gamma_P$, the larger peak height is consistent with the model. Quantitative comparison of the expected relation of peak height and width between the peaks at large and small shifts is not possible, however. The peaks with a small shift were produced by retroreflecting the red laser beam, making the excitation at 157.2° less intense due to losses from the window surfaces and at the mirror. Also, the retroreflected red beam will have a poorer temporal overlap with the UV beam due to the extra 1 to 2 nanosecond time delay involved in the extra path length to the mirror and back.

Excitation profiles of the shifted peak were taken for angles of 28.4°, 22.8°, 18.1°, and 10.1°, with xenon pressures ranging from 50 Torr to 800 Torr; a total of 35 profiles were taken. The large angle (small shift) regime was not investigated further. The centroid wavelength and FWHM of each profile was found by measuring the values off a plot of the scan; in light of the very large ratio of the shift to the width, it was felt no substantial advantage could be had by employing a computer curve-fitting program to determine the centroid and width more accurately.

It was discovered early in the course of the experiment that the fixed-frequency dye laser which drove the doubling crystal to generate light at wavelength $\lambda_1$ had an unfortunate characteristic. As mentioned before, an intracavity etalon was employed in this laser to minimize the bandwidth. It was found that the dye laser could lase simultaneously on two adjacent etalon modes (with an observed separation of about 1.6 $cm^{-1}$), producing, in the worst case, a double-peaked excitation profile, and in other cases a broadened, asymmetrical excitation profile. Careful adjustment of the angle of the etalon with respect to the axis of the laser cavity could eliminate one of the two modes; however, a change in the angle of the etalon corresponds to a change in the wavelength of the transmission maximum. It was found the etalon angle needed for

single etalon-mode operation changed from day to day, and so the wavelength of the second laser which brought $2\omega_1 + \omega_2$ into resonance changed also. Fortunately, stable single etalon-mode operation without adjustment was possible for the four to six hour duration of a data taking session, so all that was required was a means to correct data taken in different sessions to a common wavelength scale.

Data at a given beam intersection angle $\theta$ was taken in a single session; the etalon was adjusted for single-mode operation at the start of the session and not changed afterwards. The spectral output of the laser with the intracavity etalon was checked with a viewing etalon before each scan. If double-mode operation was observed, the etalon was readjusted and all the data for that session was taken again; fortunately, this happened infrequently. To correct the data sets taken in different sessions with different values of the $P_{Xe} = 0$ resonant wavelength (due to the adjustment to the etalon), a linear recursion in $P_{Xe}$ was performed on the part of each data set with $P_{Xe} \leq 400$ Torr; the pressure dependence of the shift was more nearly linear for this range of pressures. The $P_{Xe} = 0$ intercept was then the wavelength for $\lambda_2$ which made $2\lambda_1 + \lambda_2$ resonant with the unshifted ($P_{Xe} = 0$) resonance for that run. These intercept values were used to shift all the data sets to a common zero-pressure resonance wavelength of $\lambda_2 = 6500$ Å.

In Fig. 9 the shift $\Delta_\theta$ of the centroid position to the blue of the 6500 Å zero-pressure resonance wavelength is plotted *vs.* xenon pressure for each of the four angles. For angles much less than $\pi$, such as those discussed here, $\Delta_\theta$ is much larger than the other pressure dependent shifts, so $\bar{\Delta}_P = \Delta_\theta$ to very good accuracy. For $\Delta_\theta \leq 100$ Å, the shift is linear in pressure with a different slope for each angle, as predicted. For shifts of more than 100 Å, however, a departure from the linear pressure dependence is evident; this discrepancy will be discussed below. The slopes of the straight lines in Fig. 9 are calculated from the formula for $\Delta_\theta$ given in Chapter II using $F_{01} = 0.346$ for the oscillator strength. This value for $F_{01}$ was found from the data for $\theta = 28.4°$ and

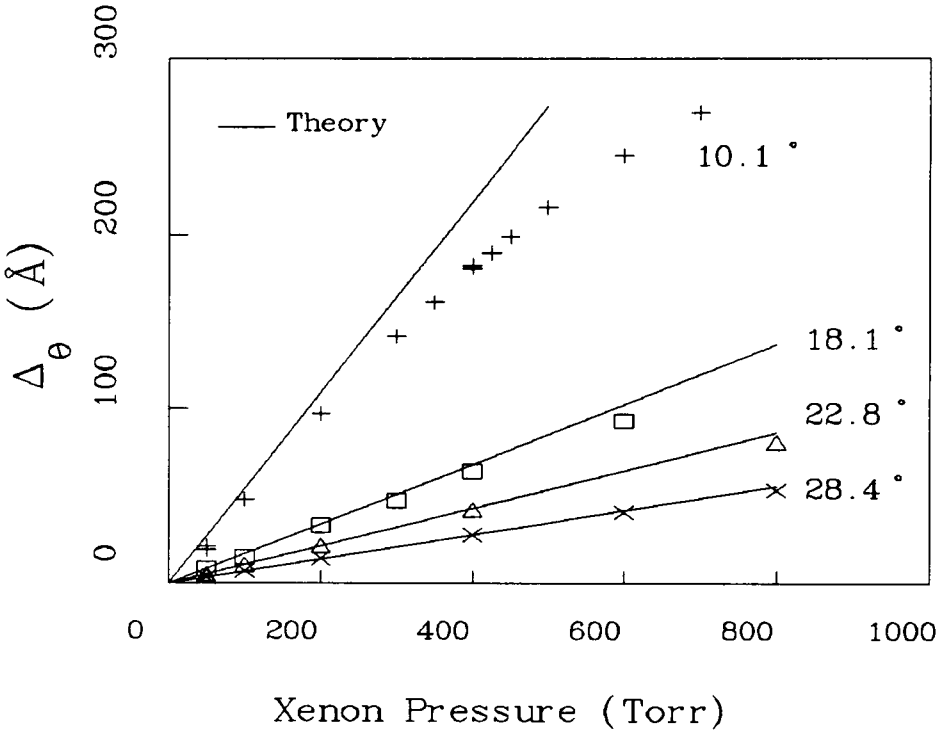


Figure 9. Shift *vs.* Xenon Pressure for Four Angles

$\Delta_\theta$ is the shift of the centroid of the excitation profile to the blue of the 6500 Å zero-pressure resonance wavelength. The straight lines have slopes calculated according to the formula for $\Delta_\theta$ in Chapter II with $F_{01} = 0.346$.

22.8° with $P_{Xe} \leq 400$ Torr; this subset of the data showed the most linear dependence of shift on pressure. The shift values $\Delta_\theta$ were then multiplied by $1 - \cos\theta$ to remove the angular dependence, the data sets combined, and a linear recursion run to find the best-fit slope. From this the value of the oscillator strength could be found.

In Ref. 40 Aymar and Coulombe calculate the absorption oscillator strength for the xenon $5p^6 \rightarrow 5d[\frac{3}{2}]_1^O$ transition to be 1.09; they use a central field model with an intermediate coupling scheme and include the effect of configuration mixing. In separate studies Geiger[41] and Castex[42] both report measured values for $F_{01}$ of 0.395. Castex employed an absorption method, while Geiger determined the oscillator strength by examining the energy distribution function of monoenergetic electrons scattered by the gas. Ferrell *et al.*[43], using the method outlined earlier of phase matching the third harmonic with a positively dispersive buffer gas,[23] finds $F_{01} = 0.37 \pm 0.019$. These values are not too dissimilar from the value of 0.346 reported here. As the exact determination of $F_{01}$ was not the primary goal of this experiment, no great care was taken to minimize the uncertainty in the experimental parameters. The principle unknown in the accuracy of the value found here is the accuracy of the manometer used to measure $P_{Xe}$; of the other experimental parameters, $\theta$ was known to within a few percent, while the observed shift $\Delta_\theta$ can in principle be known to very high accuracy, and was in fact measured to within a few percent. In principle, this method of determining oscillator strengths could be made accurate to within some fraction of the ratio of the line width to the shift, so with care in the measurement of the pressure and the angle, $F_{01}$ could be found to within 0.1%.

The potential accuracy of this method (in which phase matching is achieved with an angle between the laser beams) is much greater than with the otherwise rather similar method used by Ferrell *et al.* in which phase matching is achieved by use of a buffer gas. The addition of a buffer gas causes the formation of mixed dimers, the concentration of which is proportional to the product of the number densities of the resonant and buffer

gases. These mixed dimers have resonant transitions in the neighborhood of the resonant gas transition under investigation. To reduce the contribution of the dimer transitions to the index of refraction, and thus to reduce the effect of the dimers on the determination of the oscillator strength, the detuning of the phase matching point from the resonant gas transition must be kept small. But the determination of the oscillator strength is done by observing the shift in the position of the phase matching point as a function of resonant gas density, and if the shift is small the accurate measurement of the shift becomes more difficult, requiring, for instance, computer fitting of a predicted lineshape to the observed excitation profile, as is done in Ref. 43. Thus the determination of the shift comes to depend on the model employed for the lineshape. The current method avoids these problems entirely. The shift may be made as large as is consistent with a two-state model for the index of refraction; accurate measurements of the shift may be made independently of the details of the lineshape.

In Fig. 10 the shift data shown in Fig. 9 are plotted in the form $\Delta_\theta(1-\cos\theta)$ *vs.* $P_{Xe}$; since $\Delta_\theta$ is predicted to have a $(1-\cos\theta)^{-1}$ dependence on $\theta$, this has the effect of removing the angular dependence. If the experimental data followed the form of equation 2.52, then all the data points would fall on the line. As can be seen, the data for larger values of $\theta$ does follow the predicted linear pressure dependence quite well, while the data for smaller values of $\theta$ (especially 10.1°) shows a substantial deviation from linearity for larger values of $P_{Xe}$, just as in Fig. 9.

In Chapter II it was shown that in the large shift regime the shifted peak occurs at the detuning from three-photon resonance where $\Delta k_r = 0$. Thus far the shift has been discussed in the context of a two-state model in which all the index of refraction at the mixing frequency $\omega_M$ is due to the nearby three- and one-photon allowed transition. There are, of course, other one-photon allowed transitions from the ground state in the xenon atom. If the detuning from the $|0>\rightarrow|1>$ transition becomes large enough, the contribution to the index of refraction due to the other states becomes comparable in

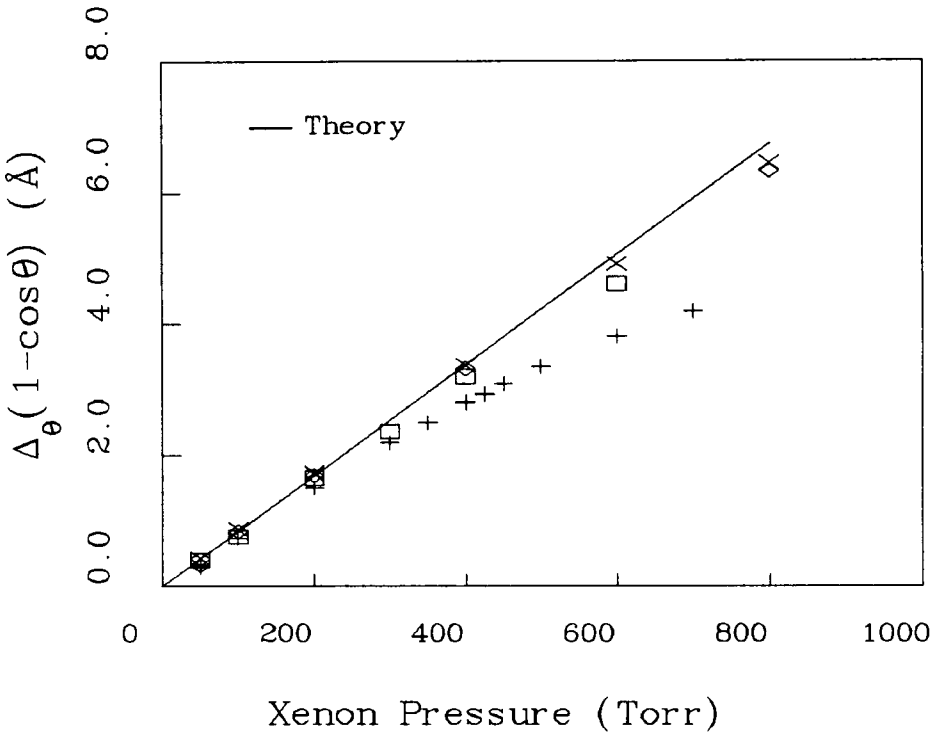


Figure 10. $\Delta_\theta(1-\cos\theta)$ *vs.* Xenon Pressure

The shift values shown in Figure 10 are multiplied by $1-\cos\theta$ to remove the angular dependence. The various angles are designated as follows: × 28.4°, △ 22.8°, □ 18.1°, + 10.1°. The straight line has the slope for $\Delta_\theta(1-\cos\theta)$ given in Chapter II with $F_{01} = 0.346$.

magnitude to that due to the $|0>\rightarrow |1>$ transition. If this is the case, then equation 2.65 must be modified to include the additional states in the calculation of the index of refraction, and the shift will no longer be linearly proportional to $P_{Xe}$. For example, the xenon $7s[\frac{3}{2}]_1^O$ level at 85440.53 $cm^{-1}$ with absorption oscillator strength[43] 0.09 is the next higher-lying one-photon allowed state above the $5d[\frac{3}{2}]_1^O$. The $7s$ state lies approximately 1550 $cm^{-1}$ above the $5d$; with $\Delta_\theta$ as large as 600 $cm^{-1}$ (for $\theta = 10.1°$ and $P_{Xe} = 800$ Torr), the detuning between $\omega_M$ and the $5p^6 \rightarrow 7s$ is small enough for the $7s$ state to have a considerable effect on the phase matching. If the $7s$ is designated state $|2>$, then equation 2.65 would be modified to

$$-\Delta k_r \approx k_M - \frac{\omega_M}{c} + \frac{\kappa_{01}}{\delta_1} + \frac{\kappa_{02}}{\delta_2}, \tag{3.1}$$

where $\kappa_{02} \approx 0.0265 N F_{02}$, and $\delta_2 = \delta_1 - (E_2 - E_1)/\hbar$ is the detuning of $\omega_M$ from resonance with the transition $|0>\rightarrow |2>$. As shown earlier, if only the $5d$ resonance is included in the phase-matching calculation, a linear dependence of shift on pressure is found; inclusion of the nearby $7s$ state has the effect of making that dependence sublinear for the larger pressures, so the expected dependence will be nearly linear in $P_{Xe}$ for small pressures and curve away below a linear dependence at higher pressures. All the other one-photon allowed transitions in xenon are at sufficiently large detunings from the $5p^6 \rightarrow 5d$ transition to have little effect on the curvature; instead they produce mainly a small shift in the position of the phase matching detuning.

In Fig. 11 the data for $\theta = 10.1°$ is plotted against both the linear shift prediction (equation 2.52) and the prediction of a model[15] in which the index of refraction at $\omega_M$ is approximated in a more detailed treatment. For small shifts ($\Delta_\theta < 100$ Å) the two models differ only slightly in the magnitude of the shift predicted; for larger shifts, where the contribution from the $|0>\rightarrow |1>$ transition becomes smaller, the predictions differ substantially. Excellent agreement with the detailed model is found.

A summary of the detailed model for phase matching (which is described in some-

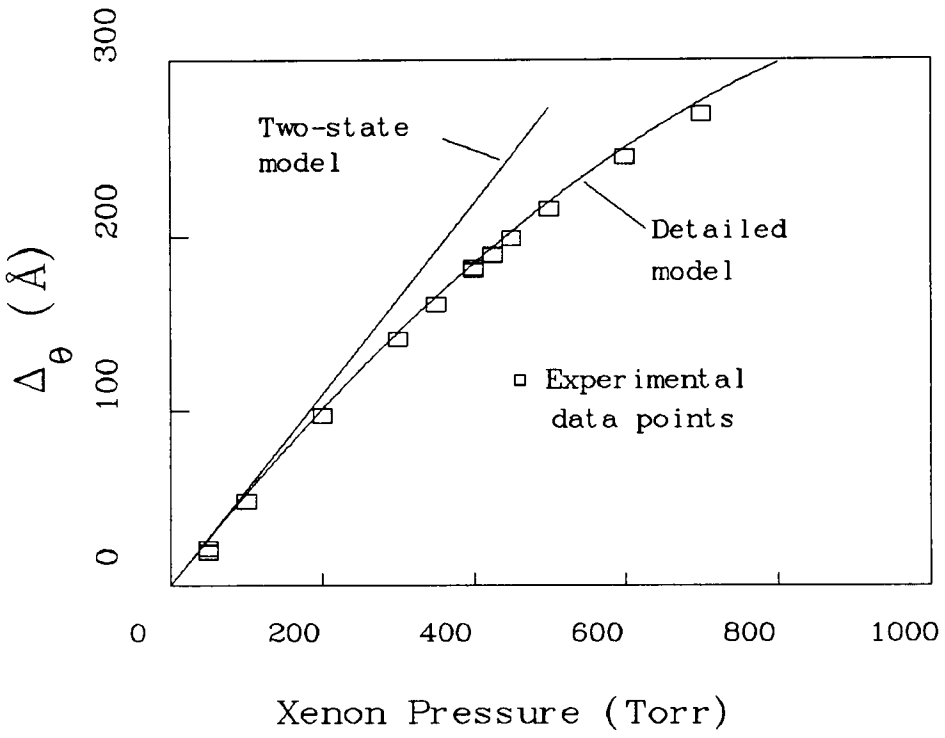


Figure 11. Correct Prediction of Large Shifts

The squares are the observed shifts for $\theta = 10.1°$. The straight line (labeled 'Two-state model') is the shift predicted by a model which includes only the $5p^6 \rightarrow 5d$ transition in the calculation of the index of refraction. The curved line (labeled 'Detailed model'), which fits the data quite well, is found using a model which more accurately estimates the index of refraction at large detunings from the $5d$.

what more detail in Ref. 15) will be given here. The phase mismatch is given by

$$\begin{aligned}\Delta k_r &= k_m - \frac{\omega_M n(\omega_M)}{c} \\ &= k_m - \frac{\omega_M}{c} - \frac{\omega_M N}{c} F(\omega_M),\end{aligned} \tag{3.2}$$

where $n(\omega_M) = 1 + NF(\omega_m)$ is the index of refraction at frequency $\omega_M$ and

$$F(\omega) = \frac{2\pi e^2}{m} \sum_{\omega_n} \frac{F_{0n}}{(\omega_n - \omega_0)^2 - \omega^2}. \tag{3.3}$$

Here $F_{0n}$ is the oscillator strength of the $|0> \rightarrow |n>$ transition, and the summation is to include an integral over transitions to the continuum. Twenty-three oscillator strengths for strong resonance transitions in xenon are known. By the Thomas-Reiche sum rule the sum of all the resonance transitions should equal 54, but all the known values sum to about 1, so the bulk of the oscillator strength therefore lies in inner-core transitions at very high energy. To estimate the effect of these high-energy transitions on optical-frequency oscillator strengths, the sum in equation 3.3 is divided into two parts: one is a sum over the known oscillator strengths, and the other a sum over three unknown oscillator strengths resonant at 0 eV, 13 eV, and 25 eV (corresponding to DC, 953 Å, and 496 Å). Note that 13 eV is just above the first ionization potential of xenon. The values of the unknown pseudo-oscillator strengths are found by fitting the formula for $n$ to known values in the range of 1 to 6 eV. The phase matching point is then found by using equation 2.12 to find the value of $k_M$ and solving equation 3.2 numerically for $\Delta k_r = 0$.

In Chapter II the dependence of the FWHM of the excitation profile $2\Gamma_{EFF}$ on the absorption coefficient $\beta$ at the detuning of the shifted peak was found. In Fig. 12 the observed FWHM of the excitation profiles is plotted against the xenon pressure for each of the four angles used. The straight line has the slope for $2\Gamma_P$ found earlier. The shifts corresponding to $\theta \geq 18°$ are less than 100 Å; in this region the observed width of the excitation profile is less than $2\Gamma_P$, so the effective value of the absorption is less than that

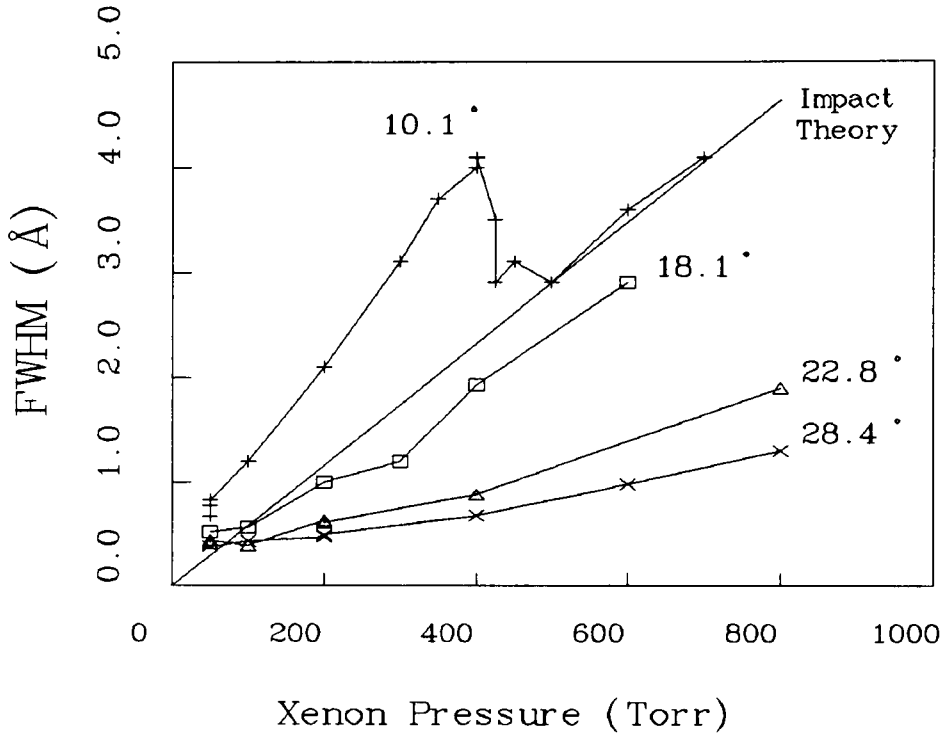


Figure 12. Width of the Excitation Profile *vs.* Xenon Pressure

The FWHM of the excitation profile is plotted against $P_{Xe}$ for each of the angles used. The straight line (labeled 'Impact Theory') has slope $2\Gamma_P$, with $\Gamma_P$ found according to the impact theory of pressure broadening. As expected, the absorption (and thus the width of the excitation profile of the shifted line) is not well described by this value of $\Gamma_P$ at the large detunings found here.

given by $\beta = 2\kappa_{01}\Gamma_P/\delta_1^2$. The data for $\theta = 10.1°$, however, shows $\Gamma_{EFF} > \Gamma_P$. However, this data may have been taken in a regime where $\beta L$ is no longer much greater than 1; in this case, the line shape is expected to start to broaden and resemble the phase matching profile rather than a Lorentzian. Inspection of the excitation profiles reveals no obvious difference in line shape between the 10° data and that taken at larger angles, but the difference in a Lorenztian and the central maximum of a sinc function (sinc(x) = sin(x)/x) might not be evident when looking at noisy data. The conspicuous dip at about 400 Torr in the 10° data is of unknown origin; it occurs at a sum-frequency wavelength of 84390 $cm^{-1}$, corresponding to a detuning of about 500 $cm^{-1}$ from resonance with the $5p^6 \rightarrow 5d[\frac{3}{2}]_1^O$ transition.

This method could obviously be used for measurements of the absorption coefficient $\beta$ at VUV wavelengths, especially at relatively large detunings from three-photon resonance. The theory presented in Chapter II for the width of the profile in the large shift regime could be modified to account for the effect of other nearby resonances on the line shape. If $\beta L$ became too small in the region of interest it might also prove necessary to fit equation 2.77 to the observed line shapes. In Refs. 23, 20, and 43 the measurement of absorption coefficients by the analogous method of phase matching with a buffer gas is described. The current method, in which phase matching is achieved by an angle between the laser beams, is superior because effects due to mixed dimers are absent.

## Summary

The pressure- and angle-dependent blue shift discussed in Chapter II and references 16 and 18 was studied experimentally at the xenon $5d[\frac{3}{2}]_1^O$ level with $\theta$ in the range from 180° to 10.1° and xenon pressures from 50 to 800 Torr. For the $\theta = 180°$ case, excellent agreement between theory and experiment for both the shift and the line width was found; also, the data of Ferrell *et al.* for this transition was found to agree with

prediction. In this regime, where the shift $\Delta_\theta$ is comparable in size to the pressure-broadened line width, the shifted line has the same width as it would in the absence of the shift. For smaller values of $\theta$, for which the shift is much larger, the shift was found to obey the predicted linear pressure dependence for shifts of less than 250 $cm^{-1}$. A new value of the oscillator strength for the transition was found from the data in this linear-shift regime. Shifts of more than 250 $cm^{-1}$ were found to show a sublinear pressure dependence which is explained well in terms of a more detailed model of the index of refraction of xenon. A $\Delta J = 3$ three-photon transition ($5p^6 \rightarrow 5d[\frac{5}{2}]_3^O$) was found to show neither three-photon cancellation nor the three-photon shift, as predicted.

# CHAPTER IV

## Theory of Four-photon Suppression

In this chapter and the next the three-photon interference effect is studied in the context of the excitation of a four-photon resonant state. Four laser photons are resonant with a transition allowed in two and four photons; the laser frequencies are chosen to make three laser photons of frequency $\omega_1$ nearly resonant with an intermediate state to which transitions are allowed with one and three photons. The frequency $\omega_2$ of the fourth photon is then chosen to make $3\omega_1 + \omega_2$ resonant with the four-photon transition. As is discussed at length in the first three chapters of this dissertation, when a three-photon excitation is tuned near a three- and one-photon allowed transition the sum-frequency field (in this case a third-harmonic field) has a profound effect on the atomic response. In the situation under discussion here, where the three-photon state is an intermediate level for the excitation of a four-photon state, the effect of the internally generated sum-frequency field is to produce a second excitation pathway between the ground state and the four-photon state; that is, the four-photon state may be excited by the absorption of one third-harmonic photon plus another laser photon as well as by the absorption of four laser photons. An interference between these two pathways can occur which can suppress or even cancel the excitation of the four-photon state.

In the first section of this chapter the action of the three-photon interference effect in a focused, two-color, four-photon resonant situation is related to the previously described model for unfocused, three-photon resonant excitation. The central importance of a mechanism to absorb or otherwise attenuate the freely propagating wave at the sum frequency is discussed. The connection between the experiment described here, in which

the sum-frequency wave is diminished by a large phase mismatch, and the experiment of Blazewicz *et al.*,[44] in which the sum-frequency wave is attenuated by two-photon absorption, is developed in this context. Reference is also made to observations[10,45] at other four-photon resonances in xenon in which interference at an intermediate three-photon resonance produces unexpected behavior. In the second section of this chapter a theoretical model for the simultaneous excitation of a four- and two-photon allowed state both by the laser fields and by the internally generated sum-frequency field is described; absorption by either one or two-photon processes is neglected. The model is used to predict the ratio of the ionization without the three-photon interference effect to the ionization when the interference is present. In Chapter V the predictions of this model are found to be in excellent agreement with experiment.

## Introduction

In the three-photon resonant cases discussed earlier, in which the laser beams were unfocused, the cancellation of the excitation of the three-photon resonance was complete when the laser excitation was by three photons all traveling in the same direction; even when an angle was introduced between the laser beams no on-resonance excitation was found until, with the beams counterpropagated, excitation was found at a frequency shifted only slightly to the blue of the three-photon resonance. Consider the situation shown in Fig. 8 a), where $\theta$ is 22.8°. Excitation (ionization) is seen only at a detuning of about 25 $cm^{-1}$ from the three-photon resonance; as shown in Chapter II, the detuning which produces a peak in the ionization is that for which the laser field and the sum-frequency field are phase matched; cancellation elsewhere is complete. If $\theta$ is zero, then the phase matching detuning becomes arbitrarily large and no excitation is seen for any detuning.

If, however, the laser beam is focused the situation is quite different. As discussed in

Chapter I, phase-matched generation of a sum-frequency field can occur with a focused beam due to the $\pi$ phase change introduced by focusing. A peak in the ionization will be found to the blue of the three-photon resonance, the detuning from resonance depending on the number density, the oscillator strength of the transition, and the confocal parameter of the focused beam. As is discussed in Refs. 9 and 10, excitation on-resonance can be seen for sufficiently low pressures, but as the pressure is raised the on-resonance excitation becomes canceled.

Now consider the situation illustrated in Fig. 13 in which two laser beams of frequencies $\omega_1$ and $\omega_2$ are employed. The beam at $\omega_1$ is focused and the frequency chosen to make it nearly three-photon resonant with a transition $|0> \rightarrow |1>$ which is allowed with both one and three photons; the detuning of $\omega_1$ from exact three-photon resonance is $\delta_1$. The frequency $\omega_2$ is chosen to make $3\omega_1 + \omega_2$ four-photon resonant with a transition $|0> \rightarrow |2>$ which is allowed in two and four photons. Ionization from state $|2>$ occurs by the absorption of additional photons. If $\omega_1$ is tuned to the blue of $|1>$ to be at the peak of the third-harmonic phase matching profile, excitation of $|2>$ will occur, principally by the absorption of one third-harmonic photon plus one photon at frequency $\omega_2$. As $\omega_1$ is tuned closer to exact three-photon resonance the phase mismatch between the three-photon laser field and the third-harmonic field will become larger and larger, resulting in a decrease in the pumping rate of $|2>$ due to the third harmonic. If $\delta_1$ is zero, three-photon cancellation will occur at state $|1>$ and the excitation of $|2>$ will be canceled as well. Observation of the ionization signal due to the excitation of state $|2>$ as $\omega_1$ is tuned closer to the three-photon resonance should thus allow the observation of the degree of suppression of the excitation of $|2>$ by the interference at $|1>$.

If the three-photon resonant laser is unfocused, as in the situation discussed in Chapter II, strong absorption is necessary at the sum frequency for three-photon cancellation to occur. At any point $z$ in the medium the field at the sum frequency has two

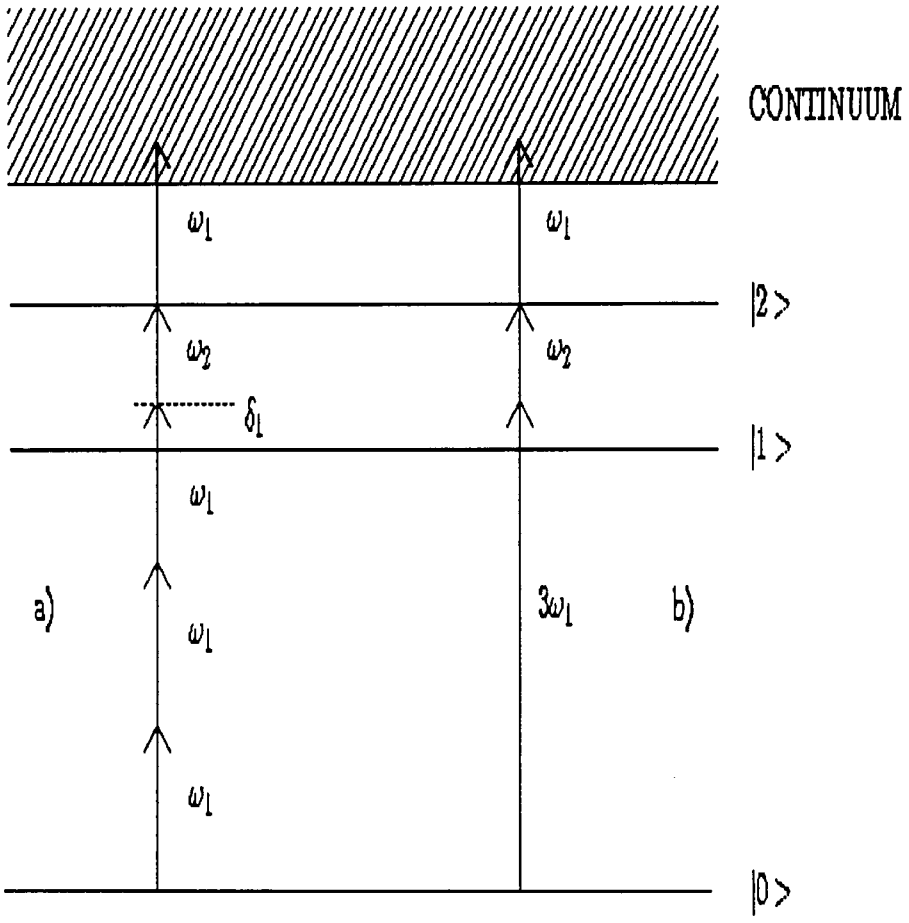


Figure 13. The Simultaneous Excitation of |2> by Two Pathways

At a) the excitation of state |2> is by three laser photons nearly resonant with |1>, plus one additional photon of another color, while at b) the excitation of |2> is by one third-harmonic photon plus one photon of another color. Interference between the two pathways to |1> can suppress the excitation of |2> and thus the MPI signal.

sources: one is the polarization occurring in the medium at $z$, and the other is the free electromagnetic wave which propagates to $z$ from other locations in the medium. The local term follows the laser adiabatically, and, as shown in Chapter II, gives rise to a one-photon Rabi frequency which exactly cancels the three-photon Rabi frequency due to the laser. In the unfocused case strong absorption is necessary to eliminate the propagating, nonlocal term. The important point here, however, is not how the propagating part of the sum-frequency field is eliminated, but merely that any means of eliminating the propagating part will allow the cancellation between the local part and the laser to be revealed.

There are at least three means of eliminating the propagating part of the electric field at the sum frequency: pressure-induced one-photon absorption on the far wing of the nearby transition $|0> \rightarrow |1>$; two-photon absorption by the $|0> \rightarrow |2>$ transition of a sum-frequency photon plus a photon of frequency $\omega_2$; and a large phase mismatch parameter $\Delta k_r b$. The theory described later in this chapter, as well as the experimental results given in Chapter V, demonstrate the last case. The suppression of the ionization observed as $3\omega_1$ is tuned closer to exact three-photon resonance is shown to be described quite well by a theory which entirely neglects both absorption processes. Earlier observations by Blazewicz *et al.*[44], which inspired the current work, are now understood to be an example of the second case, in which two-photon absorption is responsible for revealing the cancellation.[46]

The experiment reported by Blazewicz *et al.* in Ref. 44 is similar to the one described here in that four-photon resonant MPI with a nearly three-photon resonant intermediate enhancement is studied. As the nearly three-photon resonant laser is tuned through four-photon resonance with the second laser one would expect to see a peak in the ionization due to the increased resonant enhancement. For some combinations of density, detuning, and confocal parameter this was the case, but under other conditions a decrease in the ionization was observed. This quite surprising and totally counter-

intuitive observation was not understood at the time.

This behavior was seen when using the xenon $6s'[\frac{1}{2}]_1^o$ state (referred to as the $6s'$) as the three-photon intermediate state; both the $5f$ states and the $6p$ were used for the four-photon resonant level. Two-color excitation was used, but in the Blazewicz experiment laser 2 was focused, as was laser 1. As a consequence, the intensity of the light at frequency $\omega_2$ was perhaps three orders of magnitude greater than in the experiment to be described here. The two-photon absorption of light at frequency $3\omega_1$ was thus substantial. Another significant difference in the two experiments is in the selection of the state for the three-photon level. The $6s'$ level lies high enough for ionization to take place from the three-photon level by the absorption of one additional photon of frequency $\omega_1$. As a result, the four-photon resonance response was superimposed upon a spectrally broad background due to direct ionization by one third-harmonic photon plus one additional photon from the first laser. When the first laser was tuned through four-photon resonance with the second laser (that is, $3\omega_1 + \omega_2 = (E_2 - E_0)/\hbar$), the two-photon absorption of the third harmonic was sufficient to allow partial three-photon cancellation to occur at the three-photon level. This partial cancellation of the three-photon resonance resulted in a decrease in the amplitude of the third-harmonic background, and so a dip in the excitation profile was seen. The $6s[\frac{3}{2}]_1^o$ state (referred to as the $6s$), which is the three-photon level in the present experiment, lies enough lower in energy that two additional photons of frequency $\omega_1$ are required to ionize. As a result there is very little of the broad background seen at the $6s'$, and one does not see dips due to three-photon interference under any circumstances.

Also of interest is the observation by Miller and Compton (Ref. 10) of dips in the ionization spectrum of the xenon $5f'$ four-photon resonance; the $6s'$ served as a three- and one-photon allowed intermediate state. At low pressures where no third harmonic was observed the $5f'$ resonance was present as a peak in the ionization spectrum, while at somewhat higher pressures a broad response was seen in both the ionization and third-

harmonic generation spectra, with the four-photon resonance present as a dip in the third harmonic and a peak in the ionization. At still higher pressure (greater than 100 Torr), a dip was present in both the third harmonic and ionization spectra. Again, two-photon absorption of the third-harmonic by the four- and two-photon allowed resonance causes the enhancement due to the three-photon resonance to be diminished. A similar process is responsible for the partial suppression of the xenon $J = 2$ $4f$ four-photon resonances reported in Ref. 45. Here the three-photon intermediate resonance is the $6s$, so no broad background profile due to absorption of the third harmonic is observed. At low pressures, both the $J = 2$ and $J = 4$ four-photon resonances are seen. An increase in pressure results in the suppression of the $J = 2$ transition (which is coupled to the ground state in two photons) relative to the $J = 4$ transition (which is not coupled to the ground state in two photons).

In Ref. 46 a detailed theory for the effect of three-photon interference on four-photon resonant excitation is presented. Included in that work are numerical evaluations of the theory for choices of parameters comparable to the situation studied by Blazewicz *et al.*; a dip in the ionization comparable to those observed in experiment is produced. Also given there is an explanation for the observation of third-harmonic generation on the red (positively dispersive) side of a three-photon resonance,[47] where it should be forbidden by phase matching considerations; this anomalous production of third harmonic is shown to be a consequence of the non-uniform two-photon absorption of the third harmonic that can occur when both laser beams are tightly focused. Finally, Ref. 46 includes a detailed development of a theory of the effect of three-photon interference in the absence of significant absorption; this development is outlined in Ref. 48 and repeated in the following section in somewhat more detail.

# Theory

In this section the ionization from a four-photon resonant state is calculated both with and without the effect of three-photon interference occurring at an intermediate state. As discussed earlier, retroreflecting the laser beam which is nearly resonant with the three-photon allowed state provides an additional excitation pathway which effectively lacks the three-photon interference effect; a measurement of the ratio of the ionization occurring without counterpropagation of the three-photon resonant laser to that found with counterpropagation would provide a measure of the effectiveness of the three-photon interference effect in suppressing the excitation of the four-photon resonant state. Here a model for the excitation of the four-photon state is developed in which the effect of three-photon interference is included without absorption of the third-harmonic light; an expression for the ratio of ionization with and without the interference is found. In Chapter V the predictions of this expression are compared with experiment. The development in this section follows closely that given in Refs. 46 and 48.

Consider MPI with the pumping scheme shown in Fig. 13. Electric dipole transitions between the ground state $|0>$ and state $|1>$ are allowed with one and three photons, while $|2>$ is coupled to the ground state in both two and four photons, with state $|1>$ serving as a near resonant intermediate state. Laser 1 of frequency $\omega_1$ is focused with waist radius $w$ and confocal parameter $b$, and has a detuning from three-photon resonance of $\delta_1 = 3\omega_1 - (E_1 - E_0)/\hbar$; its direction of propagation is chosen to be along the $+\hat{z}$ axis. Laser 2 of frequency $\omega_2$ is unfocused, temporally coincident with laser 1, and is assumed to be of uniform intensity over the focal region of beam 1; $\delta_2 = 3\omega_1 + \omega_2 - (E_2 - E_0)/\hbar$ is the detuning from four-photon resonance.

An atom at cylindrical coordinates $\rho, z$ and time t has a state vector given in the

Schrödinger representation by

$$|\Psi(\rho,z,t)> = a_0 e^{-iE_0 t/\hbar}|0> + A_1 e^{-i\delta_1 t} e^{ik_r(3\omega_1)z}|1> + A_2 e^{-i\delta_2 t} e^{i[k_r(3\omega_1)+k(\omega_2)]z}|2> + \sum_{\mu} \int dE_c\, a_c(E_c,\mu,\rho,z,t)|E_c,\mu> e^{-iE_c t/\hbar}, \tag{4.1}$$

where the rapid parts of the temporal and spatial dependence of the amplitudes $A_1$ and $A_2$ of states $|1>$ and $|2>$ have been written out explicitly. $k_r(3\omega_1)$ is the real part of the propagation vector for light at frequency $3\omega_1$, while $k(\omega_2)$ is the propagation vector at $\omega_2$; since $\omega_2$ is far from resonance with any transition from the ground state, $k(\omega_2) \simeq k_r(\omega_2)$ to good accuracy. $E_c$ and $a_c$ are the energy and probability amplitude, respectively, of a continuum state; $\mu$ represents a set of angular momentum quantum numbers. The time dependent Schrödinger equation is applied to equation 4.1, and an adiabatic-following type approximation used to eliminate the continuum states in terms of an ionization rate. The ac Stark shift due to the coupling of state $|2>$ to the continuum is neglected, as is the spontaneous decay of the population of $|2>$.

States $|0>$ and $|1>$ are coupled both by a three-photon Rabi frequency $\Omega_{10}^{(3)}$ due to laser 1 and by a one-photon Rabi frequency $\Omega_{10}^{(1)}$ due to the internally generated third-harmonic field. An effective or net Rabi frequency $\Omega_{10}^{eff}$, defined as

$$\Omega_{10}^{eff} = e^{-i\Delta k_r z}\Omega_{10}^{(3)} + \Omega_{10}^{(1)}, \tag{4.2}$$

describes this simultaneous, coherent coupling in one and three photons. Here $\Delta k_r$ is the phase mismatch between the propagating third-harmonic field and the laser field.

With the elimination of the amplitude of $|1>$ in terms of the Rabi frequencies, and the assumption of negligible population transfer from the ground state, the equation of motion for the amplitude of state $|2>$ is found to be

$$\frac{dA_2}{dt} = i\left[\delta_2 - \frac{|\Omega_{21}^{(1)}|^2}{\delta_1} + i\frac{\Gamma_{I2}}{2}\right]A_2 - i\frac{\Omega_{10}^{eff}\Omega_{21}^{(1)}}{\delta_1}. \tag{4.3}$$

Here $\Omega_{21}^{(1)}$ is the one-photon reduced Rabi frequency due to the coupling of states $|1>$ and $|2>$ by laser 2. The second term in the bracket in equation 4.3 is the ac Stark shift

of state |2> due to laser 2, while $\Gamma_{I2}$ is the ionization rate from state |2>. Neglecting the Stark shift with respect to the ionization rate, $A_2$ is found to be

$$A_2(t) = -i \int_{-\infty}^{t} dt_1 \, e^{i\delta_2(t-t_1)} \exp\left(-\int_{t_1}^{t} \frac{\Gamma_{I2}(t')}{2} dt'\right) \frac{\Omega_{10}^{eff}(t_1)\Omega_{21}^{(1)}(t_1)}{\delta_1}. \tag{4.4}$$

Laser 2 is assumed to be a multi-mode, broadband device, while Laser 1 is here assumed to be a single-mode device with a transform limited bandwidth, though later this assumption will be relaxed. Laser bandwidth effects are included by evaluating $\rho_{22} = \ll A_2 A_2^* \gg$, where in this case the ensemble average represents an average over the fluctuations of the field of laser 2; this average is carried out by expressing $A_2$ entirely in terms of the field amplitudes and phases and using the field-field autocorrelation function describing the fluctuations of laser 2 to evaluate the ensemble average of $\Omega_{21}^{(1)}$. $A_2 A_2^*$ is given by

$$A_2 A_2^* = \frac{1}{\delta_1^2} \int_{-\infty}^{t} dt_1 \int_{-\infty}^{t} dt_2 \, e^{i\delta_2(t_2-t_1)} \exp\left(\int_{t_1}^{t_2} \frac{\Gamma_{I2}(t')}{2} dt'\right) \exp\left(-\int_{t_1}^{t} \Gamma_{I2}(t') dt'\right)$$
$$\times \, \Omega_{10}^{eff}(t_1) \, \Omega_{10}^{eff}(t_2) \, \Omega_{21}^{(1)}(t_1) \, \Omega_{21}^{(1)}(t_2). \tag{4.5}$$

The field-field autocorrelation function for a chaotic field laser is

$$G^{(n)}(t) = \frac{\ll (E^+(\tau+t))^n (E^-(\tau))^n \gg}{(\ll E^+(\tau)E^-(\tau) \gg)^n}$$
$$= n! \, e^{-n(\Gamma_{L2}t)^2}, \tag{4.6}$$

where $\Gamma_{L2}$ is the bandwidth of laser 2. The ensemble average $\ll\gg$ of equation 4.5 is then taken. Since laser 1 is assumed to be single mode, the ensemble average over its field reduces simply to $\ll \Omega_{10}^{eff}(t_1)\Omega_{10}^{eff}(t_2) \gg = \frac{1}{2}(|\Omega_{10}^{eff}(t_1)|^2 + |\Omega_{10}^{eff}(t_2)|^2)$.

The ionization rate $\Gamma_{I2}$ is assumed to be much less than the bandwidth $\Gamma_{L2}$, so the integrals of $\Gamma_{I2}(t)$ in equation 4.5 will accumulate area mainly for times much greater than the inverse bandwidth of laser 2. Thus the exponential of the integral of $\Gamma_{I2}(t)$ from $t_1$ to $t_2$ will be very nearly unity for times $t_1 - t_2$ on the order of $\Gamma_{L2}^{-1}$. However, the

autocorrelation function will decay for times $t_1 - t_2$ larger than $\Gamma_{L2}^{-1}$, and so the ensemble average of the remainder of equation 4.5 may be crudely approximated as

$$\ll \exp\left(-\int_{t_1}^{t_2} \frac{\Gamma_{I2}(t')}{2} dt'\right) \Omega_{21}^{(1)}(t_1)\Omega_{21}^{(1)}(t_2) \gg \approx \ll \Omega_{21}^{(1)}(t_1)\Omega_{21}^{(1)*}(t_2) \gg, \quad (4.7)$$

Using equation 4.6 with $n = 1$, $\tau + t = t_1$, $\tau = t_2$, and recalling that $\Omega_{21}^{(1)} \propto E^+$, where $E^+$ is the positive frequency part of the electric field due to laser 2, the remaining part of the average becomes

$$\begin{aligned} \ll \Omega_{21}^{(1)}(t_1)\Omega_{21}^{(1)}(t_2) \gg &\approx \frac{e^{-\Gamma_{L2}^2(t_1-t_2)^2}}{2}\left[\ll \Omega_{21}^{(1)}(t_2)\Omega_{21}^{(1)*}(t_2) \gg + \ll \Omega_{21}^{(1)}(t_1)\Omega_{21}^{(1)*}(t_1) \gg\right] \\ &= \frac{e^{-\Gamma_{L2}^2(t_2-t_1)^2}}{2}\left[\ll |\Omega_{21}^{(1)}(t_1)|^2 \gg + \ll |\Omega_{21}^{(1)}(t_2)|^2 \gg\right]. \end{aligned} \quad (4.8)$$

After some manipulation one then finds for $\rho_{22}$

$$\begin{aligned} \rho_{22}(\rho, z, t) = \frac{1}{\delta_1^2}\int_{-\infty}^{t} dt_1\, |\Omega_{10}^{eff}(\rho, z, t_1)|^2 \ll |\Omega_{21}^{(1)}(\rho, z, t_1)|^2 \gg \exp\left(-\int_{t_1}^{t} dt' \bar{\Gamma}_{I2}\right) \\ \times \int_{-\infty}^{t} dt_2 e^{-\Gamma_{L2}^2(t_1-t_2)^2} \cos(\delta_2(t_1 - t_2)), \end{aligned} \quad (4.9)$$

where $\bar{\Gamma}_{I2}$ is the ionization rate evaluated at the average laser power. Since $\Gamma_{I2} \ll \Gamma_{L2}$, the integral of $\Gamma_{I2}(t)$ will accumulate area only over time scales long compared to the coherence time of the laser, so the replacement of $\Gamma_{I2}(t)$ with its average involves little error. With the definition of

$$W_1(y, u) = \int_u^{\infty} dv\, e^{-v^2} \cos(yv) \quad (4.10)$$

equation 4.9 becomes

$$\begin{aligned} \rho_{22}(\rho, z, t) = \frac{1}{\Gamma_{L2}\delta_1^2}\int_{-\infty}^{t} W_1(y, -\Gamma_{L2}(t - t_1))|\Omega_{10}^{eff}(\rho, z, t_1)|^2 \\ \times \ll |\Omega_{21}^{(1)}(\rho, z, t_1)|^2 \gg \exp\left(-\int_{t_1}^{t} dt' \bar{\Gamma}_{I2}\right) dt_1. \end{aligned} \quad (4.11)$$

Here $y = \delta_2/\Gamma_{L2}$. The physical significance of $W_1$ is found by assuming that $W_1$ contains the only rapid time dependence in equation 4.11; this is equivalent to neglecting the

time variation of the temporal envelopes of the laser pulses. Evaluating the integral of $W_1$ with respect to $t_1$ using methods discussed in section II of Ref. 46, one finds the solution consists of two terms. One term is linear in $t - t_1$, and may be identified with the growth of a real population in state $|2>$; that is, the amplitude of state $|2>$ due to this term would remain nonzero even if the laser fields were switched off. The other term is independent of $t - t_1$ after a few coherence times of laser 2; it is small for $\delta_2/\Gamma_{L2}$ small, but becomes relatively more important for larger detunings $\delta_2/\Gamma_{L2}$. It represents the adiabatic following of the laser intensity by the amplitude of $|2>$; if the laser fields were switched off, the amplitude of state $|2>$ due to this term would quickly go to zero.

The evaluation of $\Omega_{10}^{eff}$ in equation 4.11 requires finding the amplitude of the third-harmonic field, which in turn requires finding the polarization in the medium at $3\omega_1$. With the assumption of negligible transfer of population from the ground state, the equation of motion for the density matrix element $\rho_{10} = \ll A_1 a_0^* \gg$ is

$$\frac{d\rho_{10}}{dt} = i\left[\delta_1 + i\left(\Gamma_1 + \frac{\Gamma_{I1}}{2}\right)\right]\rho_{10} + i\Omega_{10}^{eff} + i \ll \Omega_{12}^{(1)} A_2 a_0^* \gg, \tag{4.12}$$

where $\Gamma_1$ is the collisional dephasing rate for the transition $|0> \rightarrow |1>$ and $\Gamma_{I2}$ is the ionization rate from state $|1>$. In the experiment described in Chapter V, in which state $|1>$ is the xenon $6s[\frac{3}{2}]_1^O$, two additional photons of frequency $\omega_1$ are required for ionization by this pathway, so $\Gamma_{I1}$ is quite small and may be neglected. Also, the minimum laser detuning $\delta_1$ employed is large enough to allow a simple perturbation-theory solution of equation 4.12. This yields

$$\rho_{10} = -\frac{\Omega_{10}^{eff}}{\delta_1 + i\Gamma_1} - \frac{\ll \Omega_{12}^{(1)} A_2 \gg}{\delta_1 + i\Gamma_1}, \tag{4.13}$$

where is has been assumed that $\Gamma_1 \gg \Gamma_{L1}$ in keeping with the assumption that laser 1 has a transform limited bandwidth. The first term of 4.13 represents the contribution to the polarization at $3\omega_1$ by the combination of the laser field and the third-harmonic field, while the second term arises from the two-photon absorption of third-harmonic

photons by the $|0>\rightarrow |2>$ transition plus photons from the second laser at frequency $\omega_2$.

With the definition of

$$q = \frac{\delta_2}{\Gamma_{L2}} + i\frac{\Gamma_{I2}}{\Gamma_{L2}} \tag{4.14}$$

and

$$W(q) = \frac{\sqrt{\pi}}{2} e^{-q^2/4} \left[1 - \mathrm{erf}\left(-\frac{iq}{2}\right)\right], \tag{4.15}$$

where erf is the error function, and neglecting $(\Gamma_1 + \Gamma_{I1}/2)^2$ with respect to $\delta_1^2$, the equation for $\rho_{10}$ is

$$\rho_{10}(\rho, z, t) = \frac{\Omega_{10}^{eff}(\rho, z, t)}{\delta_1^2} \left[-\delta_1 + i(\Gamma_1 + \Gamma_{I1}/2) + i\frac{\ll |\Omega_{12}^{(1)}(\rho, z, t)|^2 \gg}{\Gamma_{L2}} W(q)\right], \tag{4.16}$$

where it has been assumed that $\ll |\Omega_{12}^{(1)}|^2 \gg$ is much less than $|\Gamma_{L2}\delta_1|$, that is, that the $|1>\rightarrow |2>$ transition is far from being saturated by laser 2. The evaluation of the ensemble average $\ll \Omega_{12}^{(1)} A_2 \gg$ in equation 4.13 is performed using the autocorrelation function for laser 2; this gives rise to the error function in equation 4.15.

$\Omega_{10}^{eff}$ has two components: one due to the three-photon laser field and one due to the third-harmonic field at $3\omega_1$. Similarly, the polarization $\mathcal{P}_{3\omega_1}$ at frequency $3\omega_1$ will consist of two components: a linear term due to the third-harmonic field and a non-linear term due to the three-photon excitation by the laser. Thus, with $\phi = k_r(3\omega_1)z - 3\omega_1 t$,

$$\mathcal{P}_{3\omega_1}^{+} = N D_{01} \rho_{10} e^{i\phi} = \mathcal{P}_{3\omega_1}^{L} + \mathcal{P}_{3\omega_1}^{NL} \tag{4.17}$$

is the positive-frequency part of the polarization in terms of the linear ($\mathcal{P}_{3\omega_1}^{L}$) and nonlinear ($\mathcal{P}_{3\omega_1}^{NL}$) components. Using equation 4.16 and the definition $\Omega_{10}^{(1)}(\rho, z, t) = e^{-i\phi} D_{10} E_{3\omega_1}^{+}(\rho, z, t)/(2\hbar)$ for the reduced one-photon Rabi frequency due to the positive-frequency part of the third-harmonic field, the linear component of the polarization

is

$$\mathcal{P}^{L}_{3\omega_1} = -\frac{N|D_{01}|^2/(2\hbar)}{\delta_1 + i(\Gamma_1 + \Gamma_{I1}/2)}\left[1 - i\frac{\Delta_S}{\Gamma_{L2}}W(q)\right]E^{+}_{3\omega_1}$$
$$= \chi_0 E^{+}_{3\omega_1}, \tag{4.18}$$

where $\Delta_S$ is the ac Stark shift in the $|0\rangle \rightarrow |2\rangle$ transition due to the first laser.

$\mathcal{P}^{NL}_{3\omega_1}$ is found similarly by using the part of equation 4.16 that depends on $\Omega^{(3)}_{10}$. In the problem under consideration, laser 1 is focused; however, a useful simplification in the form of $\mathcal{P}^{NL}_{3\omega_1}$ is found most easily by using the form of the wave equation that pertains to an unfocused geometry. That is,

$$\frac{\partial^2 E^{+}_{3\omega_1}}{\partial z^2} - \frac{1}{v^2}\frac{\partial^2 E^{+}_{3\omega_1}}{\partial t^2} = \frac{8\pi}{c^2}\frac{\partial^2 \mathcal{P}^{NL}_{3\omega_1}}{\partial t^2}, \tag{4.19}$$

where the linear part of the polarization given in equation 4.18 has been incorporated in the phase velocity $v$ through $v = c/\sqrt{1 + 4\pi\chi_0}$. With the substitution of $\mathcal{P}^{NL}_{3\omega_1}$ into equation 4.19 and some manipulation, the following useful relationship is found:

$$\frac{3\omega_1}{v} - \frac{3\omega_1}{c} \equiv \Delta k - \Delta k_0$$
$$= -\frac{2\pi N|D_{01}|^2(3\omega_1)}{\hbar c}\frac{1 - i\frac{\Delta_S}{\Gamma_{L2}}W(q)}{\delta_1 + i(\Gamma_1 + \Gamma_{I1}/2)}$$
$$\approx \frac{\kappa_{01}}{\delta_1^2}\left[-\delta_1 + i(\Gamma_1 + \Gamma_{I1}/2) + \frac{\Delta_S\delta_1}{\Gamma_{L2}}W(q)\right]. \tag{4.20}$$

Here $\kappa_{01}$ is defined as in Chapters I and II, and $\Delta k_0$ is the phase mismatch due to the non-resonant part of the index of refraction. Recall that the state vector (equation 4.1) did not include any bound states aside from $|0\rangle$, $|1\rangle$, and $|2\rangle$. $\Delta k_0$ is included to account for the effect of these neglected states. Using equation 4.20 one may write

$$\delta_1^2\left(\frac{\Delta k - \Delta k_0}{\kappa_{01}}\right) = -\delta_1 + i(\Gamma_1 + \Gamma_{I1}/2) + \frac{\Delta_S\delta_1}{\Gamma_{L2}}W(q).$$

With this relation $\mathcal{P}^{NL}_{3\omega_1}$ may be written as

$$\mathcal{P}^{NL}_{3\omega_1}(\rho, z, t) \simeq ND_{01}e^{i\phi}\Omega^{(3)}_{10}(\rho, z, t)\left[\frac{\Delta k - \Delta k_0}{\kappa_{01}}\right]e^{-i\Delta k_r z}. \tag{4.21}$$

The form for the nonlinear component of the polarization with laser 1 focused is found simply by combining equation 4.21 for $\mathcal{P}^{NL}_{3\omega_1}(\rho,z,t)$ with the appropriate expression for the electric field due to the focused beam. An unfocused laser beam with a Gaussian transverse profile, frequency $\omega_1$, and propagation vector $k$ traveling in the $+\hat{z}$ direction is described by

$$\vec{E}(\rho,z,t)=\vec{e}\,\frac{E_0}{2}e^{-\rho^2/d^2}e^{i(kz-\omega_1 t)}+c.c. \tag{4.22}$$

Here $\vec{e}$ is the polarization vector, and $d$ is the radius at which the amplitude has decreased to $e^{-1}E_0$. If this beam is focused by a lens of focal length $F$ with the focal point at $z=0$, the field is given by

$$\vec{E}(\rho,z,t)=\vec{e}\frac{E_{0F}/2}{(1+2iz/b)}e^{i(kz-\omega_1 t)}\exp\left(-\frac{\rho^2}{w^2(1+2iz/b)}\right)+c.c. \tag{4.23}$$

$w=\frac{2F}{kd}$ is the $1/e$ radius of the field strength at the focal point, and $b=kw^2$ is the confocal parameter. $E_{0F}$ is the field amplitude at $z=0$; it is related to the amplitude of the unfocused beam by $|E_{0F}|=|2FE_0/b|=|E_0 d/w|$.

By combining equation 4.21 with equation 4.23 the following expression for the nonlinear part of the polarization at $3\omega_1$ is found:

$$\begin{aligned}\mathcal{P}^{NL}_{3\omega_1}=&\frac{ND_{01}(\Delta k-\Delta k_0)\Omega^{(3)}_{10}}{\kappa_{01}(1+2iz/b)^3}e^{3i(kz-\omega_1 t)}\\&\times\exp\left(-3\frac{\rho^2}{w^2(1+2iz/b)}\right)+c.c.\end{aligned} \tag{4.24}$$

$\Omega^{(3)}_{10}$ now refers to the reduced three-photon Rabi frequency corresponding to the laser field intensity found at $z=0$ and $\rho=0$. The $z$ and $\rho$ dependence of $\mathcal{P}^{NL}_{3\omega_1}$ due to focusing is explicit in equation 4.24. With this form for the nonlinear part of the polarization the wave equation for the $e^{-\omega_1 t}$ part of the third-harmonic field is

$$\begin{aligned}\nabla^2E^{+}+k(3\omega_1)E^{+}=&-\frac{4\pi(3\omega_1)^2}{\kappa_{01}c^2}\frac{ND_{01}(\Delta k-\Delta k_0)\Omega^{(3)}_{10}}{(1+2iz/b)^3}e^{3i(kz-\omega_1 t)}\\&\times\exp\left(-3\frac{\rho^2}{w^2(1+2iz/b)}\right).\end{aligned} \tag{4.25}$$

Here $k(3\omega_1) = k_r(3\omega_1) + i\alpha$, where $k_r$ is the propagation vector and $\alpha$ is half the absorption coefficient for the third-harmonic. $\alpha$ may represent either one-photon absorption by the pressure-broadened $|0> \rightarrow |1>$ transition or two-photon absorption by the $|0> \rightarrow |2>$ transition and the second laser.

Equation 4.25 is solved in the paraxial approximation using standard two-dimensional Fourier transform methods as described in Refs. 46 and 14. The solution for the one-photon reduced Rabi frequency $\Omega_{10}^{(1)}$ due to the third harmonic field is found to be

$$\Omega_{10}^{(1)}(\rho, z, t)e^{i\Delta k_r z} = i(b/2)(1 + 2iz/b)^2 \left[\frac{-\kappa_{0,1}}{\delta_1} + i\alpha\right] g(2z/b, \Delta kb/2)\Omega_{10}^{(3)}(\rho, z, t). \tag{4.26}$$

Here

$$\frac{\Delta k_r b}{2} \simeq -\frac{\kappa_{01} b}{2\delta_1}$$

is the phase mismatch parameter, and

$$\kappa_{01} = \frac{2\pi(3\omega_1)N|D_{01}|^2}{c\hbar} = \frac{\pi N e^2 F_{01}}{mc}$$

is as previously defined. In equation 4.26, as well as in the following, $\Delta k_0$ is taken to be zero. Note that $\kappa_{01}$ is proportional to the number density N of the medium and the oscillator strength between $|0>$ and $|1>$. $\alpha$ is one-half the absorption coefficient, so $\Delta k = \Delta k_r + i\alpha$ is the quantity in square brackets in equation 4.26. If $\alpha$ is independent of position, then the function $g(u, v)$ is simply

$$g(u, v) = \int_{-\infty}^{u} \frac{e^{iv(u-u')}}{(1 + iu')^2} du', \tag{4.27}$$

which is the familiar Gaussian diffraction integral for third-harmonic generation in a focused beam with position independent absorption.[24] If $\alpha$ is not independent of $\rho$ or $z$, then $g(u, v)$ is a slightly more complicated function. The effect of absorption on the

excitation is discussed in detail in Ref. 46 in connection with the experiment of Blazewicz *et al.*[44], where the decrease in the ionization occurring at four-photon resonance is shown to be due to absorption of the third-harmonic by two-photon absorption. As noted earlier, absorption of the propagating third-harmonic light is one of the mechanisms for revealing the cancellation of the laser excitation by the adiabatic part of the polarization at $3\omega_1$. In the work reported on here, the mechanism for bringing on the three-photon interference is a large value of $\Delta k_r b$ rather than a large value of $\alpha$. A discussion of the amount of two-photon absorption actually present in the experiment under discussion is included in Chapter V (as well as in Ref. 48); in the following, $\alpha \equiv 0$. The effective Rabi frequency is then

$$\Omega_{10}^{eff} = e^{-i\Delta k_r z}\Omega_{10}^{(3)}(1+iu)^2\left[\frac{1}{(1+iu)^2} + i\frac{\Delta kb}{2}g(u,\Delta kb/2)\right], \qquad (4.28)$$

where $u = 2z/b$.

Recall that two additional photons of frequency $\omega_1$ are required to ionize from $|1>$. Following Ref. 46, this implies that the only significant contribution to the ionization is that which proceeds by way of the four-photon resonance, that is, four photons are absorbed according to $3\omega_1 + \omega_2$ to reach state $|2>$, from which the absorption of one additional photon of frequency $\omega_1$ will cause ionization. To find the number of ions produced a simple rate equation analysis is used. The equation of motion for $\rho_{22}$ is

$$\frac{d\rho_{22}}{dt} = \mathcal{R} - \Gamma_I\rho_{22}\ ,$$

where $\mathcal{R}$ is the excitation rate constant proportional to

$$\mathcal{R} \propto \frac{|\Omega_{01}^{eff}|^2|\Omega_{21}^{(1)}|^2}{\Gamma_{L2}\delta_1^2},$$

and $\Gamma_I\rho_{22}$ is the rate of ionization from $|2>$. Thus $\rho_{22}$ has the form

$$\rho_{22} = \frac{\mathcal{R}}{\Gamma_I}\left(1 - e^{-\Gamma_I t}\right).$$

The decaying exponential term reflects the decrease in the population of state |2> with time due to ionization. The number of ions will then be given by

$$N_I = \int_{-\infty}^{t} dt\, \Gamma_I\, \rho_{22}\,.$$

A more careful analysis proceeding along these lines in Ref. 46 finds the number of ions produced during a laser pulse with a square temporal profile of duration $\tau$ to be

$$N_I = \frac{N\pi w^2 b\tau}{2}\left(\frac{\ll |\Omega_{21}^{(1)}(0,0,0)|^2 \gg}{\gamma_2} V(\delta_2)\right) \times \frac{|\bar{\Omega}_{10}^{(3)}(0,0,0)|^2}{\delta_1^2}\int_{-\infty}^{\infty} du \left|\frac{1}{(1+iu)^2} + i\left(\frac{\Delta kb}{2}\right) g(u, \Delta kb/2)\right|^2 . \qquad (4.29)$$

(This is essentially equation 5.3 of Ref. 46.) The quantities in the parenthesis on the first line describe the enhancement due to the second laser coupling the fields due to the first laser to the four-photon resonance, while those in the second line of equation 4.29 come from $\Omega_{10}^{eff}$. The arguments $(0,0,0)$ in the Rabi frequencies indicate the quantities are evaluated at the focal point of laser 1 and at the peak of the average power.

$V(\delta_2)$ describes the lineshape if the frequency $\omega_1$ of laser 1 is fixed and laser 2 of frequency $\omega_2$ is tuned across the four-photon resonance. The first, Gaussian term in

$$V(\delta_2) = \sqrt{\pi} e^{-\delta_2^2/4\gamma_2^2}\left[1 - \frac{1 - e^{-\Gamma_{I2}\tau}}{\Gamma_{I2}\tau}\right] + \frac{4\Gamma_{I2}}{\gamma_2} G(\delta_2/\gamma_2), \qquad (4.30)$$

represents absorption into |2> with subsequent ionization, while the second term represents far-wing resonant enhancement by state |2>. Here $\Gamma_1$ and $\Gamma_2$ are the bandwidths of lasers 1 and 2, $\gamma_2 = \sqrt{3\Gamma_1^2 + \Gamma_2^2}$ is the effective four-photon laser bandwidth, and $\Gamma_{I2}$ is the ionization rate out of |2>. $G(y)$ is given by

$$G(y) = -\frac{1}{2} + \frac{y}{4} e^{-y^2/4}\int_0^y dv e^{v^2/4}.$$

This form for $V(\delta_2)$ results from an approximate evaluation of equation 4.10; this is treated in detail in Ref. 46.

The behavior of the interference between the fields at $\omega_1$ and $3\omega_1$ is contained in the integrand of equation 4.29. Let

$$M(u, \Delta kb/2) = \left| \frac{1}{(1+iu)^2} + i(\Delta kb/2) g(u, \Delta kb/2) \right|^2 . \tag{4.31}$$

The first term of M is the contribution due to laser 1, while the second represents the summed contributions of the third-harmonic field from all smaller values of $u = 2z/b$. $\Delta kb/2$ determines the degree of interference. For large values of $\Delta kb/2$, corresponding to small detunings or large number densities, or to large values of absorption, the second term in equation 4.31 will be similar in magnitude and opposite in sign to the first. For $|v(1+iu)| > 15$, the asymptotic series (obtained by the repeated integration by parts of equation 4.27)

$$g(u, v) \simeq -\frac{i}{(1+iu)} \sum_{j=1}^{J} \frac{j!}{(-v)^j (1+iu)^j}, \tag{4.32}$$

with $J$ chosen so that $J < |v(1+iu)|/2$, is a valid approximation to equation 4.27. Recalling that $v = (\Delta k_r + i\alpha)b/2 = (-\kappa_{01}/\delta_1 + i\alpha)b/2$, one may write for equation 4.31

$$M(u, \Delta kb/2) \simeq \left| \frac{1}{(1+iu)^2} - \frac{1}{(1+iu)^2} + \frac{2}{v(1+iu)^3} - \frac{6}{v^2(1+iu)^4} + \cdots \right|^2 . \tag{4.33}$$

The leading, $v$-independent term of the expansion represents the adiabatic part of the polarization at $3\omega_1$; it cancels the term due to three-photon pumping by the first laser. For small $\alpha$, the behavior of M is dominated by $\Delta k_r b/2$. As $\delta_1$ approaches zero, the phase mismatch becomes larger and the remaining terms in the expansion approach zero; this is the three-photon interference effect canceling the excitation. As $\delta_1$ is tuned away from three-photon resonance, the phase mismatch is lessened and the remaining terms in the expansion produce excitation. It is this dependence of the interference on the phase mismatch that is examined in the experiment described in Chapter V.

If the first, near three-photon resonant laser is reflected back on itself an excitation pathway involving the absorption of two photons traveling in one direction plus one from

the other direction (plus one from the second laser) is created; due to the radically different phase-matching condition, this pathway may be considered for the situation here as lacking the interference effect. (See, however, Refs. 15 through 19 and Chapters II and III of this dissertation.). With counterpropagated excitation, one would see increased ionization. The ratio between the ionization with and without counterpropagation will depend on the degree of interference occurring in the uncounterpropagated case, which depends on the value of $\Delta kb/2$.

Defining $R$ as the ratio between ionization with the first laser counterpropagated and ionization with unidirectional excitation, assuming $|\alpha| << |\Delta k_r|$, and using equation 4.29, one may write

$$\begin{aligned} R = & \frac{\int_{-\infty}^{\infty} du \left[ M + (F/3) \frac{1}{(1+u^2)^2} \right]}{\int_{-\infty}^{\infty} du M}, \\ = & 1 + \frac{\pi F/6}{\int_{-\infty}^{\infty} du M(u, \Delta k_r b/2)} \end{aligned} \tag{4.34}$$

The relative simplicity of this equation results from the cancellation of most of the factors in equation 4.29. Here the quantity $(F/3)(1+u^2)^{-2}$ represents the additional ionization due to the counterpropagated excitation pathway. The reflected beam is assumed to be refocused to have the same confocal parameter as the forward beam, with F the fraction of the forward energy reflected.

In the development up to this point laser 1 has been assumed to have a single mode, transform limited output; however, the laser used as laser 1 in the experiment described in Chapter V was a multimode device. This is significant because laser 1 pumps a three-photon transition and the rapid temporal structure of the multimode laser will affect the pumping rate of the transition in different ways for the unidirectional and counterpropagated cases; thus the statistics of laser 1 must be incorporated into the calculation of R.

The physical basis for the effect of the mode structure is the following. The envelope of the laser output will vary on a time scale estimated by $1/\Gamma_L$, where $\Gamma_L$ is the bandwidth

of the multimode laser. This variation is due to the beating together of the various simultaneously lasing cavity modes, and results in a rapid spikiness in the laser output. These spikes will have a length given approximately by $c/\Gamma_L$. This rapid variation has relatively little significance for unidirectional pumping, since all three photons may be absorbed from the same spike. For counterpropagated pumping, however, where there is no correlation between the spikes in the forward and reflected beams, a net reduction in the pumping rate occurs due to the frequent lack of spatial overlap of the spikes in the two beams. The effect of this lack of correlation may be modeled at least approximately by assuming laser 1 to be described by the chaotic field model with an autocorrelation function of the form of equation 4.6. This assumption leads to the factor of $\frac{1}{3}$ in the numerator of the expression for R.

## Summary

An expression for the suppression of the ionization from a four-photon resonance with a three-photon intermediate enhancement by the three-photon interference has been found. The expression predicts the ratio of the ionization with counterpropagation of the near three-photon resonant beam to that without counterpropagation. The ratio depends on the real phase mismatch parameter $\Delta k_r b$ and the fraction $F$ of the forward intensity that is retroreflected. The ratio is independent of laser intensities or pulse lengths. The phase mismatch $\Delta k_r b$ depends on the detuning from three-photon resonance $\delta_1$, the number density $N$, the oscillator strength of the transition, and the confocal parameter $b$. In the experiment described in Chapter V $R$ is measured for fixed $F$ and $b$ as a function of $N$ and $\delta_1$.

# CHAPTER V

## The Four-photon Suppression Experiment

In this chapter experimental observation of the suppression of the excitation of a four-photon resonance by four-wave sum-frequency generation occurring near an intermediate three-photon resonance is reported. The $6p[\frac{1}{2}]_0$ state of xenon (referred to as the $6p$) is excited by three blue photons plus one infrared photon. One beam, focused to $I_1 \simeq 7 \times 10^9$ watts/cm$^2$, is nearly three-photon resonant with the $6s[\frac{3}{2}]_1^O$ resonance (referred to as the $6s$); the second, unfocused beam ($I_2 \simeq 2 \times 10^7$ watts/cm$^2$) is tuned to maintain exact four-photon resonance. One additional blue photon ionizes from the four-photon level. Third harmonic light is generated by the first, near three-photon resonant beam by four-wave sum-frequency mixing. One third-harmonic photon plus one photon from the second laser form a second excitation pathway to the four-photon level; destructive interference between the two pathways results in a reduction in the observed ionization. The degree of reduction depends on the xenon density and the detuning from three-photon resonance. This interference may be overcome by retroreflecting the near three-photon resonant beam to provide an additional excitation pathway which generates no third-harmonic. Comparison is made between the observed reduction in ionization and the predictions made in Chapter IV and elsewhere[46,48]; excellent agreement is observed. Also reported is the observation of suppression of pressure-induced absorption on the wing of the $5p^6 \rightarrow 6s$ transition. Almost all of the material presented in this chapter appears in Ref. 48.

# Experimental Apparatus and Procedures

Light is generated at $\lambda_1 \simeq 440.8$ nm (referred to as blue) and $\lambda_2 \simeq 828.2$ nm (referred to as IR) with, respectively, a Lumonics HD-300 dye laser using Coumarin 440 dye and a side-pumped Quanta-Ray PDL-1 dye laser using LDS-820 dye. Each laser is pumped by the appropriate harmonic of a single Nd:YAG laser. Both dye laser beams were linearly polarized, with the directions of polarization parallel. Pulse lengths were approximately 7 ns, and the laser bandwidths were approximately 0.2 $cm^{-1}$ and 1 $cm^{-1}$, giving an effective four-photon bandwidth $\gamma_2$ of about 1 $cm^{-1}$. The blue laser had an unfocused beam diameter of about 1 mm and a beam divergence of about 0.3 mRad. The lasers were calibrated in wavelength by observing the enhancement of the MPI at the $5p^6 \rightarrow 6s$ and $6s \rightarrow 6p$ transitions for $\lambda_1$ and $\lambda_2$ respectively.

The blue beam was focused into the center of the 10 cm long xenon cell with a lens with a focal length measured to be 5.5 cm; after passage through the cell the light was recollimated with a 15 cm focal length lens and retroreflected with a dichroic mirror. The 828 nm light from laser 2 was brought into the cell through the dichroic mirror along a direction almost opposite to that of the forward blue beam. A slight angle between the blue and IR beams was necessary to allow the retroreflected blue beam to be blocked while still admitting the IR beam to the cell. The 15 cm lens which recollimated the blue beam plus a third lens formed a telescope for the IR beam, which was thus unfocused in its passage through the cell.

The cell contained both a wire-type proportional counter and a charge collection plate mounted on an insulating standoff on the opposite side of the focal region from the wire. An electrometer could be connected to the charge collection plate. The most satisfactory results were obtained by placing +200 to +300 volts on the wire and observing the positive ion current with the electrometer.

Maintaining a constant overlap between the forward and retroreflected blue beams

was critical in obtaining repeatable results; a large, heavy mount for the retroreflection mirror proved to provide adequate stability for data taking runs of an hour or so. To optimize the overlap, laser 1 was tuned to the $6s[\frac{3}{2}]_1^o$ three-photon resonance and the mirror adjusted to maximize the MPI signal.

The photoionization cross-section $\sigma_I$ for the $6p[\frac{1}{2}]_0$ state of xenon is approximately $1.6 \times 10^{-17}\text{cm}^2$ for 440 nm light.[49] With the intensities employed this transition is fully saturated, and so one expects an ${I_1}^3$ power dependence of the four-photon resonant MPI signal as the intensity of the blue laser is varied. Employing only the proportional counter and a charge-sensitive preamp an ${I_1}^3$ dependence was observable only with $I_1$ so weak that the four-photon MPI signals were uselessly small and noisy; this is thought to be due to a combination of space-charge effects limiting the electron mobility to the ion diffusion rate, and the limited integration time of the (pulse-type) preamp. Employing the electrometer, which integrated the ion current over long times, allowed operation with both adequate signal levels and the proper $I^3$ power dependence. The experiment was performed with $I_1 \simeq 7\times10^9$ Watts/cm$^2$ at the focus and $I_2 \simeq 1.5\times10^7$ Watts/cm$^2$. $I_2$ was determined by observing the transverse profile of the beam with a linear photodiode array, while the value for $I_1$ is calculated from the known focal length of the lens and the measured values of the unfocused beam diameter and divergence. Using $\Gamma_I = \sigma_I F$, with $F$ the photon flux at 440 nm, one finds $\Gamma_I \simeq 1.2$ cm$^{-1}$, which, in combination with the expected laser bandwidths, is in reasonable agreement with the observed FWHM of the four-photon resonance of about 2 cm$^{-1}$.

To measure a value of R $\lambda_2$ was fixed to place the four-photon resonance at a known detuning $\delta_1$ from three-photon resonance. The blue laser was scanned across the four-photon peak with the output from the electrometer recorded on a chart recorder. The retroreflected beam was then blocked and the scan repeated. By using different values of $\delta_1$ and $P_{Xe}$ (the xenon pressure) the dependence of R on $\Delta k_r b$ could be determined. To guard against any systematic errors (due, for example, to a change in the overlap

between forward and retroreflected beams) the detuning and pressure were varied in an irregular fashion. Repeated values of R taken at a given value of $\Delta k_7 b$ indicate the repeatability of the measurements is better than 10%. Xenon pressures of two and four Torr were employed. R was measured on both sides of the three-photon resonance, with $|\delta_1|$ in the range of 20 to 50 $cm^{-1}$. Reliable values for R could not be obtained for detunings closer to three-photon resonance than about 20 wavenumbers, since as $\delta_1$ decreases the four-photon MPI signal without counterpropagation of the blue beam becomes comparable with the noise level, leading to large uncertainties in R. This was especially significant for the values taken on the red side of three-photon resonance, where, since the third-harmonic is very badly phase mismatched, the suppression is greater than at the same detuning on the blue side.

## Experimental Results and Comparison With Theory

In Fig. 14 typical scans across the four-photon resonance are shown. The scans labeled a, a′ are taken without counterpropagation of the blue beam, that is, with the three-photon interference effect acting to suppress excitation of the four-photon level. Those labeled b, b′ are taken with counterpropagation. The two pairs a, b and a′, b′ differ in the detuning from three-photon resonance, with the upper pair taken closer to resonance, and thus showing more suppression in the uncounterpropagated scan.

In Fig. 15 the four-photon MPI signal is shown as a function of $\delta_1$ for both unidirectional and counterpropagated excitation. With the blue beam counterpropagated, approximately the expected $\delta_1^{-2}$ dependence due to near-resonant enhancement by the nearby three-photon level is seen. Without counterpropagation, the MPI signal decreases drastically as the detuning from three-photon resonance becomes smaller and the system comes closer to complete three-photon cancellation.

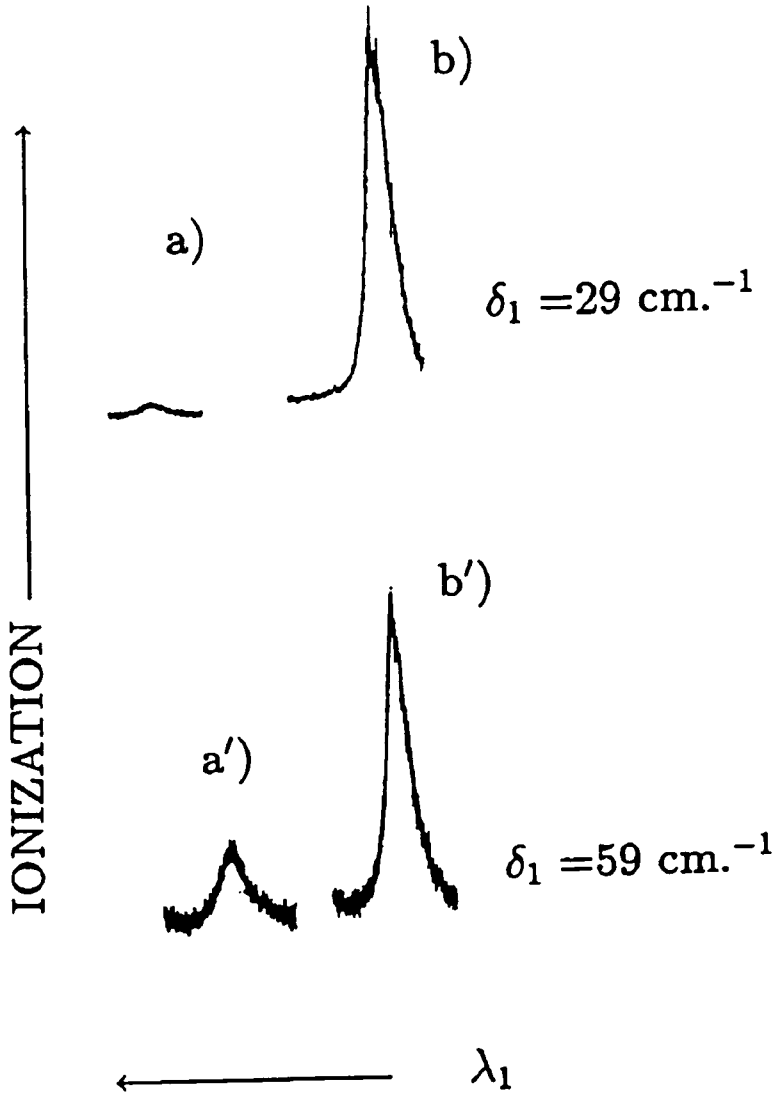


Figure 14. MPI as the First Laser is Scanned Across the Four-photon Resonance

Scans labeled a, a′ are taken without retroreflection of the near three-photon resonant beam, while in b, b′ the retroreflected excitation overcomes the three-photon interference. The upper and lower pairs are for blue-side detunings from three-photon resonance of 29 and 59 cm$^{-1}$, respectively, with $P_{Xe}$ = 4 Torr. A smaller detuning produces more suppression.

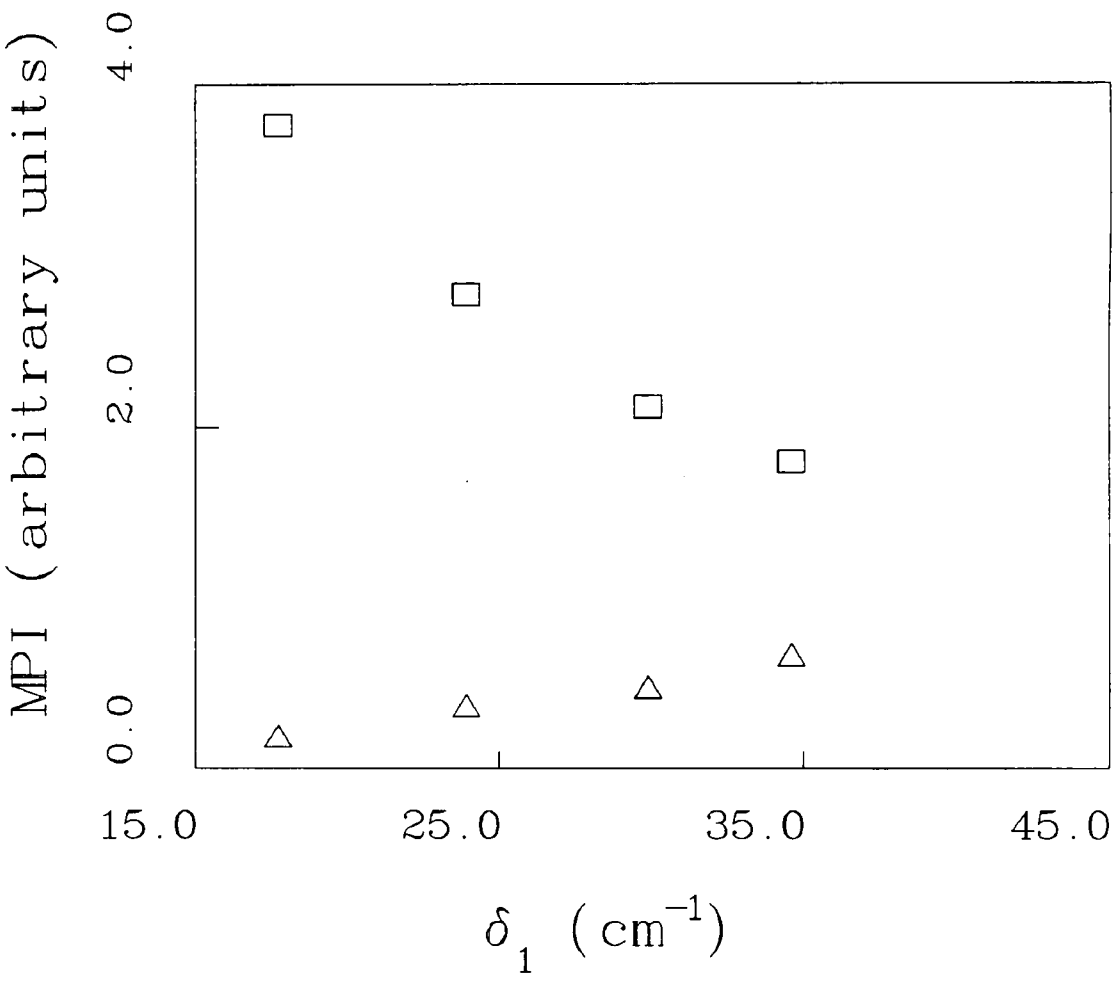


Figure 15. Four-photon MPI as a Function of Detuning

The upper curve (squares) shows MPI with the near three-photon resonant beam retroreflected; it shows an increase in ionization as the laser is tuned closer to the enhancing three-photon resonance. The lower curve (triangles), taken with the beam not retroreflected, shows the result of the three-photon interference effect; the ionization decreases as three-photon resonance is approached. Both curves are at the same laser intensities and detection sensitivities.

In Fig. 16 the data are plotted against the predicted behavior from equation 4.30 in the form $(R-1)/F$ *vs.* $-\Delta k_r b/2$. Here $F$ is taken to be the fraction of the intensity of the forward beam at the focus of the reflected beam; since the reflected beam is focused with a lens with a focal length three times that of the lens used in the forward beam, $F = 0.1$ is used. To find $\Delta k_r b$ the laser is treated as if it had a diffraction-limited Gaussian beam; using $f_{01} = 0.269$ for the oscillator strength of the $5p^6 \rightarrow 6s[\frac{3}{2}]$ transition (Ref. 39, chapter 5), one finds

$$-\frac{\Delta k_r b}{2} = 102.9\frac{P_{Xe}}{\delta_1},$$

with $P_{Xe}$ in Torr and $\delta_1$ in $\text{cm}^{-1}$. The solid line in Fig. 16 is the result of evaluating equation 4.34 numerically using techniques outlined in Ref. 46.

To achieve the fit shown the experimental values of $\Delta k_r b$ were multiplied by 1.25 and the observed values of $(R-1)/F$ by 0.6. The adjustment to $\Delta k_r b$ is insignificant, given that the focused laser beam is modeled as being axially symmetrical with a Gaussian intensity distribution, whereas in fact the laser beam employed is neither Gaussian nor symmetrical. Some of the discrepancy between predicted and observed values of $(R-1)/F$ may also be attributed to this source; other souces for the difference are residual two-photon absorption of the third harmonic and an inadequate model of the temporal structure of the output of laser 1. As will be shown below, both would have the effect of increasing the observed suppression ratio above the predicted value.

The expression for $R$ (equation 4.34) is found with the assumption of a chaotic field model for laser 1. The chaotic field model assumes the laser output to consist of a very large number of simultaneously lasing modes with randomly chosen phases; it is thus something of a limiting case chosen for analytical convenience rather than accuracy. The laser used for laser 1 typically shows three or four cavity modes operating on a given shot, and so the statistics of the temporal fluctuations of its output may not be well described by the autocorrelation function equation 4.6. The assumption of a chaotic field model gave the factor of $\frac{1}{3}$ in the numerator of the first form of equation

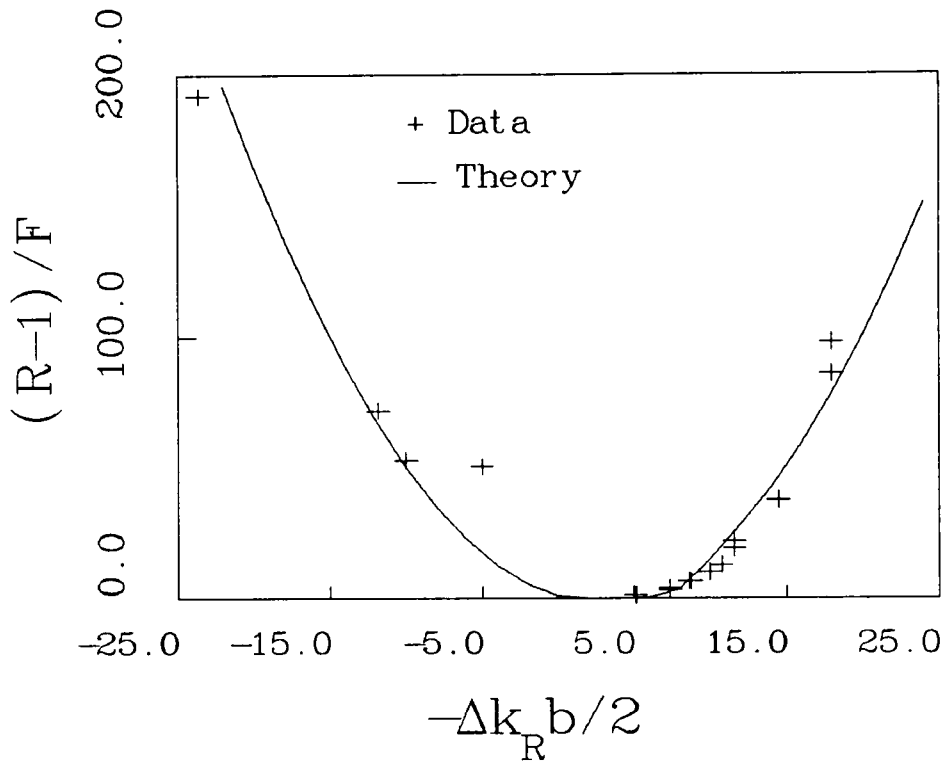


Figure 16. Suppression of Four-photon MPI *vs.* Phase Mismatch

R is the ratio of MPI with and without counterpropagation of the near three-photon resonant beam. $F$ is the fraction of the forward intensity in the reflected beam. $-\Delta k_r b/2 = 102.9\ P_{Xe}(\text{Torr})/\delta_1(\text{cm}^{-1})$, so three-photon resonance is approached from the blue(red) side on the right(left) side of the graph. The theoretical curve is the result of evaluating numerically equation 4.34. Xenon pressures of 2 and 4 Torr were used when taking the data points.

4.34; the assumption of a single mode laser would give a factor of 1 instead. Although the idea has not yet been investigated in detail, it seems likely that a laser with an output intermediate between the chaotic field case and the single mode case would give a value for the coefficient intermediate between 0.33 and 1, and so increase the predicted magnitude of the suppression.

In the analysis of the data it has been assumed that $\Delta k = \Delta k_r$; that is, both one-photon absorption on the far wing of the $|0> \rightarrow |1>$ transition and two-photon absorption by the $|0> \rightarrow |2>$ transition have been neglected. At the relatively large detunings ($\delta_1 > 28\text{cm}^{-1}$) and low pressures ($P_{Xe} = 4$ Torr or less) employed, one-photon absorption is insignificant. Evaluating equation 2.84 for the absorption coefficient $\beta$ one has

$$\begin{aligned}\beta &= 2\frac{\kappa_{01}\Gamma_P}{\delta_1^2} \\ &= 0.37\frac{\kappa_{01}^2\lambda_R}{\delta_1^2},\end{aligned}$$

where $\lambda_R$ is the resonant wavelength in cm, and $\delta_1$ is the detuning from resonance in radians $\text{s}^{-1}$. With $\lambda_R = 1470$ Å, $P_{Xe}$ in Torr, and the detuning $\delta_1$ in $\text{cm}^{-1}$, this is

$$\beta \approx 8.0\frac{P_{Xe}^2}{\Delta^2},$$

where, of course, $\beta$ has dimensions of $\text{cm}^{-1}$. For a detuning of 28.6 $\text{cm}^{-1}$ and a pressure of 4 Torr, $\beta = 0.16$ $\text{cm}^{-1}$, corresponding to an absorption length of 6.4 cm. This is clearly negligible.

To estimate the two-photon absorption coefficient, one may write for the excitation rate $\mathcal{R}$ of state $|2>$ by the absorption of one photon at frequency $3\omega_1$ and one at $\omega_2$

$$\mathcal{R} \simeq 2\frac{|\Omega_{02}^{(2)}|^2}{\Gamma_L} \simeq 2\frac{|\Omega_{01}^{(1)}|^2|\Omega_{12}^{(1)}|^2}{\Gamma_L\delta_1^2},$$

where $\Omega_{02}^{(2)}$ is the reduced two-photon Rabi frequency and $\Gamma_L$ is the HWHM of the transition. With $N$ the number density, $F_{3\omega_1}$ the photon flux at $3\omega_1$, and $\beta$ the two-photon absorption coefficient for light at $3\omega_1$ one finds

$$N\mathcal{R} = \beta F_{3\omega_1}$$

by equating the volume rate of excitation to the volume rate of absorption. Then

$$\alpha = \frac{\beta}{2} = \frac{N\mathcal{R}}{2F_{3\omega_1}} = \kappa_{01}\frac{|\Omega_{12}^{(1)}|^2}{\Gamma_L\delta_1^2}$$

where $|\Omega_{01}^{(1)}|^2$ has been evaluated in terms of $F_{3\omega_1}$ and $\kappa_{01}$. Following Ref. 39 one finds $|\Omega_{12}^{(1)}|^2 = 1.7 \times 10^{16} I_2$, where $I_2$ is the intensity of laser 2 in watts/cm$^2$. Then

$$\begin{aligned}\Delta k &= \Delta k_r + i\alpha \\ &\simeq -\frac{\kappa_{01}}{\delta_1}\left[1 - i\frac{|\Omega_{12}^{(1)}|^2}{\delta_1\Gamma_L}\right] \\ &\simeq -\frac{\kappa_{01}}{\delta_1}\left[1 - i\frac{\Delta_S}{\Gamma_L}\right], \end{aligned} \tag{5.1}$$

where $\Delta_S$ is the ac Stark shift in state $|2>$ due to laser 2. Note that two-photon absorption can increase the magnitude of $\Delta k$ by at most a factor of $\sqrt{2}$, since if $\Delta_S$ becomes large compared to the other widths which make up $\Gamma_L$ ( $\gamma_2$ and $\Gamma_I$ ), one must use $\Gamma_L \simeq \Delta_S$.

From the measured energy and transverse spatial FWHM of the beam of laser 2, and assuming a Gaussian intensity distribution, the peak intensity of laser 2 is found to be $I_2 = 1.5 \times 10^7$ Watts/cm$^2$; from the scans of the four-photon resonance one can estimate $\Gamma_L \simeq 1$ cm$^{-1}$. For $\delta_1$ =28.6 cm$^{-1}$ and $P_{Xe}$ = 4 Torr (corresponding to the largest value of $\Delta k_r b/2$ used), one has

$$\Delta k = -171(1 - i0.25) \quad [\text{cm}^{-1}].$$

For this value of $\Delta kb$ the series expansion of the diffraction integral (equation 4.27) given in equation 4.32 is valid. To suggest the effect of an imaginary part of $\Delta k$ one may write to first order in v

$$M \propto \left|\frac{1}{(\Delta k)}\right|^2 = \frac{1}{\Delta k_r^2 + \alpha^2},$$

so absorption of the magnitude predicted here should not have a large effect on M or R, although observation of the total (far-field) third-harmonic might show a dip at four-photon resonance, since the large IR beam will cause absorption over a distance many times as large as b.

In addition, from equation 5.1 one sees that two-photon absorption comparable in magnitude to $\Delta k_\tau$ should be accompanied by observable ac Stark broadening of the four-photon resonance. In the data there is in fact a small decrease in the width of the four-photon resonance peak as $\delta_1$ decreases from 50 $cm^{-1}$ to 20 $cm^{-1}$ on the blue side of three-photon resonance, rather than any increase. For these reasons the effect of absorption is thought to be relatively small, and so the observed suppression is due mainly to large $\Delta k_\tau b$.

In Fig. 16 it may be seen that as the three-photon resonance is approached from either the blue side (the right side of Fig. 16) or the red, the suppression of the four-photon resonance by the interference occurring at the three-photon level reaches very large values. In contrast, as the phase-matched value of $-\Delta k_\tau b/2 = 2$ is approached the suppression becomes negligible. As one tunes closer to the three-photon resonance, the phase mismatch becomes larger, so destructive interference among components of the third-harmonic light generated at smaller values of z results in less net third-harmonic intensity. Expressed another way, the correlation length for third-harmonic generation $l_c = \pi/\Delta k_\tau$ becomes smaller, and an atom at any given position z sees third-harmonic produced over a shorter region. The first term in the expansion of the diffraction integral in equation 4.33 does not depend on the phase mismatch; it is the adiabatic polarization which follows (and cancels) the three-photon laser field exactly. So for large $\Delta k_\tau b$ one has 1) little excitation by one third-harmonic photon plus one photon at $\omega_2$, since the bad phase mismatch kills the propagating third harmonic, and 2) little excitation by laser photons since the adiabatic part of the polarization at $3\omega_1$ cancels the contribution from three laser photons.

For $\Delta k_\tau b$ near the phase-matching point, the third-harmonic intensity can grow large enough to provide substantial pumping of the four-photon level by the absorption of one photon at $3\omega_1$ and one at $\omega_2$; note that for equal intensities the two-photon process is vastly more likely than the four-photon $(\omega_1 + \omega_1 + \omega_1 + \omega_2)$ process. Thus

near $-\Delta k_r b/2 = 2$ one sees little evidence of suppression. In fact, in this region the ionization is largely due to the third-harmonic field.

## Hybrid Resonance Experiment

In the absence of three-photon interference, a bright laser tuned close to a three-photon resonance will create some population in the three-photon level by pressure-induced wing absorption. If a second laser were tuned resonant-resonant between the three-photon level and a higher lying level which is dipole-coupled to the three-photon level, an enhancement in the MPI would be observed as a result of pumping of population from the three-photon state to the higher-lying state and subsequent ionization. This is a classic "hybrid" resonance.

The first laser is tuned 19 $cm^{-1}$ to the blue of the $6s[\frac{3}{2}]_1^O$ three photon transition. The second, infrared laser is now time delayed by 12 ns so that it no longer overlaps temporally with the first laser. Tuning the IR laser across the $6s[\frac{3}{2}]_1^O \rightarrow 6p[\frac{1}{2}]_0$ resonance should produce a peak in the MPI signal proportional to the population excited into the 6s during the blue laser pulse; note that any population in the $6s$ is effectively trapped on the time scale of the delay between laser pulses due to the opacity of the medium to resonant light. In Fig. 17 two scans of this sort taken with and without counterpropagation of the near three-photon resonant laser are shown. Here the xenon density has been raised to 25 Torr to increase the absorption; $I_1$ is the same as before, while $I_2$ is about four times smaller. In Fig. 17 a), taken without counterpropagation, there is no peak, while in 17 b), taken with the blue beam counterpropagated and the sensitivity reduced by a factor of 10, there is a prominent peak. This demonstrates clearly that the three-photon interference effect suppresses wing absorption into the three-photon level.

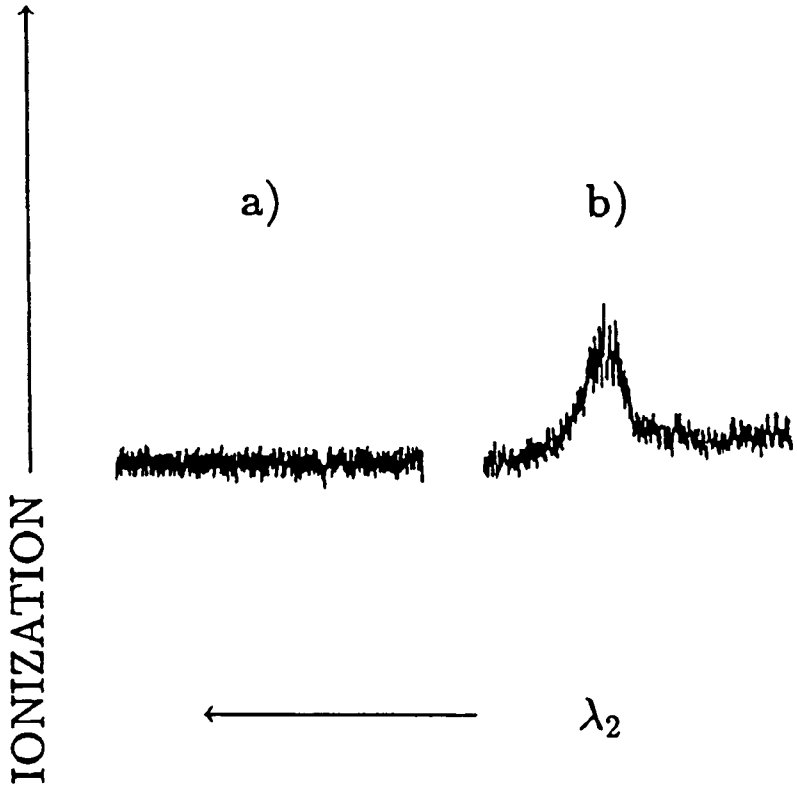


Figure 17. Suppression of Wing Absorption into the Three-photon Resonance

$\lambda_2$ is scanned across the $6s \rightarrow 6p$ transition with the beam time delayed. $\lambda_1$ is tuned 19 $cm^{-1}$ to the blue of the 6s and $P_{Xe} = 25$ Torr. In a), $\lambda_1$ is not counterpropagated and the three-photon interference effect prevents absorption. In b), counterpropagation overcomes the interference and MPI due to population in the three-photon state is seen.

# Summary

The suppression of the excitation of a four- and two-photon allowed transition by a three-photon interference effect occuring at an intermediate three- and one-photon allowed resonance is observed in a focused geometry. The three-photon interference is caused, not by absorption of the third-harmonic light, but by a large phase mismatch between the third harmonic and the laser field. Good agreement between the observed degree of suppression and the predictions made in chapter IV of this dissertation and in Refs. 46 and 48 is found. Also, it is shown with a hybrid resonance experiment that the three-photon interference effect can suppress the growth of a population in the three-photon intermediate state.

# CHAPTER VI

## Summary and Conclusions

The two experiments reported in this dissertation both demonstrate surprising results of the odd-photon interference effect; the combined action of the applied laser field and the internally generated sum-frequency field is shown to produce, in one experiment, a shift in the apparent resonant frequency of a three-photon resonant transition, and, in the other experiment, a suppression of the excitation of a four-photon resonant transition. Excellent agreement with the prediction of fairly simple theoretical models is found in both cases.

Work on what is described here as the three-photon shift stems from the observations of Ferrell *et al.*[4,43] of a pressure-dependent blue shift in the resonant frequency of three- and one-photon allowed transitions is xenon and other noble gases when the three-photon laser excitation was counterpropagated to overcome the three-photon cancellation effect. Theoretical explanations due to Friedberg *et al.*[18,19] and to Payne *et al.*[16,15] explain the effect in terms of the combined pumping of the three-photon transition by the laser field and the internally generated sum-frequency field; phase matching between the applied and generated fields turns out to be centrally important to a cohesive understanding of the shift and the related on-resonance cancellation. In Chapter II of this dissertation an expanded presentation of the model described in Ref. 16 is given; two-color excitation with an angle $\theta$ between the two laser beams is applied to a two-state model in which the sum-frequency field is treated self-consistently. The model is used to demonstrate on-resonace cancellation of the excitation for collinear ($\theta = 0$) laser pumping, a small pressure-dependent blue shift for the $\theta = 180°$ case (corresponding to

the counterpropagated excitation employed by Ferrell), and much larger blue shifts if the angle between the laser beams is much smaller than 180° or if the wavelength of one of the two colors employed is much longer than the wavelength of the other color. In Chapter III and in Ref. 17 the predictions of this model are tested in xenon for various combinations of laser wavelengths, angles, and number densities. Excellent agreement is found between theory and experiment for the $\theta = 180°$ case for a pressure range of 50 to 800 Torr and two different combinations of laser wavelengths. The larger shifts predicted for smaller values of $\theta$ are also found to be in excellent agreement with experiment, though for the very largest shifts observed a two-state model for the index of refraction is found to be inadequate; use of a more detailed approximation for the index gives excellent agreement for even the largest shifts.

The use of the angle phase matching technique for the measurement of the absorption oscillator strengths of VUV transitions is demonstrated; the utility of this method for the measurement of absorption coefficients in the VUV is also discussed. Thus both the real and imaginary parts of $n(\omega)$ for $\omega$ in the vacuum ultraviolet can be easily determined through the use of three-photon, two-color, angle phase matched excitation of the transition under investigation.

The observation by Blazewicz *et al.*,[44] of a dip in the MPI spectrum at exact four-photon resonance when pumping two- and four-photon allowed transitions in xenon with the $5p^6 \rightarrow 6s'$ as a three-photon intermediate resonance was the impetus for the theoretical study reported by Payne *et al.* in Ref. 46. The dip is found to be the result of a partial three-photon cancellation caused by two-photon absorption of the propagating third-harmonic light by the focused second laser and the two-photon transition. Also discussed in Ref. 46 is the case in which the second laser is unfocused, thus reducing two-photon absorption of the third harmonic to a negligible level. It is found there that three-photon cancellation can be caused by the diminution of the intensity of the free third-harmonic wave caused solely by a large phase mismatch. In Chapter IV of this

dissertation (which draws on and expands the exposition given in Ref. 46) a three-state model with self-consistent treatment of the third-harmonic field is used to predict the ionization to be expected for the case where absorption is negligible; the ratio R between the ionzation with copropagating excitation at the three-photon level and the ionization with counterpropagated three-photon excitation is found as a function of number density, confocal parameter, and detuning from exact three-photon resonance. In Chapter V and Ref. 48 experimental measurements of R are presented and found to agree quite well with prediction.

The two experiments reported here add to the surprisingly varied range of behavior of the nonlinear optical response of the noble gases that may be understood in terms of the odd-photon interference effect. That sum-frequency light generated by nonlinear optical processes should have some effect on the overall response of the system is, at least in retrospect, not at all surprising, given that the conditions for the efficient generation of such light (small detuning from a transition allowed in both one and some odd number of photons) are the same as the conditions for the generated light to have the largest effect on the system. It is nevertheless surprising that sum-frequency generation should have effects as counterintuitive as those discussed here. Nature, as always, will find strange ways of being simple.

# LIST OF REFERENCES

# LIST OF REFERENCES


1. N. Bloembergen, *Nonlinear Optics* (W.A. Benjamin, Inc., Reading, Massachusetts, 1965).
2. Y. R. Shen, *The Principles of Nonlinear Optics* (John Wiley & Sons, New York, 1984).
3. D. C. Hanna, M. A. Yuratich, D. Cotter, *Nonlinear Optics of Free Atoms and Molecules* (Springer-Verlag, Berlin, 1979).
4. Wanda R. Ferrell, M. G. Payne, and W. R. Garrett, Phys. Rev. A 36, 81 (1987).
5. Steven D. Kramer, C. H. Chen, M. G. Payne, G. S. Hurst, and B. E. Lehmann, Applied Optics 22, 3271 (1983).
6. M. G. Payne, "Theory of Four-Wave Mixing for VUV Generation," Proceedings of the Second International Symposium of Resonance Ionization Spectroscopy and Its Applications, (Adam Hilger Ltd., Bristol, England, 1984).
7. K. Aron and P. M. Johnson, J. Chem. Phys. 67, 5099 (1977).
8. R. N. Compton, J. C. Miller, A. E. Carter, and P. Kruit, Chem. Phys. Lett. 71, 87 (1980).
9. J. C. Miller, R. N. Compton, M. G. Payne, and W. R. Garrett, Phys. Rev. Lett. 45, 114 (1980).
10. John C. Miller and R. N. Compton, Phys. Rev. A 25, 2056 (1982).
11. J. H. Glownia and R. K. Sander, Phys. Rev. Lett. 49, 21 (1982).
12. D. J. Jackson, J. J. Wynne, and P. H. Kes, Phys. Rev. A 28, 781 (1983).
13. D. J. Jackson and J. J. Wynne, Phys. Rev. Lett. 49, 543 (1982).

14. M. G. Payne and W. R. Garrett, Phys. Rev. A 28, 3409 (1983).

15. M. G. Payne, W. R. Garrett, Roger C. Hart, and Irene Datskou, Phys. Rev. A 42, 2756 (1990).

16. M. G. Payne and W. R. Garrett, Phys. Rev. A 42, 1434 (1990).

17. W. R. Garrett, Roger C. Hart, James E. Wray, Irene Datskou, and M. G. Payne, Phys. Rev. Lett. 64, 1717 (1990).

18. R. Friedberg, S. R. Hartmann and Jamal T. Manassah, J. Phys. B 22, 2211 (1989).

19. R. Friedberg, S. R. Hartmann, Jamal T. Manassah, Phys. Rev. A 39, 93 (1989).

20. W. R. Garrett, W. R. Ferrell, M. G. Payne, and John C. Miller, Phys. Rev. A 34, 1165 (1986).

21. W. R. Garrett, Stuart D. Henderson, and M. G. Payne, Phys. Rev. A 35, 5032 (1987).

22. W. Demtröder, *Laser Spectroscopy* (Springer-Verlag, Berlin, 1982).

23. M. G. Payne, W. R. Garrett, and Wanda R. Ferrell, Phys. Rev. A 34, 1143 (1986).

24. J. F. Ward and G. H. C. New, Phys. Rev. 185, 57 (1969).

25. P. Laporte and H. Damany, J. de Physique 40, 9 (1979).

26. P. Laporte and H. Damany, J. Quant. Spect. Rad. Transfer 22, 447 (1979).

27. M. G. Payne, W. R. Garrett and H. C. Baker, Chem. Phys. Lett. 75, 468 (1980).

28. M. G. Payne and W. R. Garrett, Phys. Rev. A 26, 356 (1982).

29. M. Poirier, Phys. Rev. A 27, 934 (1983).

30. J. J. Wynne, Phys. Rev. Lett. 52, 751 (1984).

31. J. J. Wynne, in *Multiphoton Processes*, Proceedings of the Fourth International Conference on Multiphoton Processes, Boulder, CO, 1987, edited by S. J. Smith and P. L. Knight (Cambridge Univ. Press, Cambridge, 1987).

32. G. S. Agarwal, Surya P. Tewari, Phys. Rev. A 29, 1922 (1984).

33. Surya P. Tewari, Phys. Rev. A 37, 1223 (1988).

34. Ce Chen, Yi-Yian Yin, and D. S. Elliot, Phys. Rev. Lett. 64, 507 (1990).

35. I. I. Sobel'man, *Introduction to the Theory of Atomic Spectra* (Pergamon Press, Oxford, 1972).

36. Yu. A. Vdovin and V. M. Galitskii, Zh. Eksp. Teor. Fiz. 52, 1345 (1967) [Sov. Phys. - JETP 25, 894 (1967)].

37. P. R. Berman and W. E. Lamb, Phys. Rev. 187, 221 (1969).

38. A. P. Kazantsev, Zh. Eksp. Teor. Fiz. 51, 1751 (1966) [Sov. Phys. - JETP 24, 1183 (1967).

39. G. S. Hurst, M. G. Payne, *Principles and Applications of Resonance Ionization Spectroscopy* (Adam Hilger, Bristol and Philadelphia, 1988), Chp. 5.

40. M. Aymar and M. Coulombe, At. Data Nucl. Data Tables 21, 537 (1978).

41. J. Geiger, Z. Phys. A 282, 129 (1977).

42. M. C. Castex, J. Chem. Phys. 66, 3854 (1977).

43. Wanda R. Ferrell, M. G. Payne, and W. R. Garrett, Phys. Rev. A 35, 5020 (1987).

44. P. R. Blazewicz and J. C. Miller, Phys. Rev. A 38, 2863 (1988).

45. D. Charalambidis, X. Xing, J. Petrakis, and C. Fotakis, Phys. Rev. A, to be published.

46. M. G. Payne, J. C. Miller, R. C. Hart and W. R. Garrett, Phys. Rev. A, to be published.

47. P. R. Blazewicz, M. G. Payne, W. R. Garrett, and J. C. Miller, Phys. Rev. A 34, 5171 (1986).

48. R. C. Hart, W. R. Garrett, and M. G. Payne, submitted to Phys. Rev. A.

49. C. Duzy and H. A. Hyman, Phys. Rev. A 22, 1878 (1980).

50. M. G. Payne, W. R. Garrett, J. P. Judish, and M. P. McCann, "New Coherent Cancellation Effect Involving Four-Photon Excitation and the Related Ionization," Proceedings of the Fourth International Laser Science Conference (ILS IV), (Advances in Laser Sciences - IV), pp. 282-284 (American Institute of Physics - 1989).

51. D. Charalambidis and A. Lyras, P. Lambropoulos and X. Tang, S. J. Bajic and R. N. Compton, Phys. Rev. A 41, 1457 (1990).

# BIBLIOGRAPHY

# BIBLIOGRAPHY


Baldwin, George C. *An Introduction to Nonlinear Optics*, Plenum Press (1969).

Bloembergen, N. *Nonlinear Optics*, W. A. Benjamin (1965).

Bransden, B. H., and Joachain C. J. *Physics of Atoms and Molecules*, Longman Group Lmtd. (1983).

Condon, E. U., and Shortley, G. H. *The Theory of Atomic Spectra*, Cambridge University Press (1979).

Delone, Nikolai B., and Krainov, Vladimir P. *Fundamentals of Nonlinear Optics of Atomic Gases*, John Wiley & Sons (1988).

Demtröder, Wolfgang. *Laser Spectroscopy Basic Concepts and Instrumentation*, Springer-Verlag (1981).

Dicke, Robert H., and Wittke, James P. *Introduction to Quantum Mechanics*, Addison-Wesley (1960).

Eisberg, Robert, and Resnick, Robert. *Quantum Physics of Atoms, Molecules, Solids, Nuclei, and Particles*, John Wiley & Sons (1974).

Feld, Michael S., Thomas, John E. and Mooradian, Aram. *Laser Spectroscopy IX Proc. Ninth Int. Confer. on Laser Spec*, Academic Press (1989).

Hanna, David C., Yuratich, M. A., and Cotter, D. *Nonlinear Optics of Free Atoms and Molecules*, Springer-Verlag (1979).

Hurst, G. S., and Payne, M. G. *Principles and Applications of Resonance Ionization Spectroscopy*, Adam Hilger (1988).

James, J. F., and Sternberg, R. S. *The Design of Optical Spectrometers* , Chapman and Hall Ltd. (1969).

Messiah, Albert. *Quantum Mechanics*, John Wiley & Sons (1961).

Shen, Y. R. *The Principles of Nonlinear Optics*, John Wiley & Sons (1984).

Shimoda, Koichi. *Introduction to Laser Physics*, Springer-Verlag (1984).

Slater, John C. *Quantum Theory of Atomic Structure*, McGraw-Hill Book Co., Inc. (1960).

Sobel'man, I. I. *An Introduction to the Theory of Atomic Spectra*, Pergamon Press (1972).

Zare, Richard N. *Angular Momentum*, John Wiley & Sons (1988).

# VITA

Roger Charles Hart was born in Elizabethton, Tennessee on March 3, 1955. He graduated from Elizabethton High School in 1973. He attended several undergraduate institutions (including East Tennessee State University in Johnson City, Tennessee, the University of the South in Sewanee, Tennessee, and the University of Tennessee in Knoxville, Tennessee) for varying periods of time over the succeding decade or so before finally receiving a Bachlor of Arts degree from the University of Tennessee in 1985. He immediately thereafter entered the graduate program in physics at the University of Tennessee. He served briefly as a teaching assistant before finding more rewarding employment as a research assistant. His initial graduate research experience involved developing methods to grow monocrystals of lanthanide and actinide trihalides. Although ultimately successful, this work (involving as it did radiochemistry) proved to be not to his taste. In 1988 he began his dissertation research with the Photophysics Group at Oak Ridge National Laboratory, pursuing a series of investigations into the nonlinear optical response of alkali metal vapors and noble gases. He received the Doctor of Philosophy degree with a major in Physics in December 1991. His immediate postgraduate plans involve post-doctoral work at the Joint Institute for Laboratory Astrophysics at the University of Colorado in Boulder, Colorado.